

EPR spectroscopy for Bio-Inorganic Chemistry

Principles and Applications

FrenchBIC summer school

Carry-Le-Rouet / Marseille – 17-21 September 2017



Bruno GUIGLIARELLI

Unité de Bioénergétique et Ingénierie des Protéines – UMR 7281

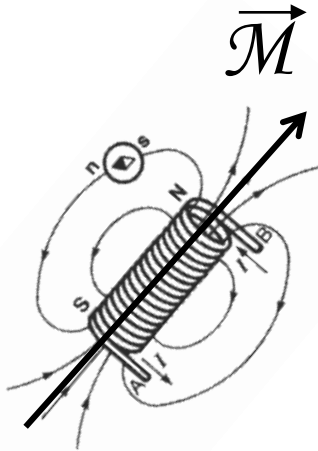
CNRS et Aix-Marseille Université



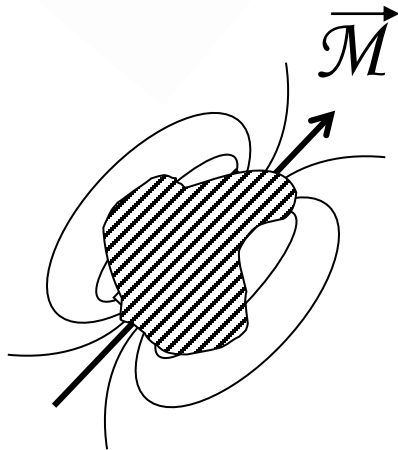
Summary

- 1- Basic principles
- 2- Improving EPR sensitivity
- 3- Transition metal ions: magnetic and EPR properties
- 4- Low spin Fe^{3+} systems: hemes
- 5- High spin Fe^{3+} systems
- 6- Spin transitions
- 7- Electron spin relaxation
- 8- Fe-S clusters and exchange interaction
- 9- Hyperfine coupling
- 10- HYSCORE spectroscopy on Mo(V) cofactor
- 11- Detection of intercenter magnetic couplings

Basic principles



Magnetism is related to motion of electric charges



In matter : moving charges are electrons and protons

- Electron magnetism :
 L , orbital momentum
 S , spin momentum

$$\begin{aligned}\vec{\mu}_e &= -\beta_e (\vec{L} + g_e \vec{S}) \\ &= -g \beta_e \vec{S}\end{aligned}$$

EPR

- Nuclear magnetism
 I , nuclear spin

$$\vec{\mu}_N = g_N \beta_N \vec{I} = \gamma_N \hbar \vec{I}$$

NMR

$$\beta_e = e \hbar / 2 m_e = 9.274 \cdot 10^{-24} \text{ A} \cdot \text{m}^2 \gg \beta_N = e \hbar / 2 m_p = 5.05 \cdot 10^{-27} \text{ A} \cdot \text{m}^2$$

Bohr's magneton \gg Nuclear magneton

Basic principles : the magnetic resonance phenomenon

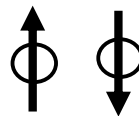
Electron Paramagnetic Resonance (EPR): A spectroscopy specific of **single electron systems**

For a system with spin $S = 1/2$ in a magnetic field \mathbf{B} : $\vec{\mu} = -g \beta_e \vec{S}$

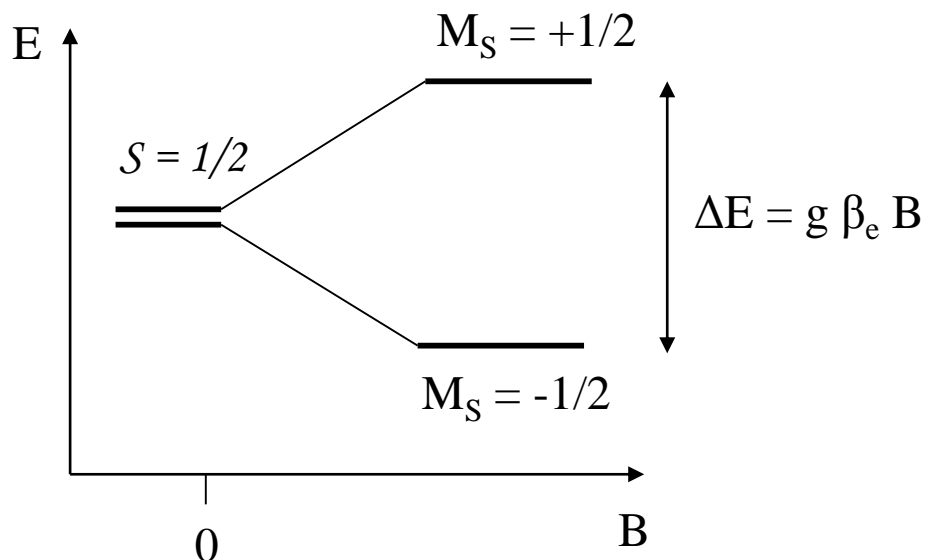
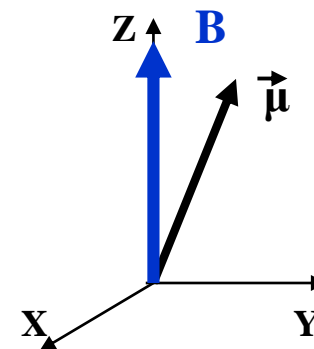
$$\mathbf{E} = -\vec{\mu} \cdot \vec{\mathbf{B}} \quad \longrightarrow \quad \mathbf{H} = -\vec{\mu} \cdot \vec{\mathbf{B}} = g \beta_e \vec{S} \cdot \vec{\mathbf{B}}$$

Taking $\vec{Z} // \vec{\mathbf{B}} \Rightarrow \mathbf{H} = g \beta B S_Z$

S_Z is quantified: only two values $M_S = \pm 1/2$



Energies : $E = g \beta_e B M_S = \pm 1/2 g \beta B$ (Zeeman effect)



Basic principles : the magnetic resonance phenomenon

Electron Paramagnetic Resonance (EPR): A spectroscopy specific of single electron systems

For a system with spin $S = 1/2$ in a magnetic field B

$$E = -\vec{\mu} \cdot \vec{B} \quad \longrightarrow \quad H = -\vec{\mu} \cdot \vec{B} = g \beta_e \vec{S} \cdot \vec{B}$$

Taking $\vec{Z} // \vec{B} \Rightarrow H = g \beta_e B S_Z$

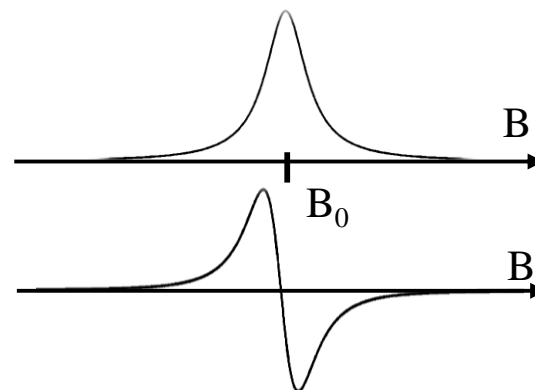
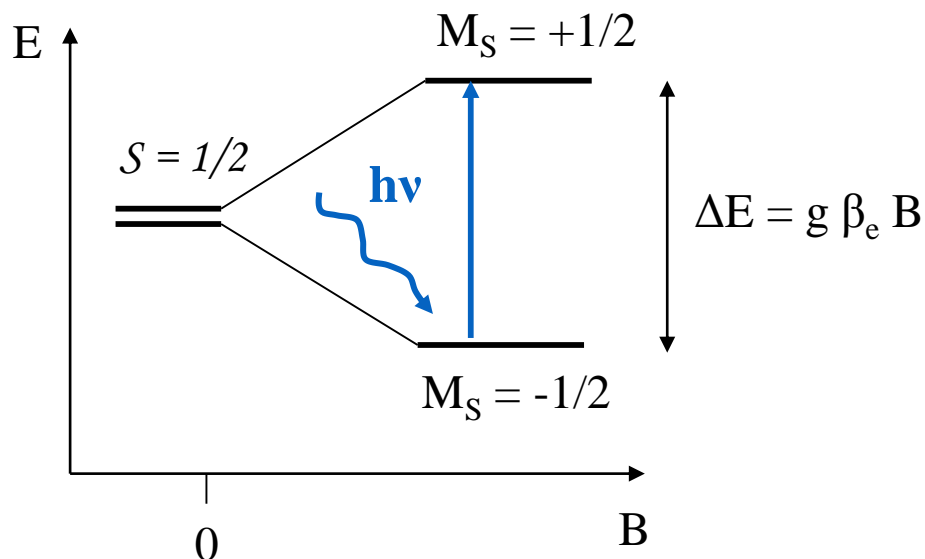
S_Z is quantified: only two values $M_S = \pm 1/2$



Energies : $E = g \beta B M_S = \pm 1/2 g \beta_e B$ (Zeeman effect)

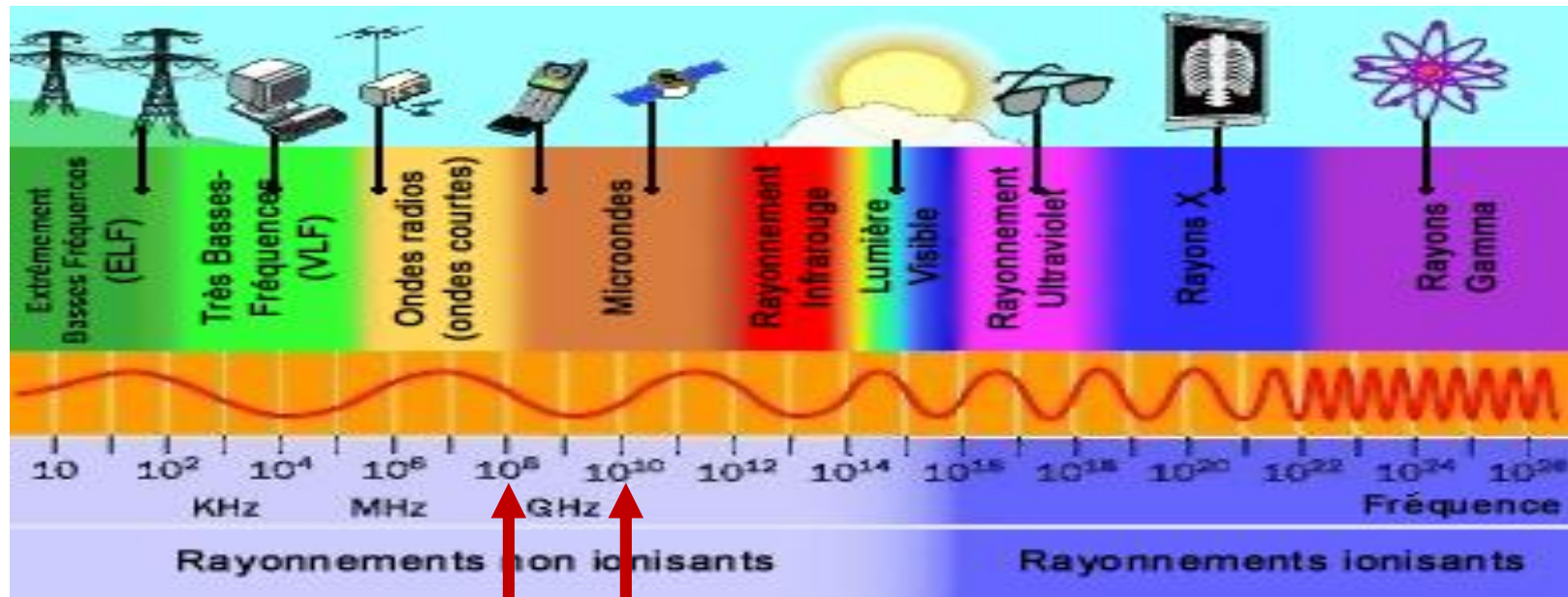
Resonance condition

$$h\nu = g \beta_e B_0$$



$g = 2.00, B_0 = 0.3 \text{ T}$
 $\nu = 10 \text{ GHz}, \lambda = 3 \text{ cm}$
Microwaves (X-band)

Basic principles : the magnetic resonance phenomenon



NMR **EPR**

2nd World War: development of **RA**dio **D**etecting **A**nd **R**anging (RADAR)

- Microwave sources: klystron (Bernard Rollin 1940)
- Highly sensitive detection crystals
- Antenna, Magic-T, ...
- Lock-in amplifiers



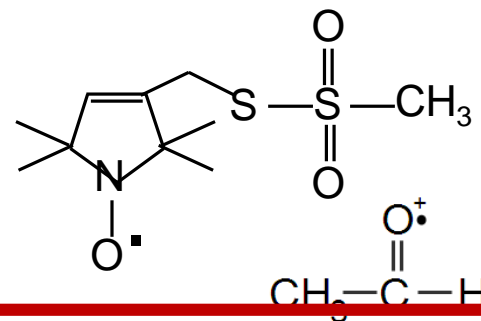
Basic principles:

EPR detectable systems:

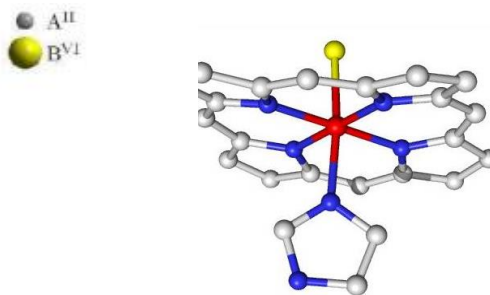
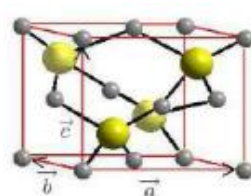
$$\mu_e \neq 0 \longrightarrow S \neq 0$$

➤ Odd electron number:

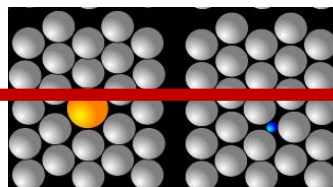
- Free radicals (organics, OH^\bullet , NO^\bullet , NO_2^\bullet , HCO_3^\bullet , ...)



- Transition metal ion compounds (Cu^{2+} , Fe^{3+} , Ni^{3+} , Mo^{5+} , V^{3+} , Ti^{3+} , ...)

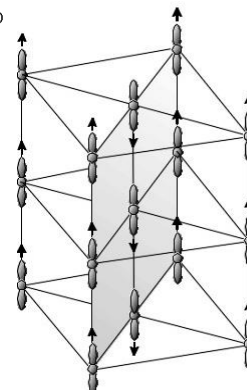
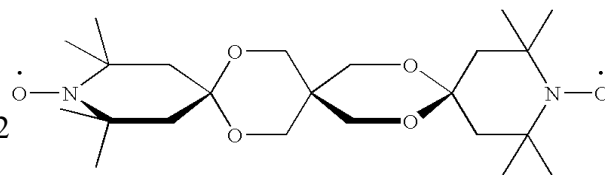


- Impurities (doping) and defects in solids



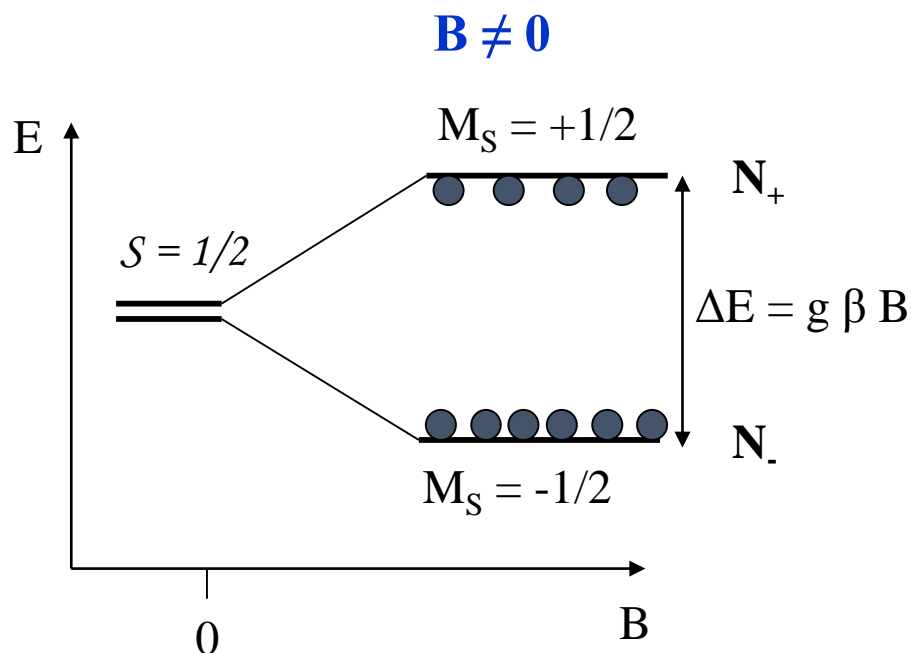
➤ Even electron number:

- Triplet states (excited or not), biradicals, O_2
- Conduction electrons, organic/inorganic molecular conductors, ferromagnets,



Basic principles : the sensitivity of EPR

Thermal equilibrium and spin state populations



Weak value of $\Delta E = g \beta B$

$$B = 0.3 \text{ T} \quad \Delta E \sim 0.3 \text{ cm}^{-1}$$

Thermal equilibrium (Boltzmann's law)

$$N_+ / N_- = \exp(-\Delta E / k_B T)$$

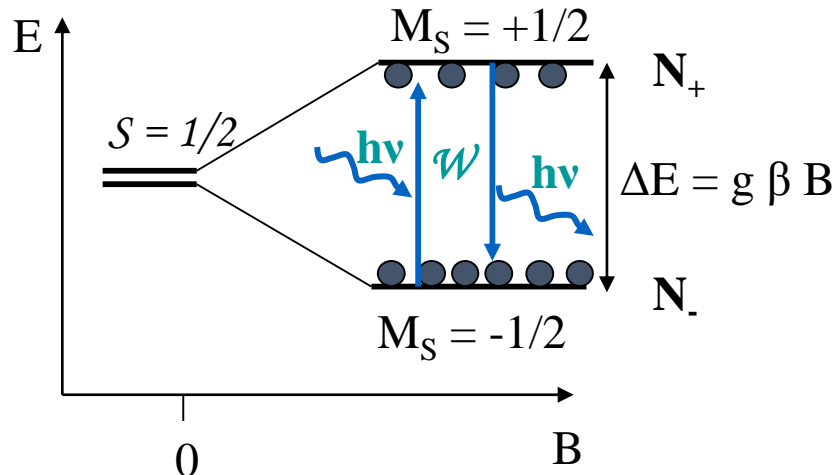
$$N_+ / N_- = \exp(-g \beta B / k_B T)$$

$$T = 298 \text{ K}, \quad N_+ / N_- = 0.9986$$

Very weak spin polarization

$$p = (N_- - N_+) / (N_- + N_+) = 7 \cdot 10^{-4}$$

Basic principles : the sensitivity of EPR



Microwave induced transitions

$$B_1(t) = B_1 \cos(\omega t)$$

Same transition probability for absorption and emission

$$W \propto B_1^2 \propto P_1 \text{ (mW)}$$

EPR signal : net absorbed power

$$P_{\text{abs}} = h\nu (WN_- - WN_+) = h\nu W n \quad \text{with } n = N_- - N_+$$

EPR signal intensity is directly related to n

Important consequence : Curie's law

$$I \propto n/N_0 = \tanh(g\beta B_0 / 2k_B T) \approx g\beta B_0 / 2k_B T$$

EPR signal intensity obeys the Curie's law $I \cdot T = \text{Cte}$

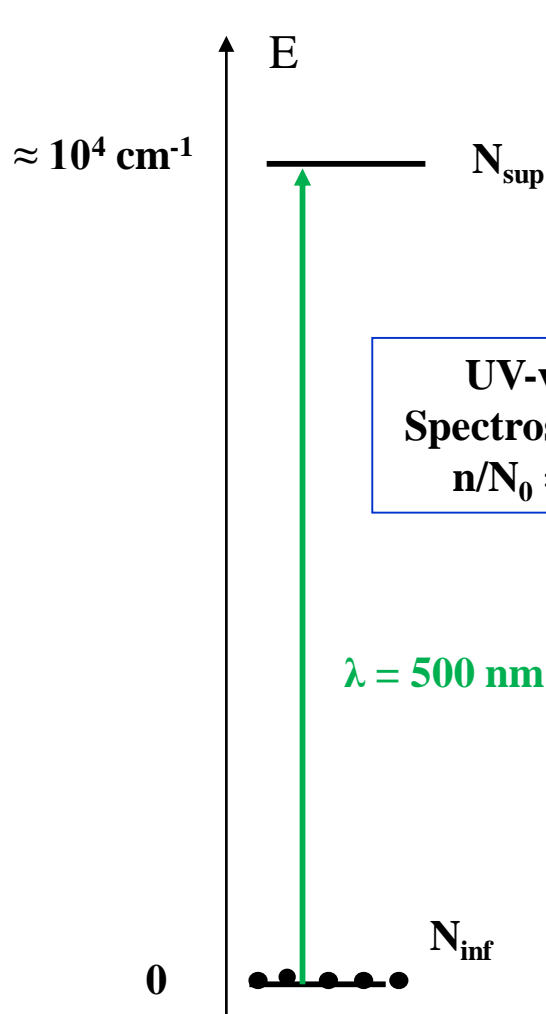


Pierre Curie

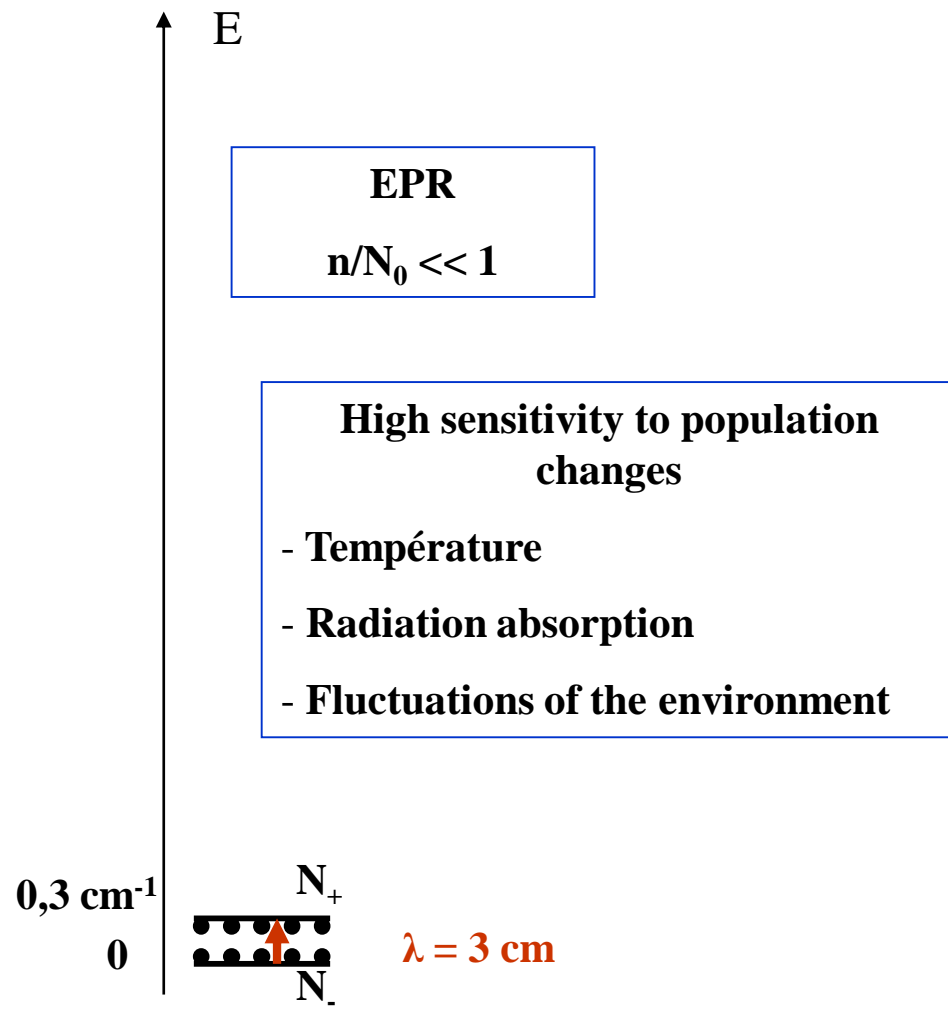
Basic principles : the sensitivity of EPR

$n = N_{\text{inf}} - N_{\text{sup}}$ population difference

Signal $\propto n$



UV-vis
Spectroscopy
 $n/N_0 = 1$



EPR

$n/N_0 \ll 1$

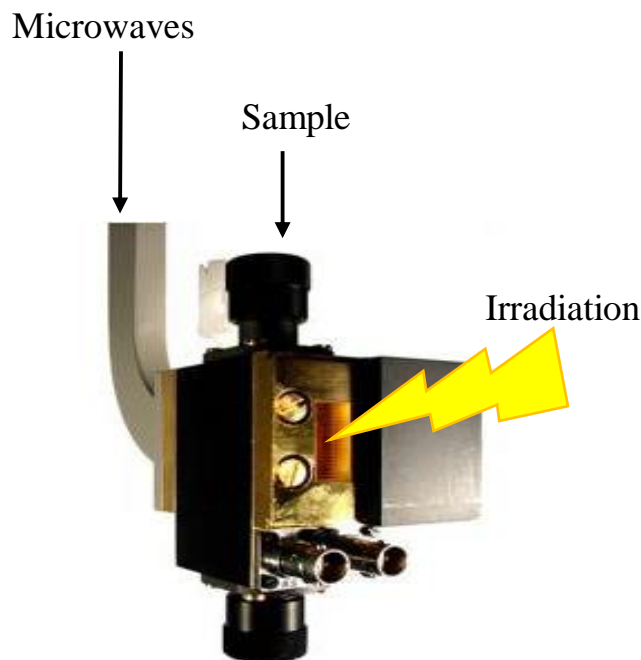
High sensitivity to population changes

- Température
- Radiation absorption
- Fluctuations of the environment

Basic principles: improving EPR sensitivity

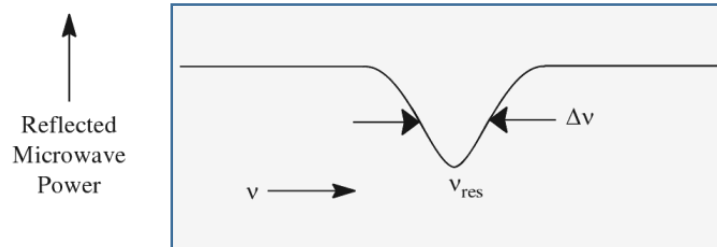
EPR signal intensity: $I \propto N_0 g \beta B / 2k_B T$

- Sample concentration (N_0)
- Low temperatures (cryogeny: liquid N_2 , He)
- High magnetic field / high frequency: Q-band 35GHz, W-band 95 GHz, 300 GHz
- Resonant cavity: Quality factor $Q \sim 5-6000$



Rectangular cavity TE102

$$Q = 2\pi \text{ \acute{e}nergie stock\acute{e}e / \acute{e}nergie dissip\acute{e}e} = \nu_{\text{res}} / \Delta\nu$$



Sensitivity \propto Q factor

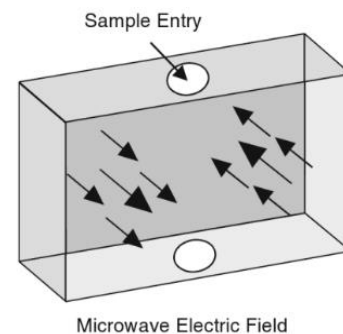
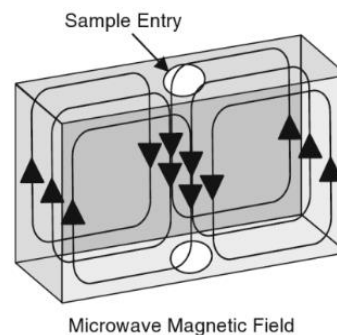
Basic principles: improving EPR sensitivity

EPR does not like polar solvent: H₂O, CH₃OH, ...

Dielectric absorption (ϵ_r)



decrease of Q-factor



NMR tube: \varnothing_{ext} 5mm

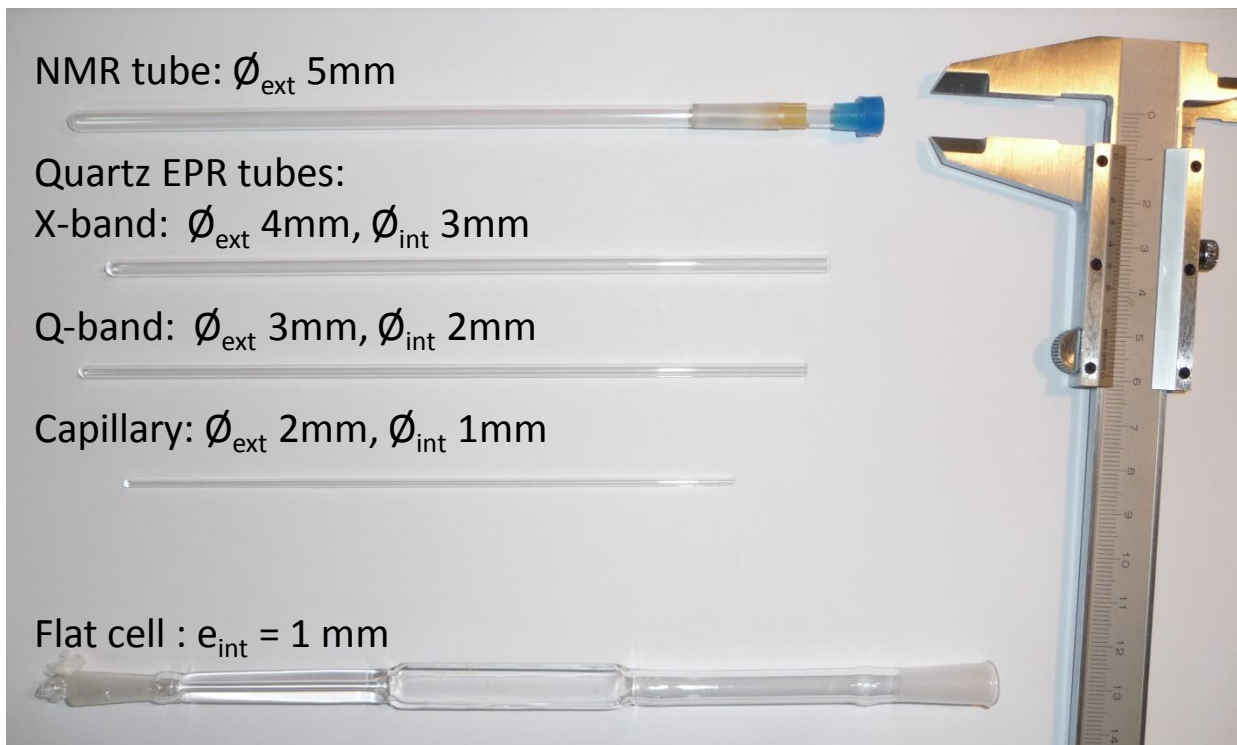
Quartz EPR tubes:

X-band: \varnothing_{ext} 4mm, \varnothing_{int} 3mm

Q-band: \varnothing_{ext} 3mm, \varnothing_{int} 2mm

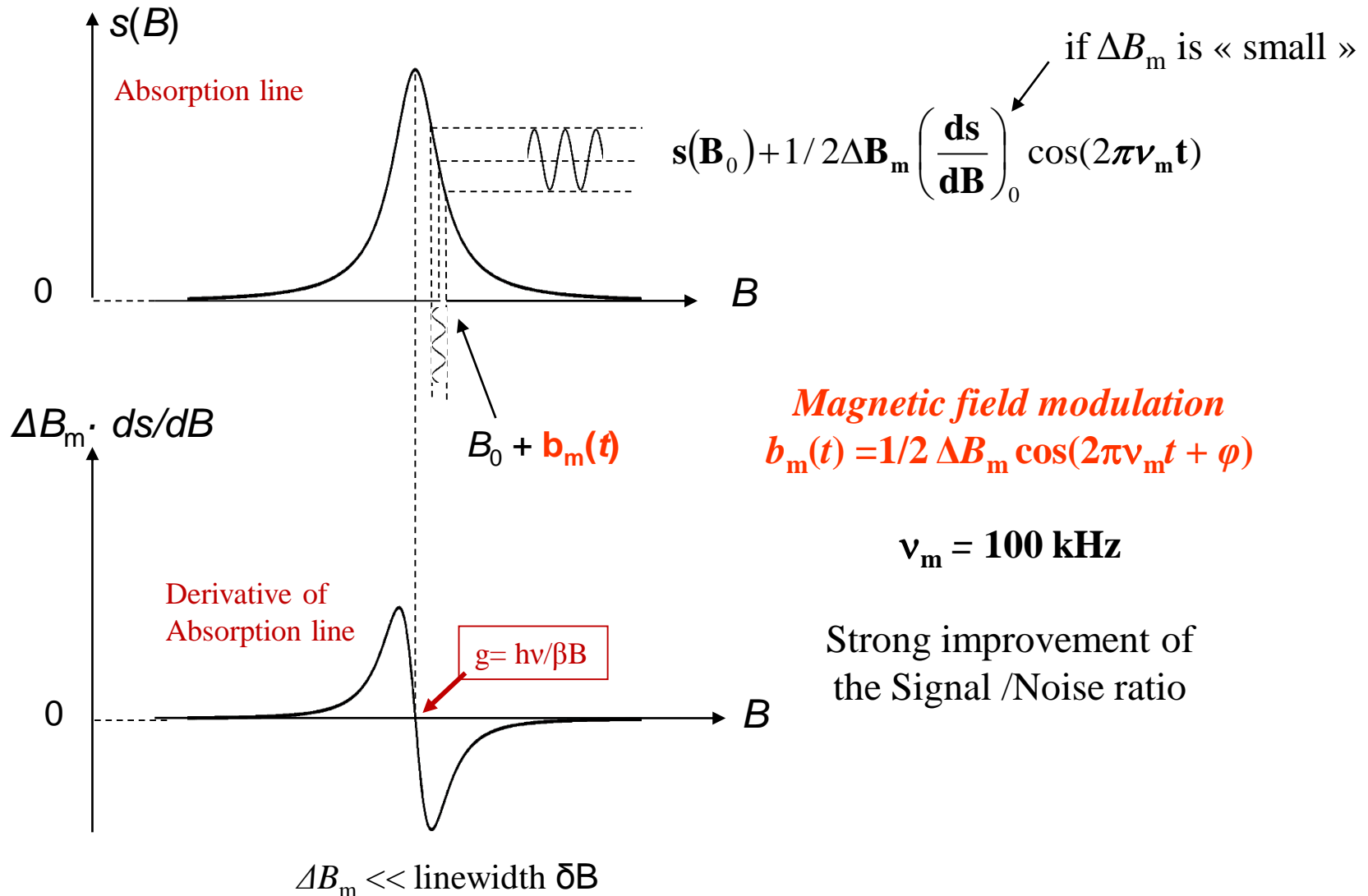
Capillary: \varnothing_{ext} 2mm, \varnothing_{int} 1mm

Flat cell : e_{int} = 1 mm

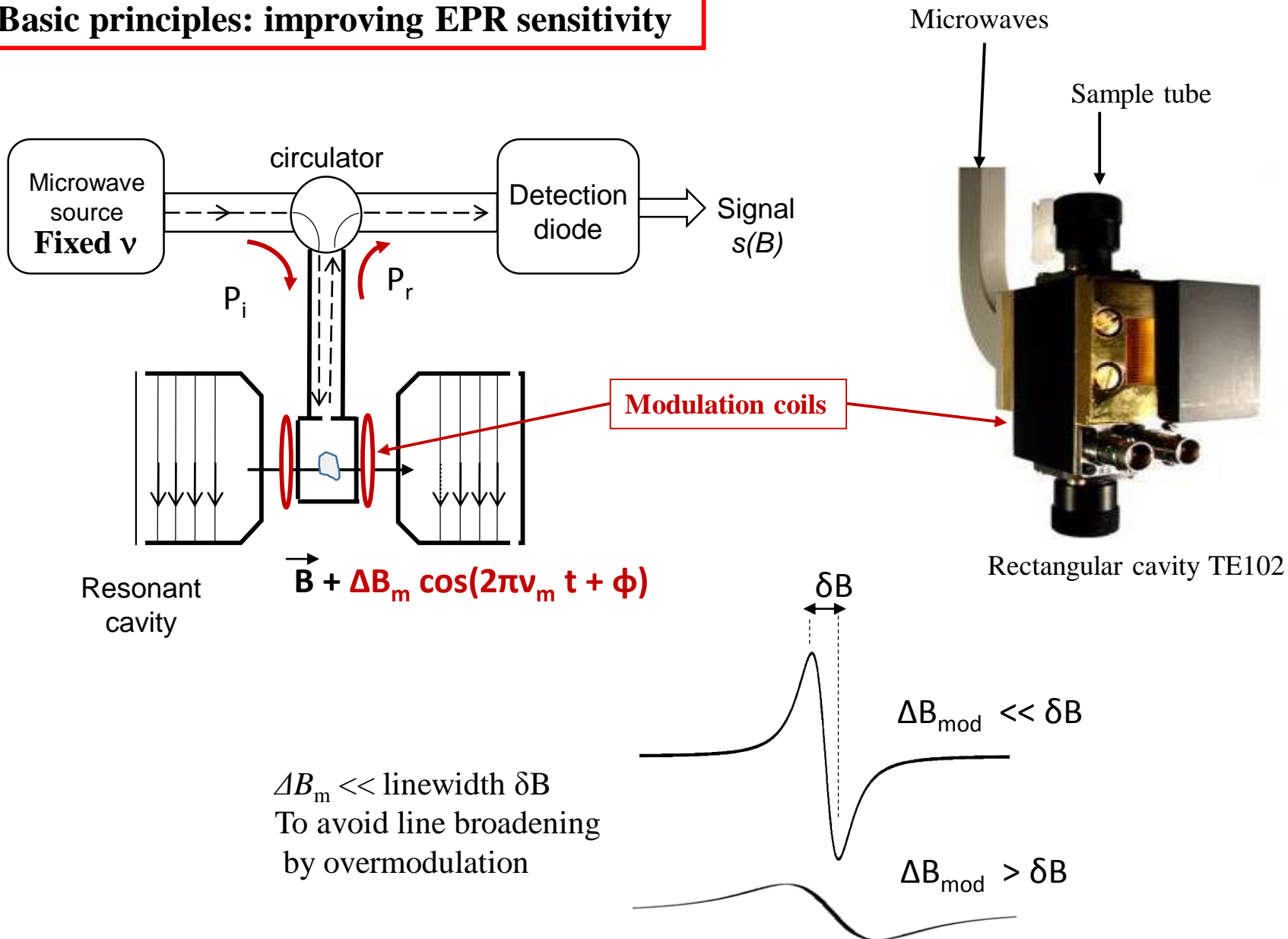


Basic principles: improving EPR sensitivity

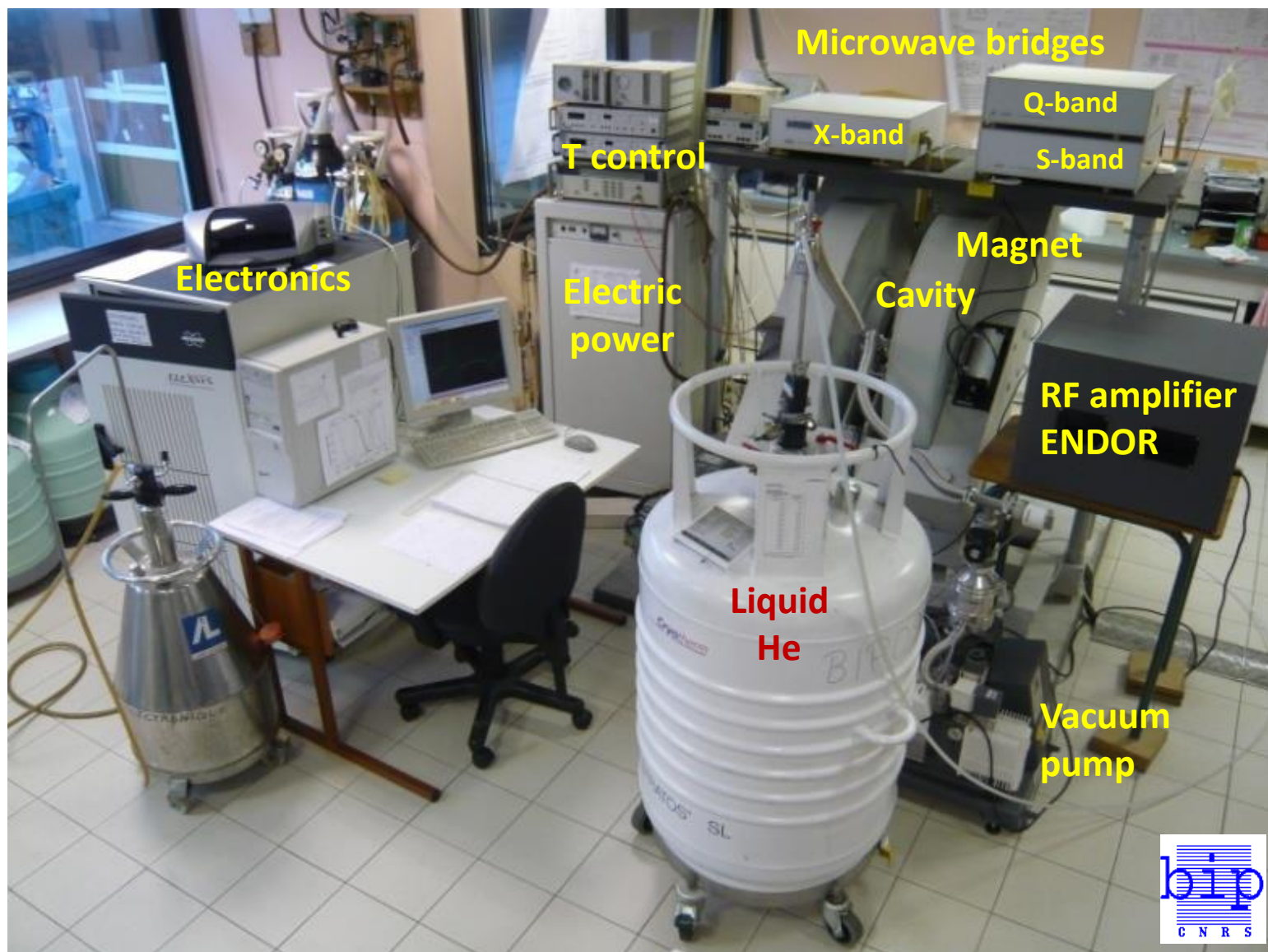
Decrease the noise: Magnetic field amplitude modulation



Basic principles: improving EPR sensitivity

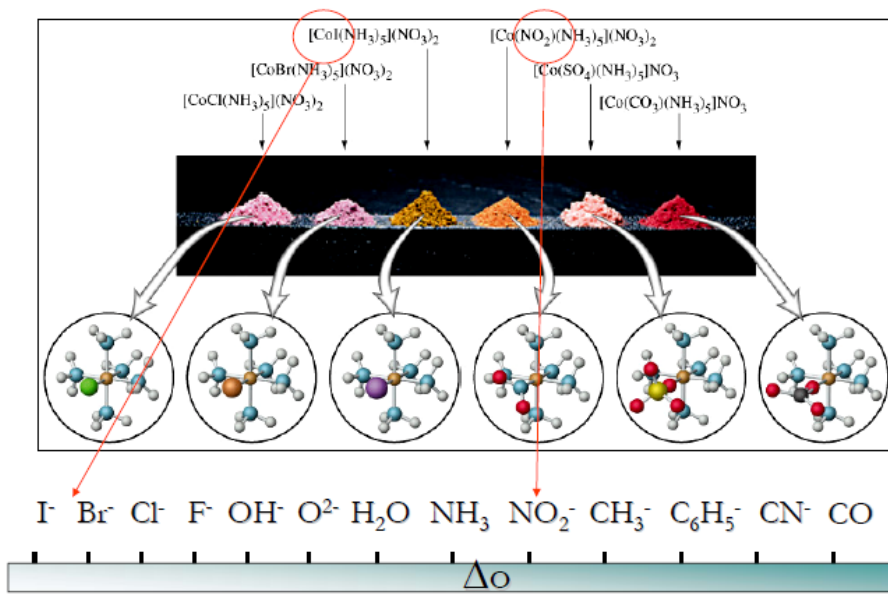
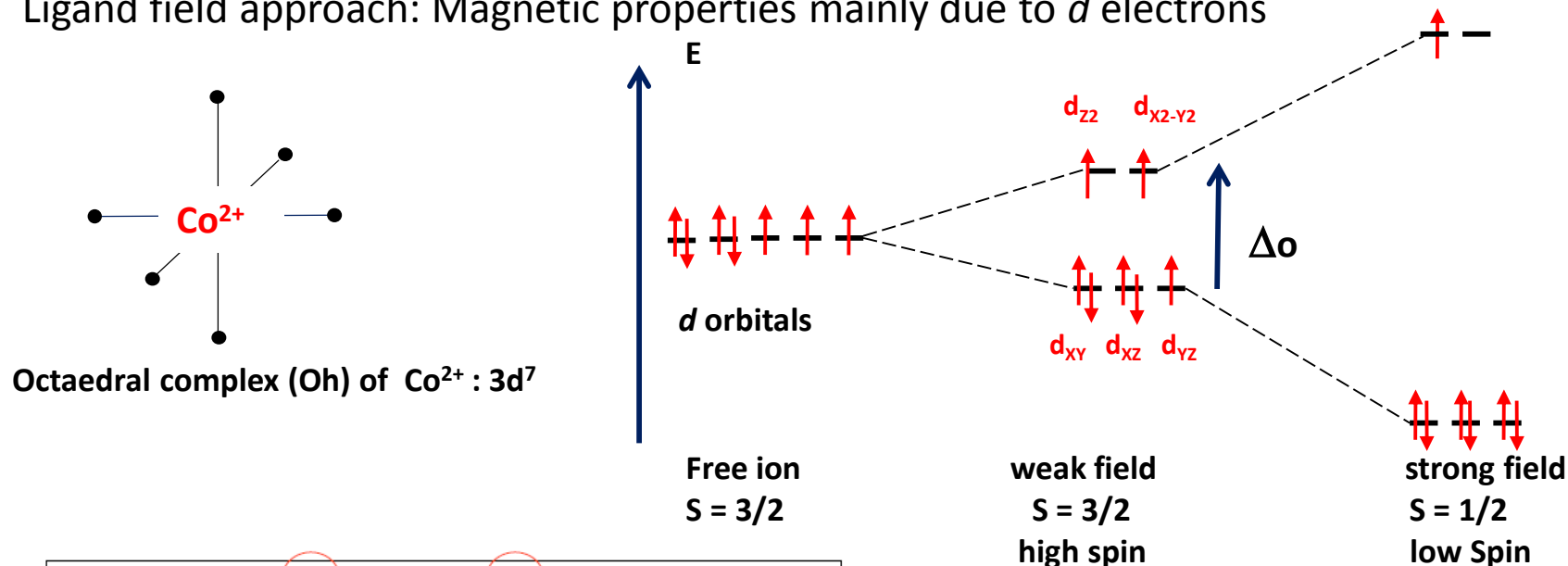


Multifrequency CW-EPR equipment



Transition metal compounds: Magnetic properties

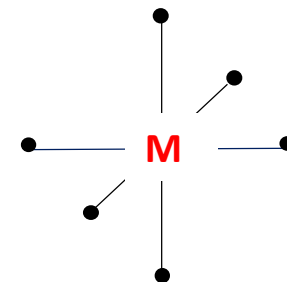
Ligand field approach: Magnetic properties mainly due to d electrons



Transition metal compounds: Magnetic properties

Hamiltonian $H = T_e + V_{en} + V_{ee} + V_L + H_{SO} + \text{magnetic terms}$

Requires the orbital part of the wavefunction to be calculated



Phenomenological approach: The spin hamiltonian H_S

$$H = \lambda \vec{L} \cdot \vec{S} + \beta (\vec{L} + g_e \vec{S}) \cdot \vec{B} + \text{couplages} (\mu_e, \mu_n) \dots$$

Zero field splitting
(fine structure term)

Anisotropy

Zeeman
Effect

Hyperfine couplings e-nuclei

$$H_S = \vec{S} \tilde{D} \vec{S} + \beta \vec{S} \tilde{g} \vec{B} + \vec{S} \tilde{A} \vec{I}$$

Terms : Fine structure Zeeman Hyperfine

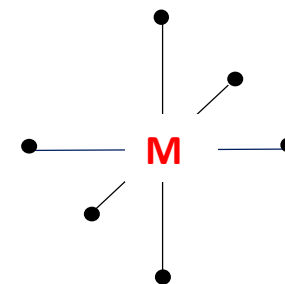
$$\tilde{D}, \tilde{g}, \tilde{A}$$

Rank 2 tensors \Rightarrow 3 x 3 matrix

$$\tilde{g} = \begin{bmatrix} g_{xx} & g_{xy} & g_{xz} \\ g_{yx} & g_{yy} & g_{yz} \\ g_{zx} & g_{zy} & g_{zz} \end{bmatrix}$$

Transition metal compounds: Magnetic properties

$$H_S = \vec{S} \tilde{D} \vec{S} + \beta \vec{S} \tilde{g} \vec{B} + \vec{S} \tilde{A} \vec{I}$$



Zeeman term: Zeeman effect + 2nd order effect of spin-orbit coupling

$$H_{Zeeman} = \beta \vec{S} \tilde{g} \vec{B}$$

$$H_{Zeeman} = \beta (S_X g_X B_X + S_Y g_Y B_Y + S_Z g_Z B_Z)$$

- Departure of g values from $g_e = 2.0023$
- Anisotropy

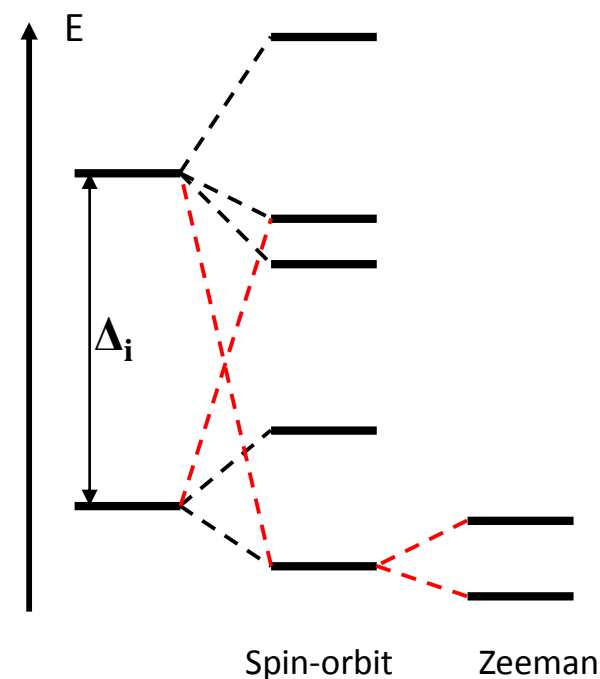
$$g_i = g_e - \alpha_i \cdot \frac{\lambda}{\Delta_i} \quad (i = x, y, z)$$

λ = spin-orbit coupling constant

dⁿ configuration

$$n < 5, \lambda > 0 \Rightarrow g_i < g_e = 2.00$$

$$n > 5, \lambda < 0 \Rightarrow g_i > g_e = 2.00$$



Transition metal centers: Magnetic properties

Anisotropic \tilde{g} tensor

(X, Y, Z) principal axes of g :
(g_X , g_Y , g_Z) principal g -values

*Magnetic axes are related to symmetry axes
and atomic positions*

$$H_{Zeeman} = \beta \vec{S} \tilde{g} \vec{B}$$

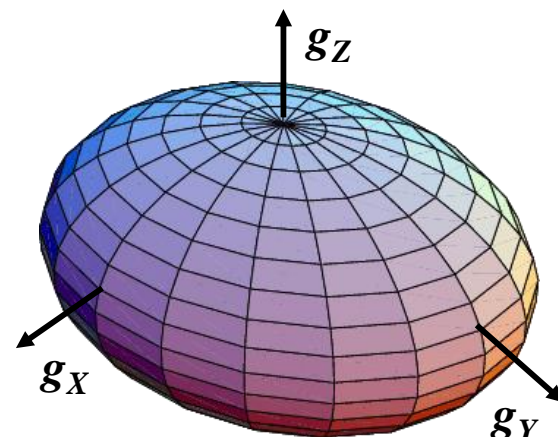
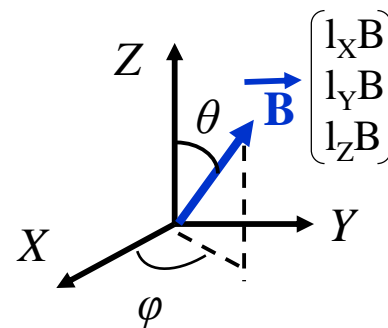
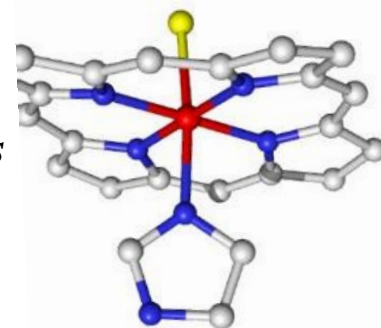
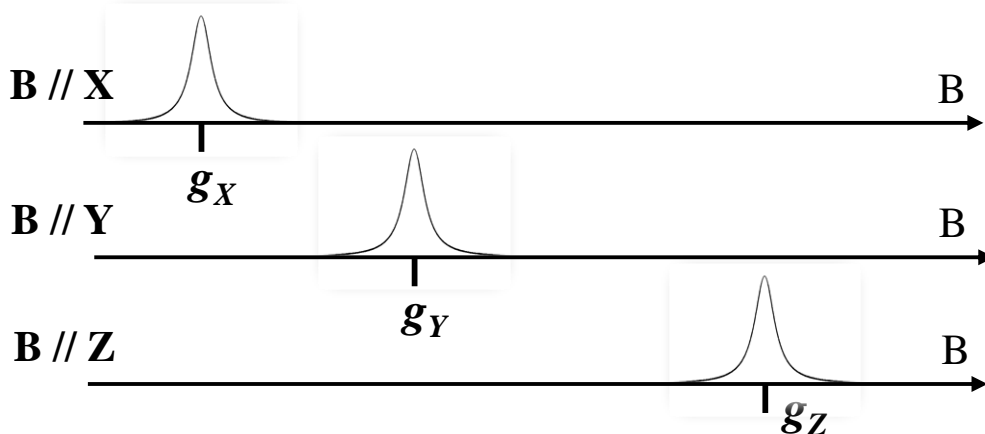
$$H_{Zeeman} = \beta (S_X g_X B_X + S_Y g_Y B_Y + S_Z g_Z B_Z)$$

$$H_{Zeeman} = \beta g' \vec{S} \cdot \vec{B}'$$

→ The line position g' depends on the B orientation

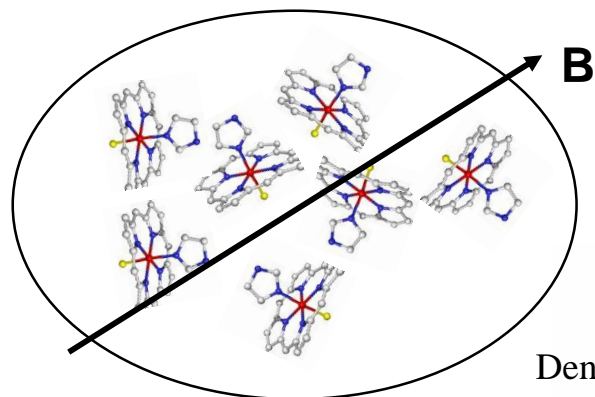
$$g'^2 = l_X^2 g_X^2 + l_Y^2 g_Y^2 + l_Z^2 g_Z^2$$

$$g'^2 = \cos^2 \varphi \cdot \sin^2 \theta g_X^2 + \sin^2 \varphi \cdot \sin^2 \theta g_Y^2 + \cos^2 \theta g_Z^2$$

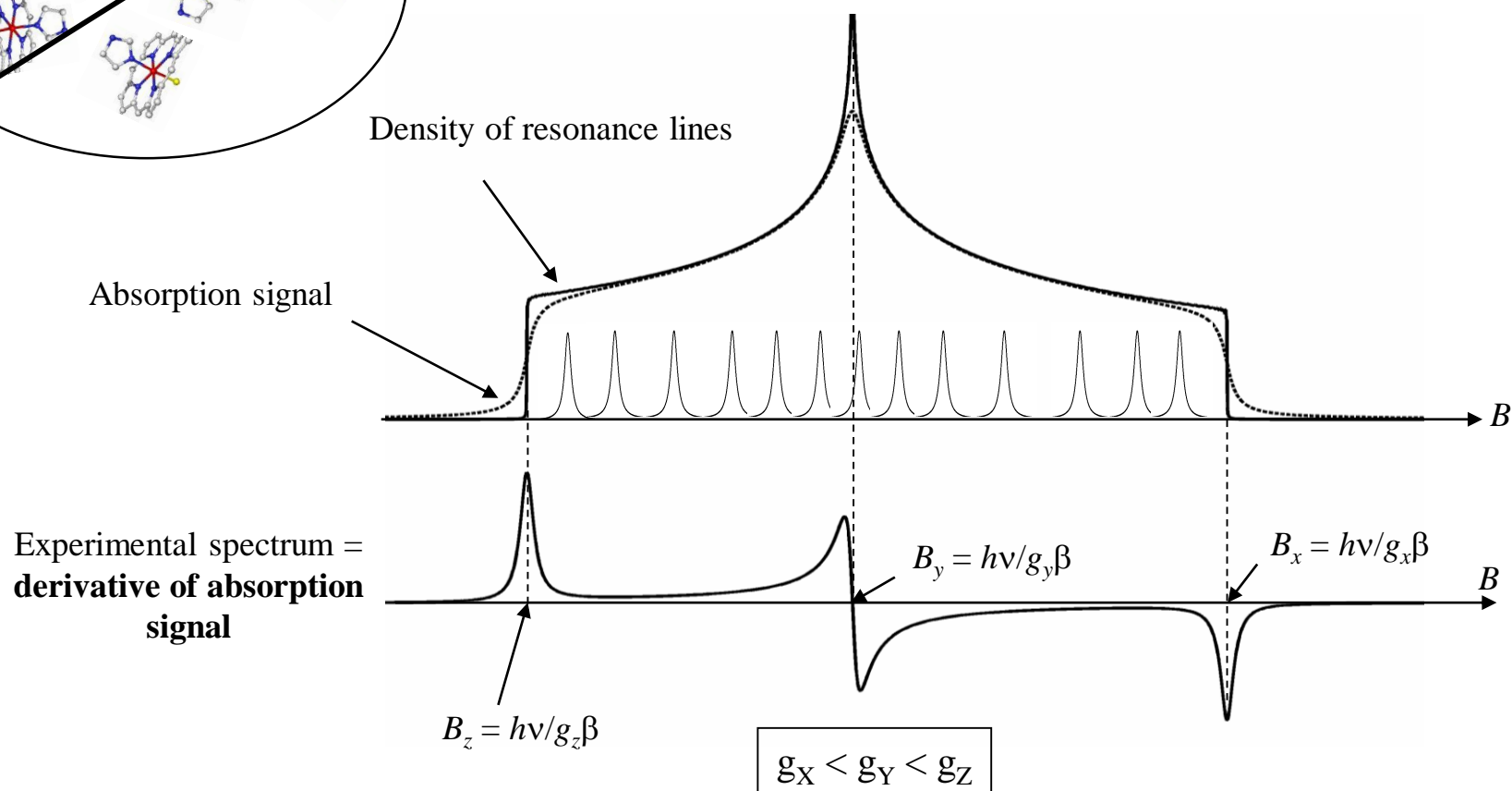


Transition metal compounds: Magnetic properties

Anisotropic g tensor– Powder or frozen solution spectrum

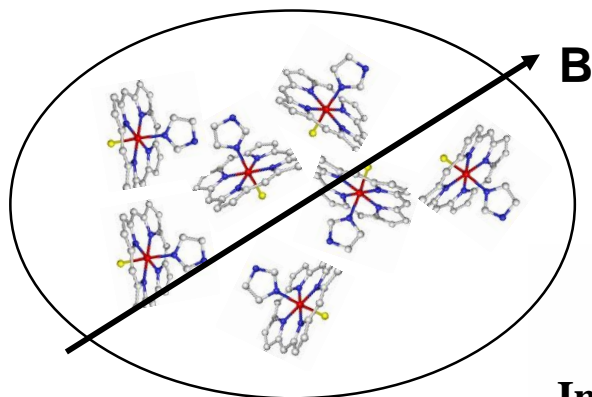


Disordered system: all the B orientations are present



Transition metal compounds: Magnetic properties

Anisotropic g tensor– Powder or frozen solution spectrum



Disordered system: all the B orientations are present

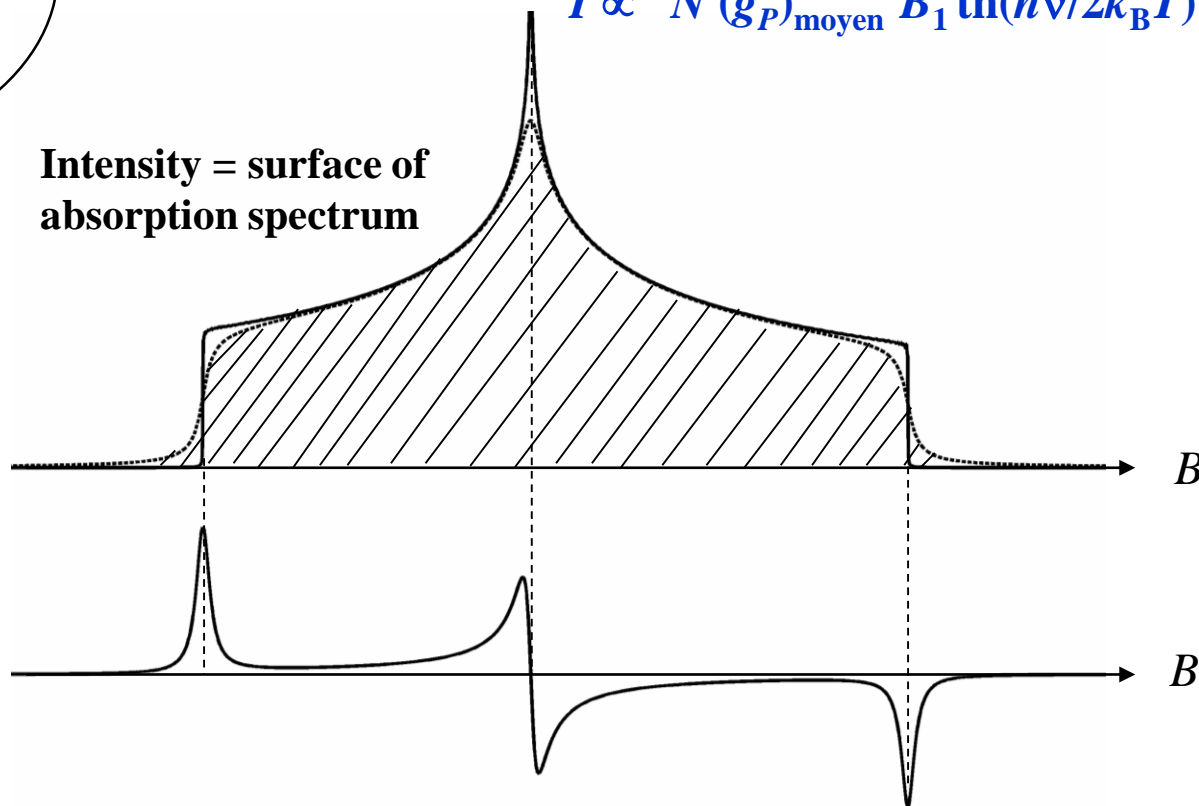
EPR signal intensity:

$$I \propto N (g_P)_{\text{moyen}} B_1 \text{th}(h\nu/2k_B T)$$

**Intensity = surface of
absorption spectrum**

*double
numerical
integration*

**Experimental spectrum
(absorption derivative)**



Spin quantitation by comparison to a reference sample: $I/I_0 = N/N_0$

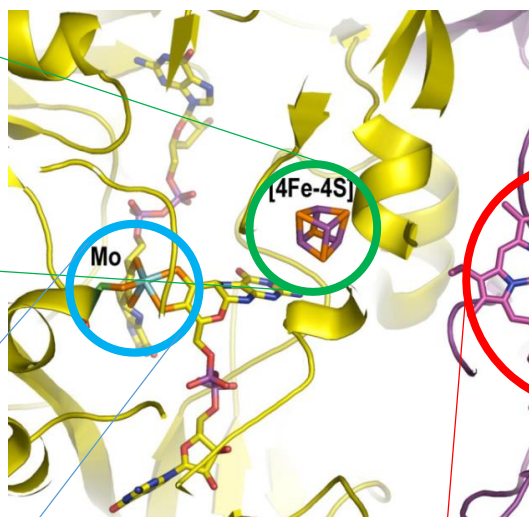
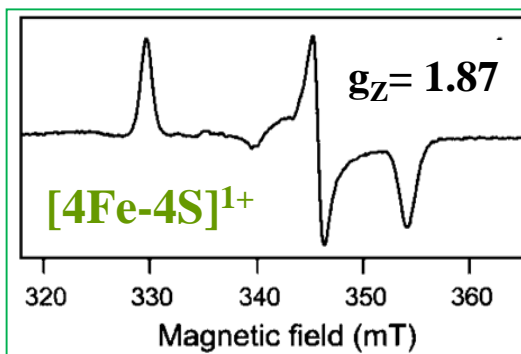
Transition metal compounds: Magnetic properties

g-tensor analysis

- Identification of magnetic centers
- Selective view of magnetic centers and of their environment (nuclei)
- No limit in size or physical state: solution, powder, crystals, membranes, cells...

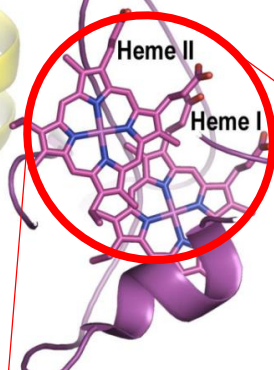
$g_X = 2.04$ $g_Y = 1.94$

15 K



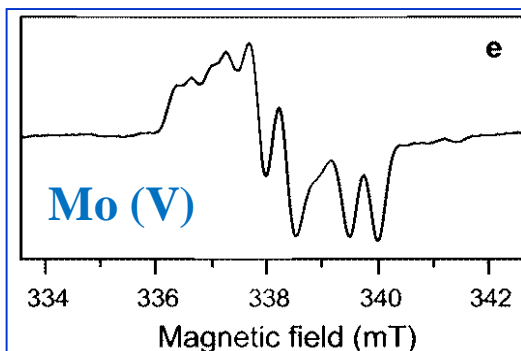
R. Sphaeroides periplasmic
Nitrate reductase - NapAB

Arnoux et al., Nat. Struct. Biol. 2003

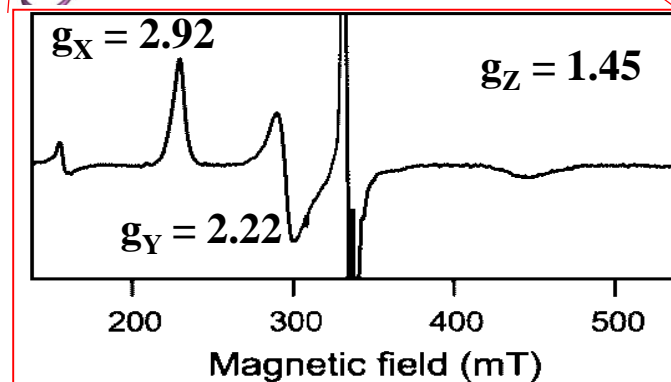


Hemes (Fe^{3+})

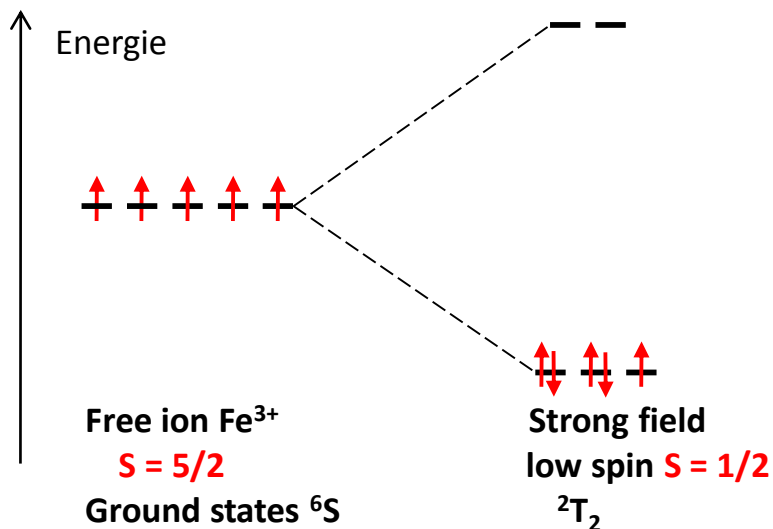
55 K



15 K



Low spin Fe^{3+} systems: hemes

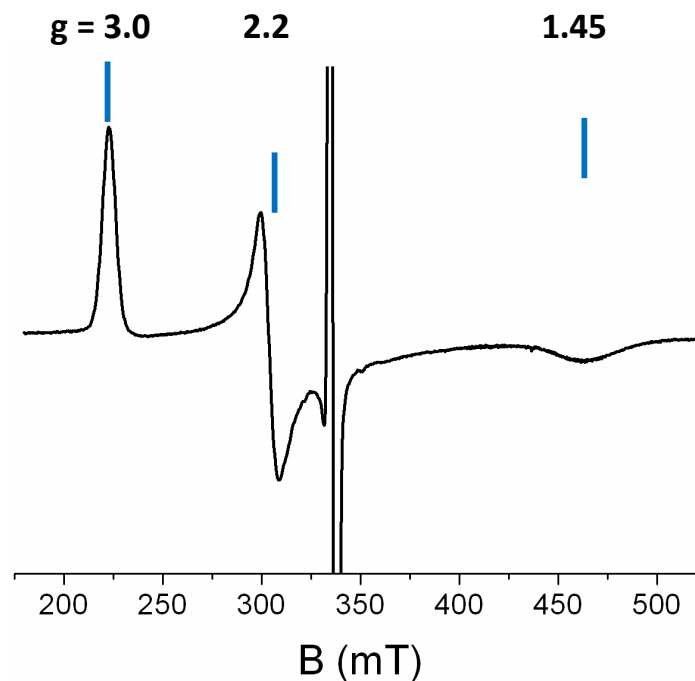
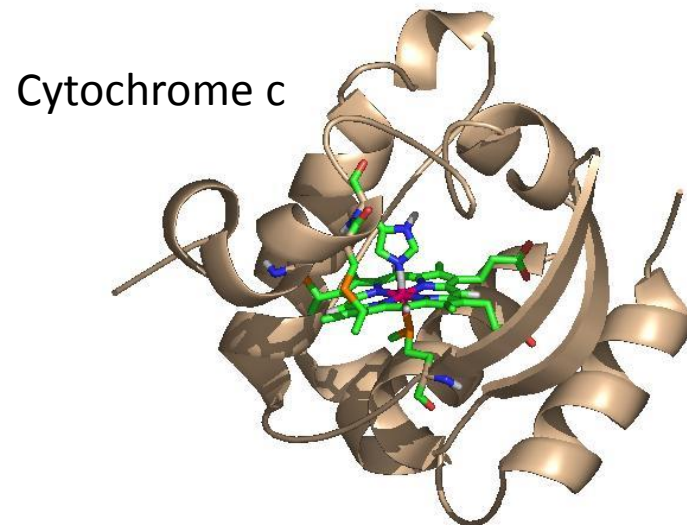


Ground state ${}^2T_{2g}$

Orbital triplet state, $S = 1/2$

No fine structure term, but strong influence of Spin-Orbit coupling on g-tensor anisotropy.

$$H_s = \beta \vec{S} \tilde{g} \vec{B}$$



Low spin Fe^{3+} systems: hemes

Magneto-structural correlations:

t_{2g} hole model (Griffith, 1971)

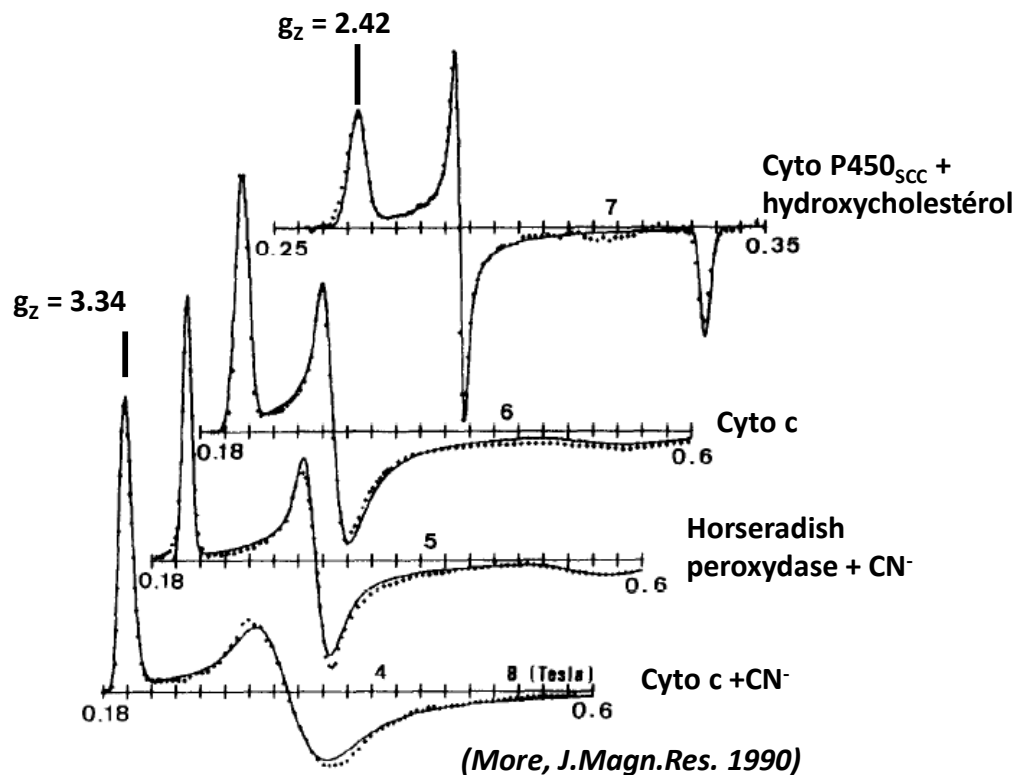
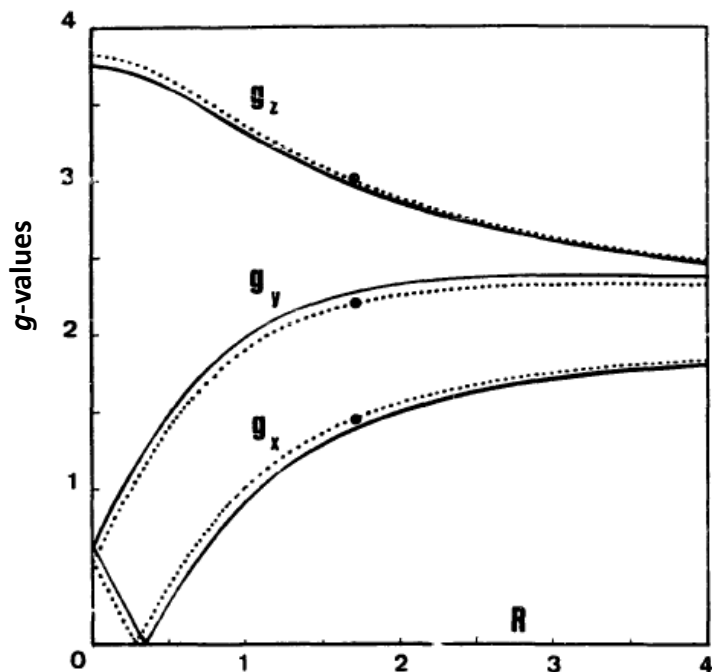
Fe^{3+} ion in strong distorted octaedral ligand field

$$\mathcal{H}(\mu, R, \lambda) = -\lambda \mathbf{L} \cdot \mathbf{S} + \frac{\mu}{9} (3L_z^2 - L(L+1)) + \frac{R}{12} (L_+^2 + L_-^2)$$

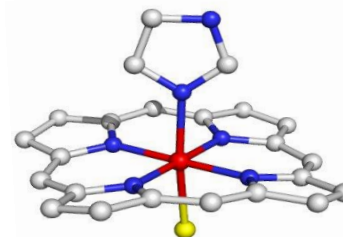
μ and R , axial and rhombic components of the ligand field

$$g_i = f(\lambda, \mu, R) : g_x^2 + g_y^2 + g_z^2 = 16$$

Also accounts for g-strain broadening



Cytochromes

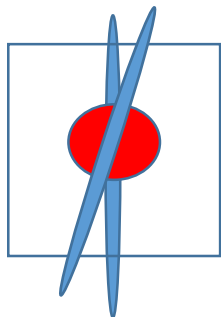


Low spin Fe^{3+} systems: hemes

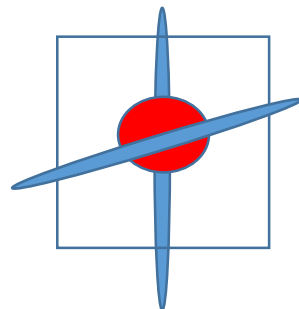
Magneto-structural correlations: Hemes with bis-Histidine axial coordination

The rhombicity depends on the ϕ angle between imidazole planes

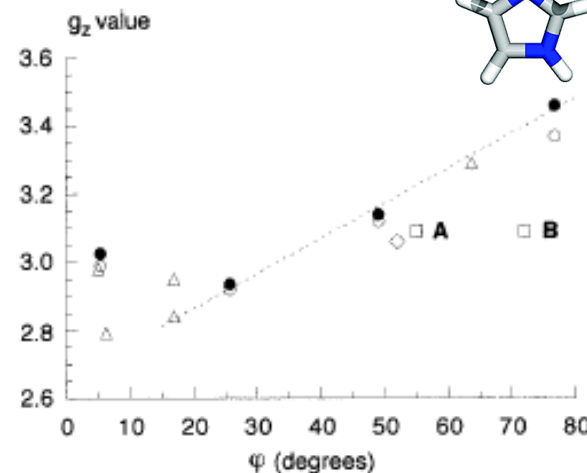
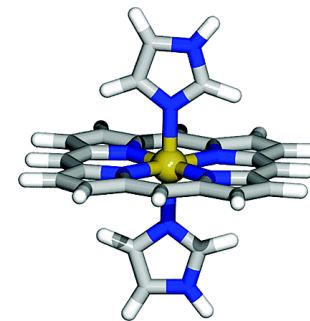
g_z increases when ϕ increases



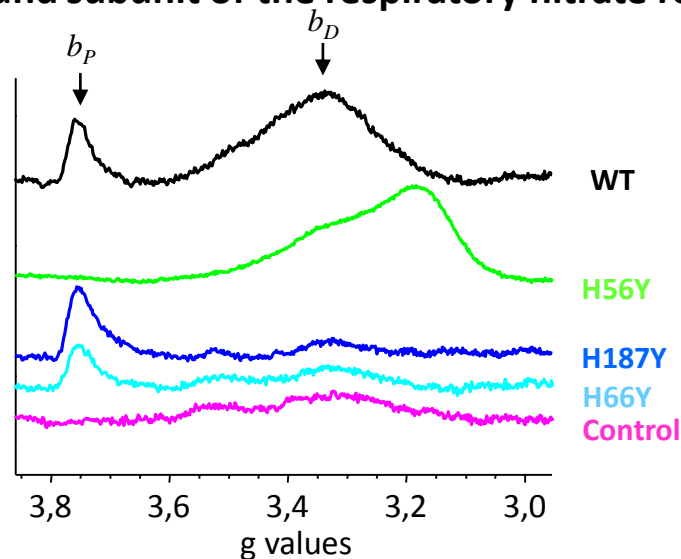
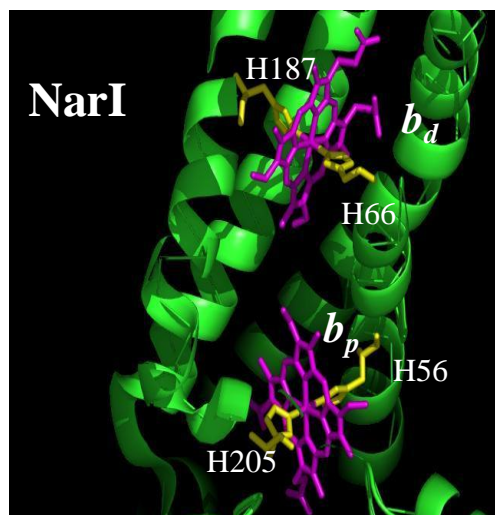
$\phi \approx 10-20^\circ$
 $g_z = 3.0$



$\phi \approx 80-90^\circ$
 $g_z = 3.8$
HALS hemes



b-type hemes of the membrane-bound subunit of the respiratory nitrate reductase NarGHI



EPR of *E. coli*
membrane fractions

Low spin Fe^{3+} systems: hemes

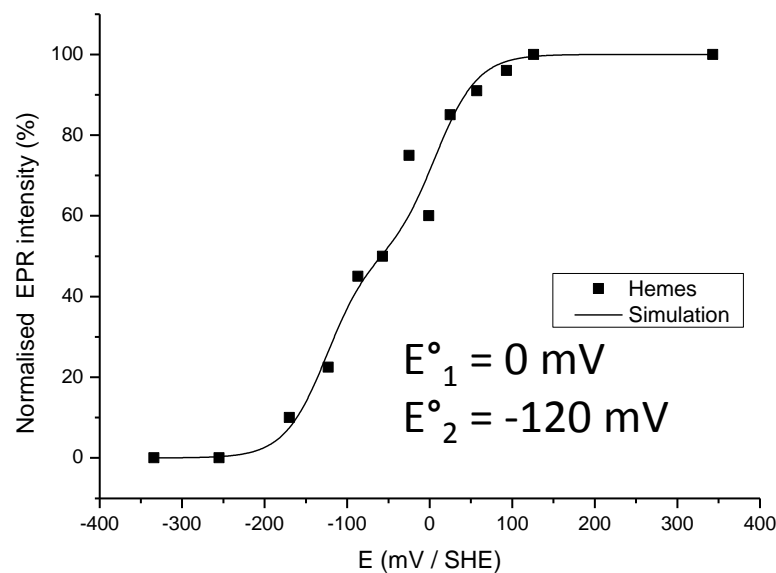
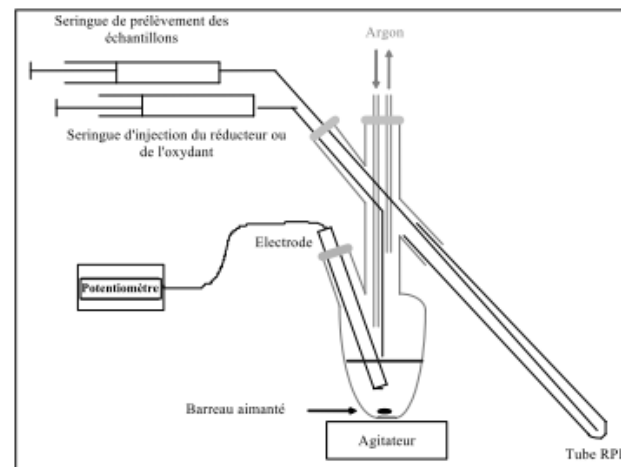
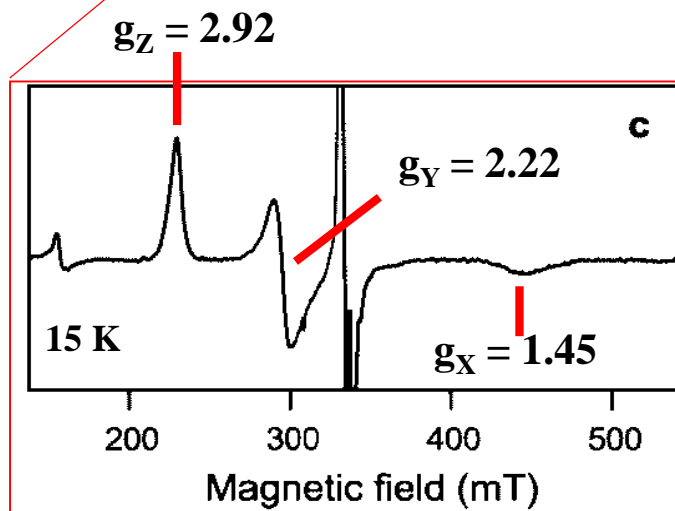
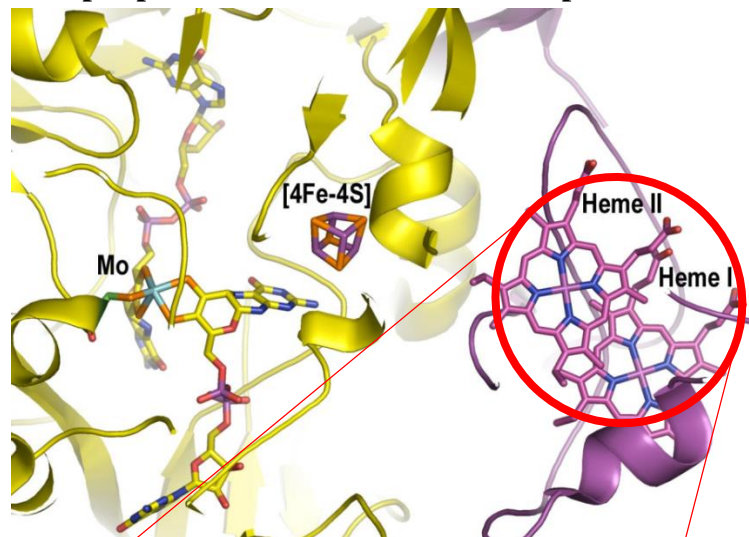
Redox titrations: E° measurements



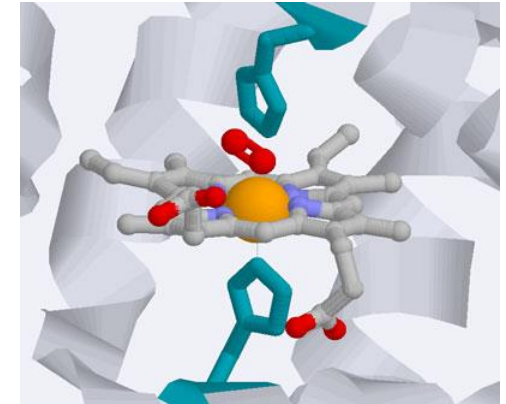
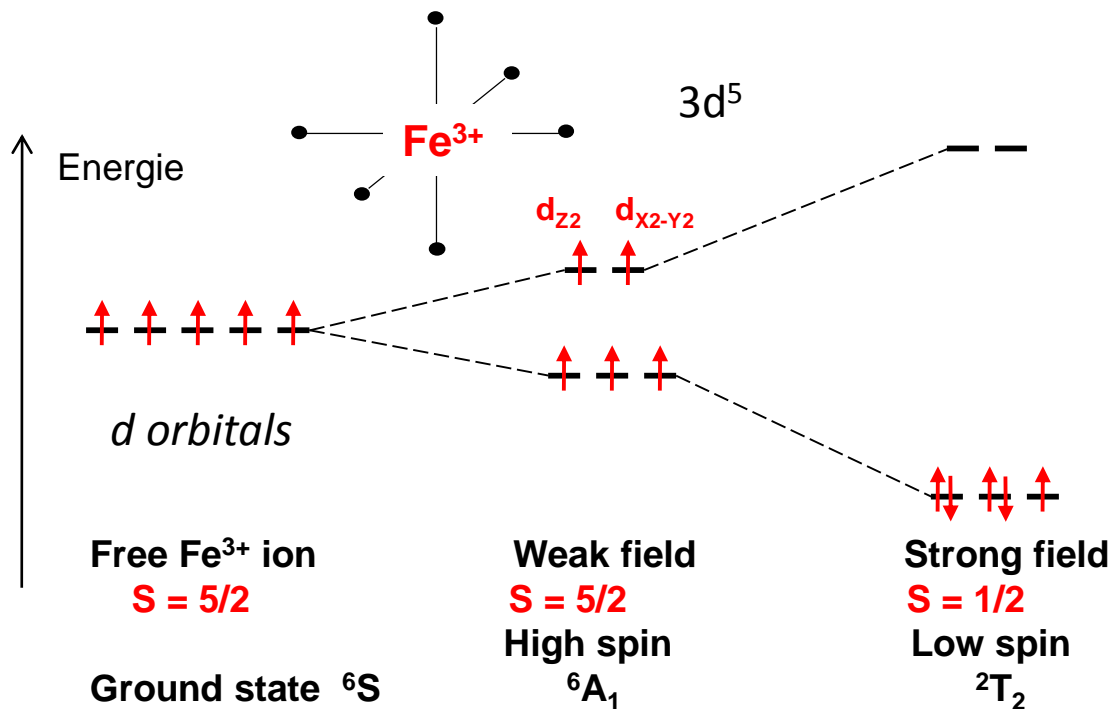
$S=1/2$

$S=0$

R. Sphaeroides periplasmic Nitrate reductase - NapAB



High spin Fe^{3+} systems



Myoglobin
 $g_{\perp} = 6.0$, $g_{\parallel} = 2.0$

Cytochrome b_2
 $g = 2.92, 2.27, 1.5$

High spin Fe^{3+} systems

$$S = 5/2, M_S = -5/2, -3/2, -1/2, +1/2, +3/2, +5/2$$

6 states $\{|S, M_S\rangle\}$

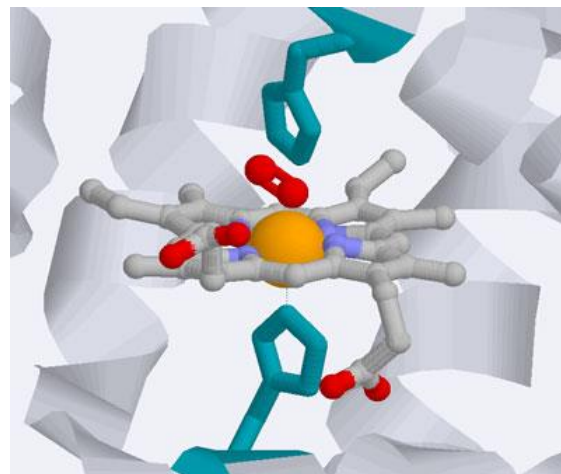
Axial symmetry– Influence of fine structure (Zero field splitting)

D axial, g isotropic

$$H_S = \vec{S} \tilde{D} \vec{S} + \beta \vec{S} \tilde{g} \vec{B}$$

$$H_{SF} = D \left(S_Z^2 - \frac{1}{3} S(S+1) \right) + g \beta \vec{S} \cdot \vec{B}$$

Heme in Myoglobin



Case $D \gg g \beta B$ (0.3 cm^{-1} at 0.3 T)

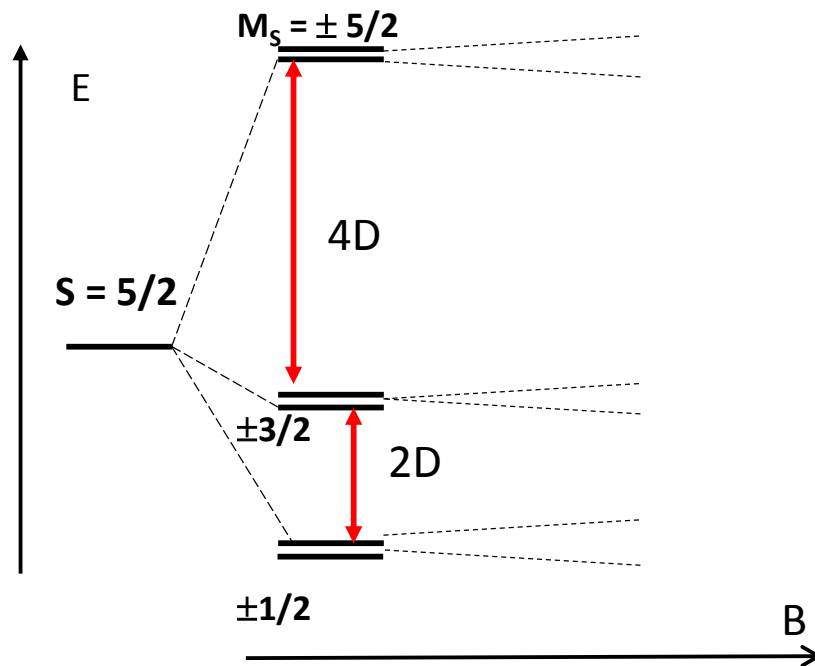
- $B = 0$: Zero field splitting

$$S_Z |S, M_S\rangle = M_S |S, M_S\rangle \quad \Delta M_S = 0$$

$$S_Z^2 |S, M_S\rangle = M_S^2 |S, M_S\rangle$$

$$E(M_S) = D \left(M_S^2 - \frac{1}{3} S(S+1) \right)$$

$$E(M_S) = D \left(M_S^2 - \frac{35}{12} \right)$$



High spin Fe³⁺ systems

– Axial symmetry – Influence of fine structure

Case $D \gg g \beta B$ (0.3 cm⁻¹ at X-band)

- $B \neq 0$:

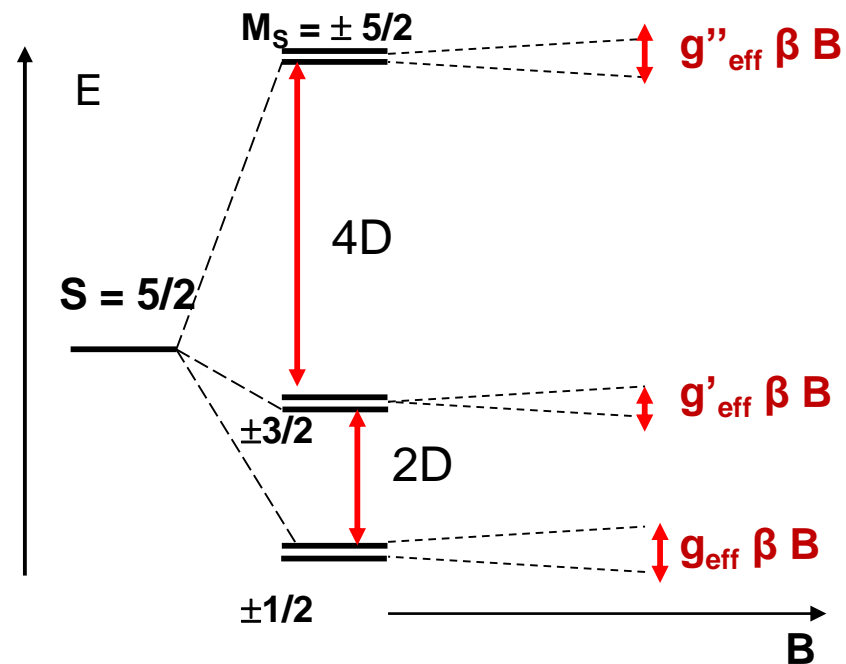
$$H_{Zeeman} = g \beta (S_x B_x + S_y B_y + S_z B_z)$$

$$= g \beta B (S_z \cos \theta + 1/2 (S_+ + S_-) \sin \theta)$$

$$\Delta M_S = 0$$

$$\Delta M_S = \pm 1$$

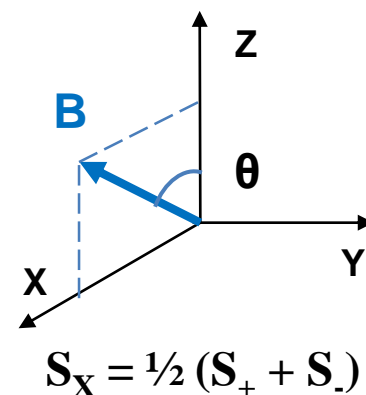
Perturbation approach:



$|M_S\rangle$ $|-5/2\rangle$ $|+5/2\rangle$ $|-3/2\rangle$ $|+3/2\rangle$ $|-1/2\rangle$ $|+1/2\rangle$

$$H_{Zeeman} = \frac{1}{2} g \beta B$$

$-5 \cos \theta$	0	X	0	0	0	$ -5/2\rangle$
0	$+5 \cos \theta$	0	X	0	0	$ +5/2\rangle$
X	0	$-3 \cos \theta$	0	X	0	$ -3/2\rangle$
0	X	0	$+3 \cos \theta$	0	X	$ +3/2\rangle$
0	0	X	0	$-\cos \theta$	$3 \sin \theta$	$ -1/2\rangle$
0	0	0	X	$3 \sin \theta$	$+\cos \theta$	$ +1/2\rangle$



$$S_+ |S, M_S\rangle = [(S(S+1) - M_S (M_S + 1))]^{1/2} |S, M_S + 1\rangle$$

$$S_- |S, M_S\rangle = [(S(S+1) - M_S (M_S - 1))]^{1/2} |S, M_S - 1\rangle$$

High spin Fe^{3+} systems

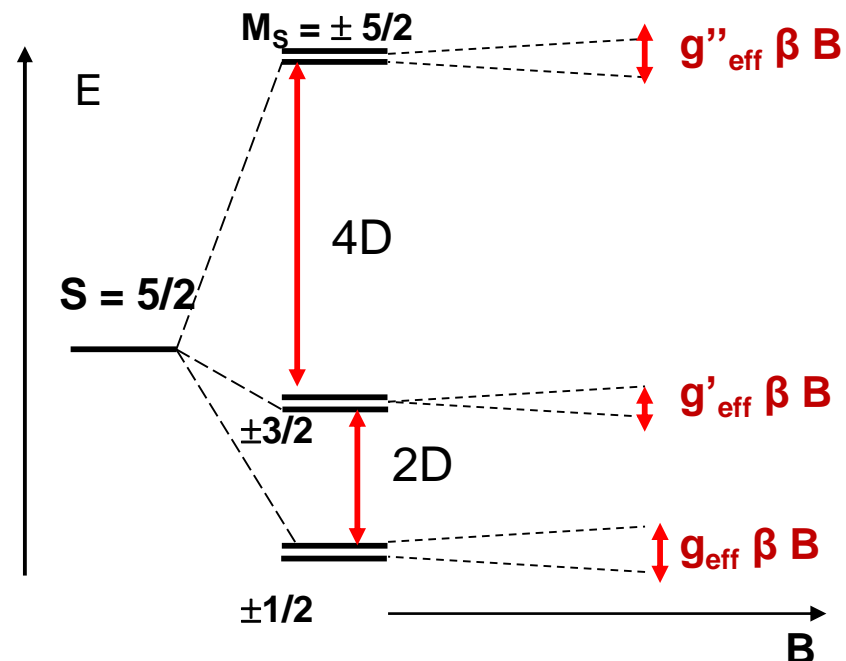
Axial symmetry - $D \gg g \beta B$

$M_S = \pm 5/2$ g''_{eff} axial : $g''_{\text{eff} //} = 5g = 10$, $g''_{\text{eff} \perp} = 0$

$M_S = \pm 3/2$ g'_{eff} axial : $g'_{\text{eff} //} = 3g = 6$, $g'_{\text{eff} \perp} = 0$

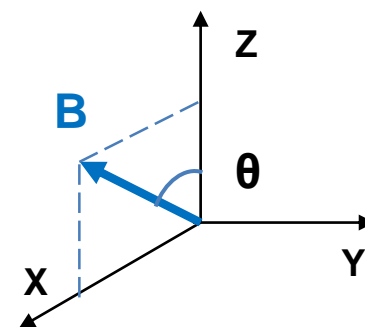
$M_S = \pm 1/2$ g_{eff} axial : $g_{\text{eff} //} = g = 2$, $g_{\text{eff} \perp} = 3g = 6$

1st order perturbation calculation



$H_{\text{Zeeman}} = \frac{1}{2} g \beta B$

$ M_S\rangle$	$ -5/2\rangle$	$ +5/2\rangle$	$ -3/2\rangle$	$ +3/2\rangle$	$ -1/2\rangle$	$ +1/2\rangle$
	$-5 \cos\theta$	0	X	0	0	0
	0	$+5 \cos\theta$	0	X	0	0
	X	0	$-3 \cos\theta$	0	X	0
	0	X	0	$+3 \cos\theta$	0	X
	0	0	X	0	$-\cos\theta$	$3 \sin\theta$
	0	0	0	X	$3 \sin\theta$	$+\cos\theta$



High spin Fe^{3+} systems

Axial symmetry- $D \gg g \beta B$

$M_S = \pm 5/2$ g''_{eff} axial : $g''_{\text{eff} //} = 5g = 10$, $g''_{\text{eff} \perp} = 0$

$M_S = \pm 3/2$ g'_{eff} axial : $g'_{\text{eff} //} = 3g = 6$, $g'_{\text{eff} \perp} = 0$

$M_S = \pm 1/2$ g_{eff} axial : $g_{\text{eff} //} = g = 2$, $g_{\text{eff} \perp} = 3g = 6$

Allowed EPR transitions: $\Delta M_S = \pm 1$

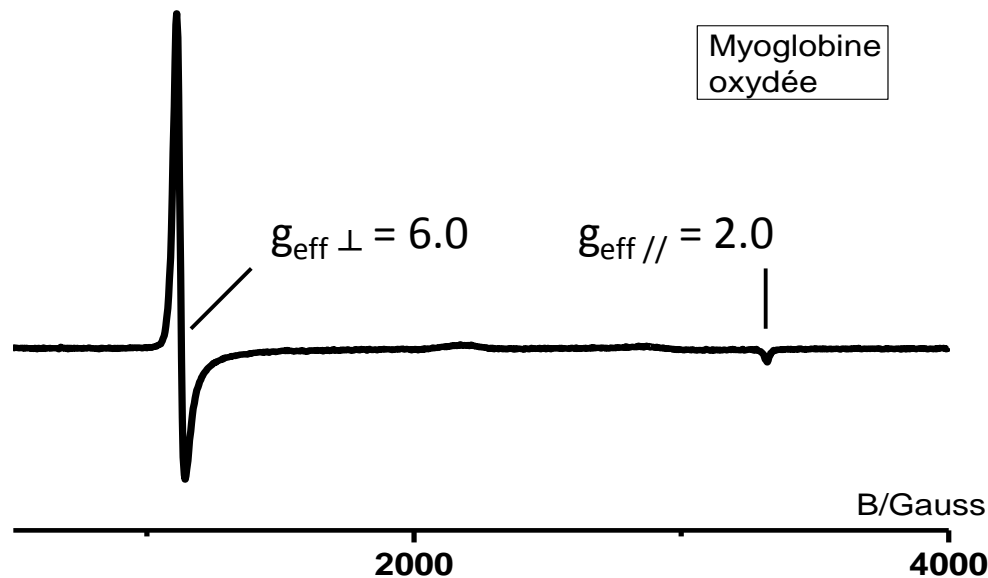
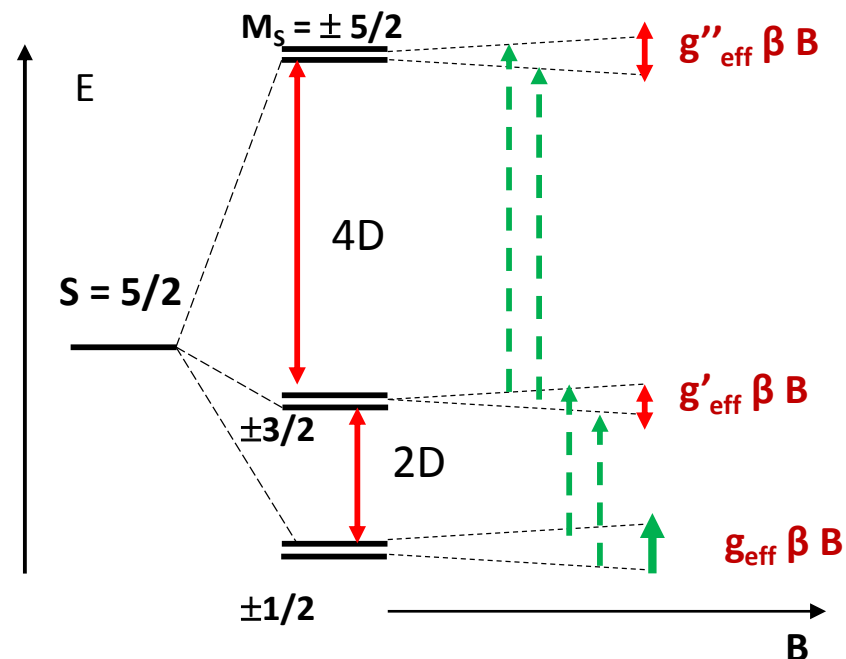
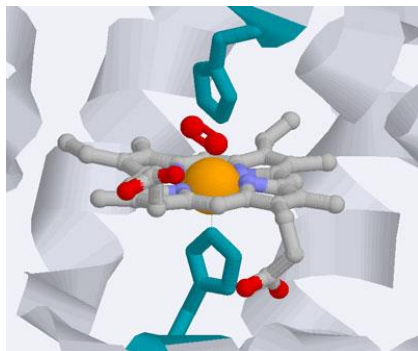
5 allowed transitions

Only one is energetically accessible :

$$h\nu \approx g\beta B \ll D$$

Forbidden transitions

$$\Delta M_S = \pm 3 ; \Delta M_S = \pm 5$$



High spin Fe^{3+} systems

Axial Symmetry - $D \gg g \beta B$

Measurement of D : Temperature study

$M_S = \pm 1/2$ EPR spectrum intensity

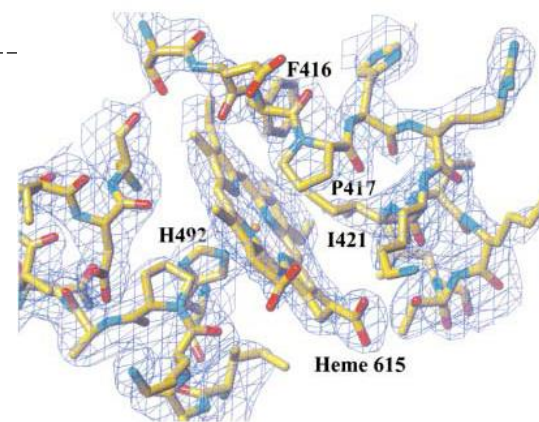
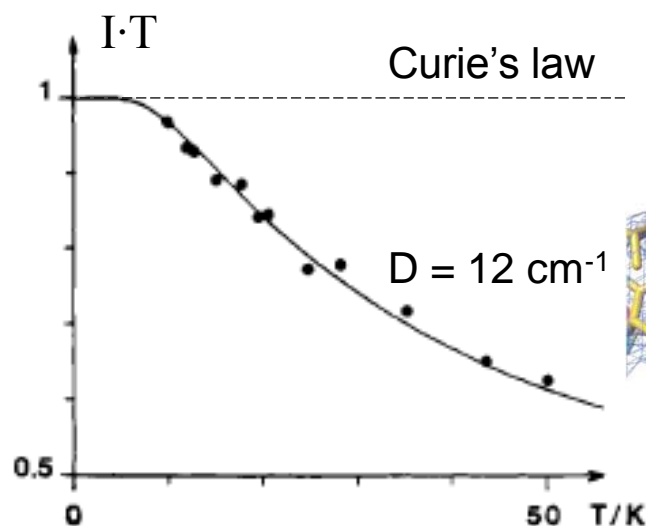
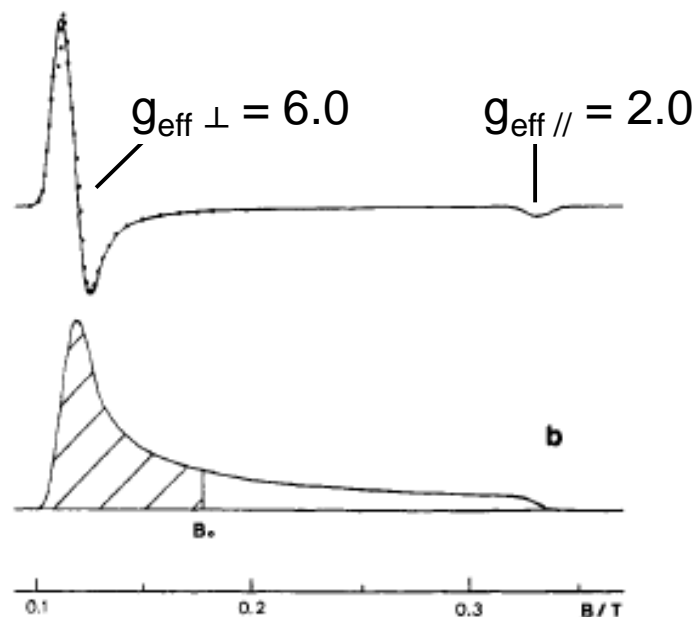
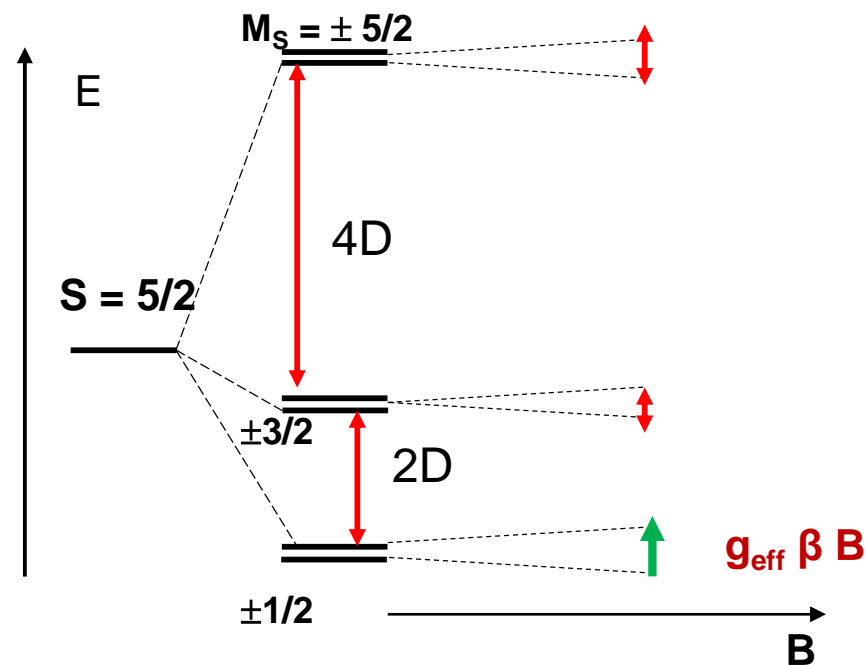
$$I \propto N_{(\pm 1/2)} / T$$

$$N_0 = N_{(\pm 1/2)} + N_{(\pm 3/2)} + N_{(\pm 5/2)}$$

$$N_{(\pm 3/2)} / N_{(\pm 1/2)} = \exp(-2D/kT) \quad (\text{Boltzmann})$$

$$N_{(\pm 5/2)} / N_{(\pm 1/2)} = \exp(-6D/kT)$$

$$I \cdot T \propto 1 / [1 + \exp(-2D/kT) + \exp(-6D/kT)]$$



High spin Fe^{3+} systems

Rhombic fine structure: $(D, E) \gg g \beta B$

$$H_{\text{SF}} = D \left(S_z^2 - \frac{1}{3} S(S+1) \right) + E(S_x^2 - S_y^2)$$

$$H_{\text{SF}} = D \left(S_z^2 - \frac{1}{3} S(S+1) \right) + \frac{E}{2} (S_+^2 + S_-^2)$$

Mixing of states $\Delta M_S = \pm 2$

Forbidden transitions become allowed !

$\Delta M_S = \pm 3$; $\Delta M_S = \pm 5$

But the g_{eff} calculations are more complex...

Weak rhombicity: $E/D < 0.1$

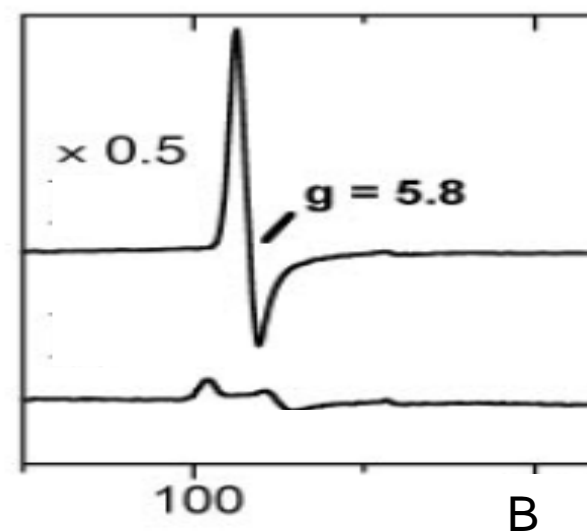
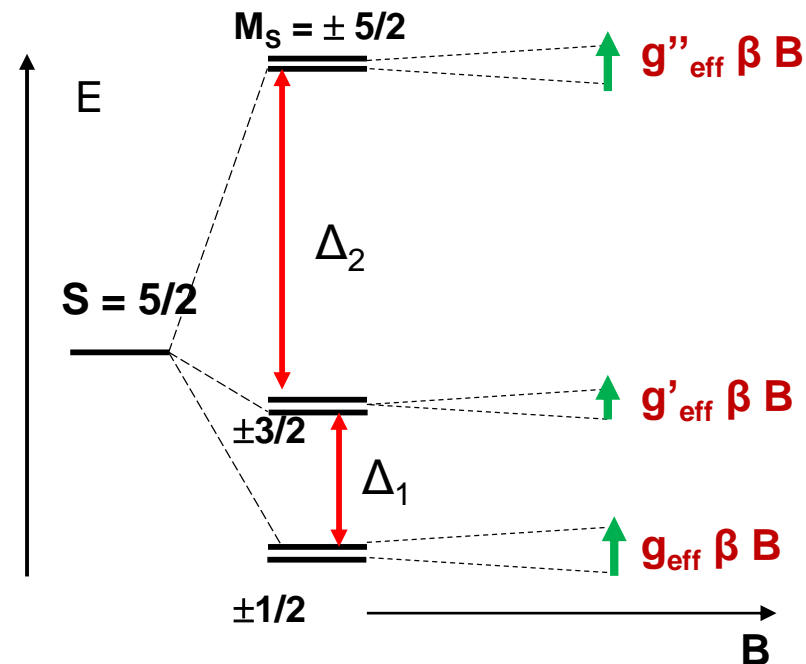
In manifold $M_S = \pm 1/2$

$$g_{\text{eff } X} = 6 + 24 E/D$$

$$g_{\text{eff } Y} = 6 - 24 E/D$$

$$g_{\text{eff } Z} = 2.0$$

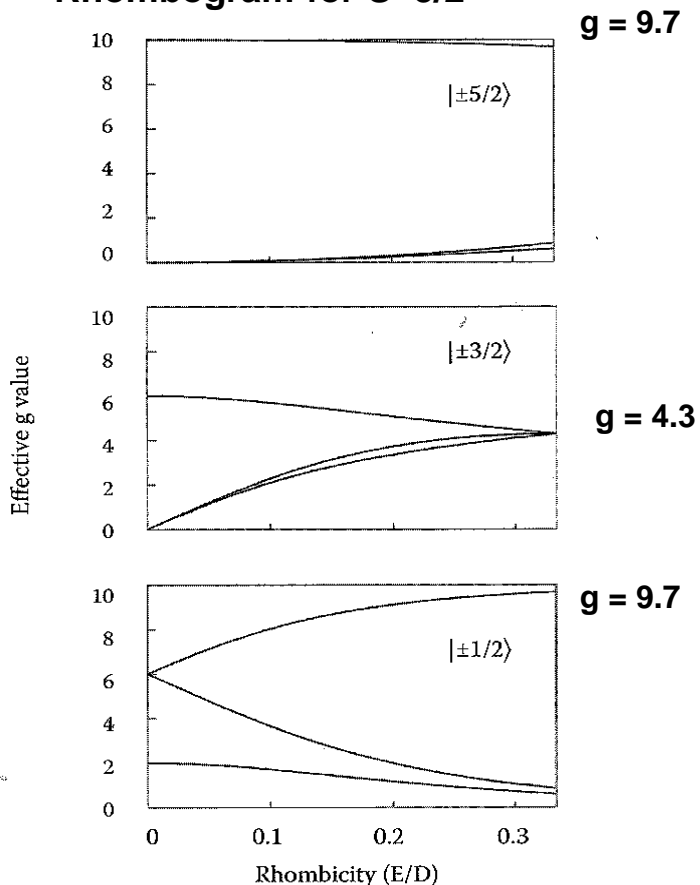
=> Determination of E/D



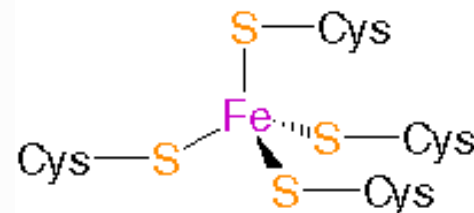
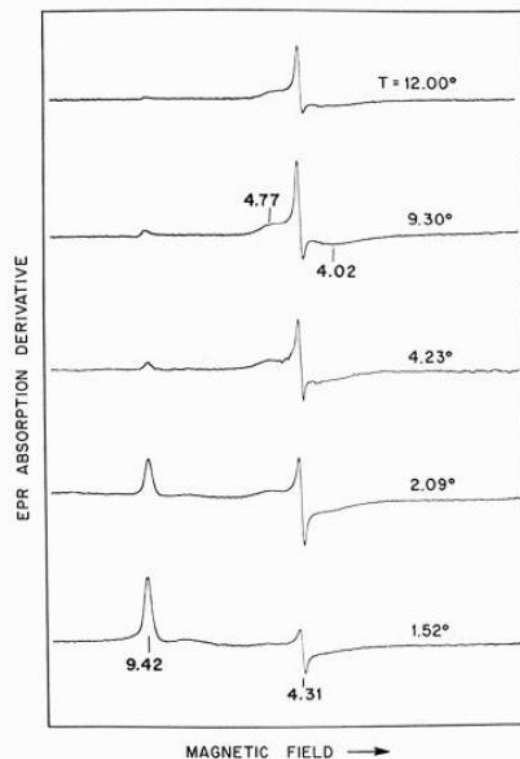
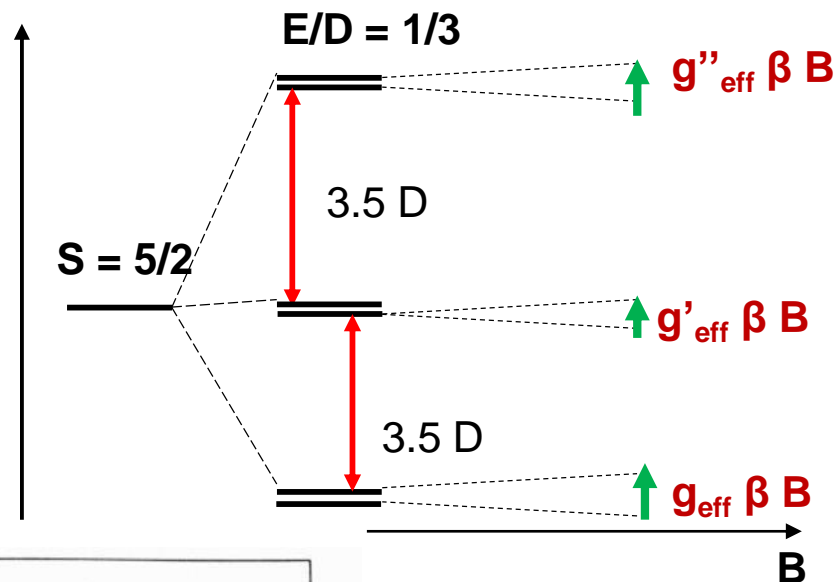
High spin Fe^{3+} systems

Rhombic fine structure: $(D, E) \gg g \beta B$

Rhombogram for $S=5/2$



Isotropic line at $g = 4.3$ for adventitious Fe^{3+}



Oxidized Rubredoxin

$g = 9.4, 1.2, 0.9$

$g = 4.77, 4.3, 4.0$

$D = 1.76 \text{ cm}^{-1}$ $E = 0.495 \text{ cm}^{-1}$
(Peisach 1971)

B

High spin / Low spin Fe^{3+} systems

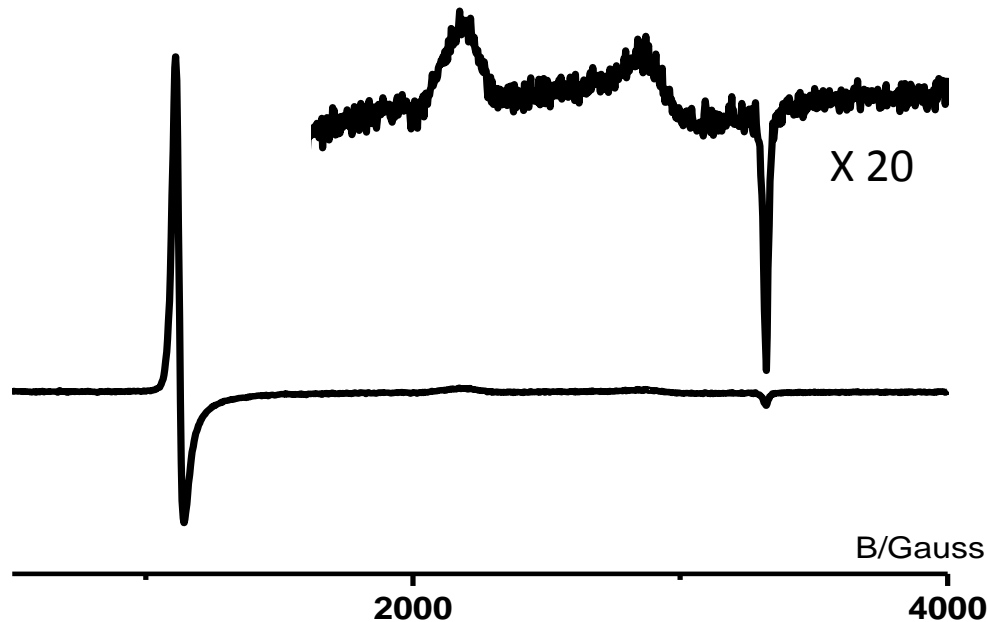
EPR Signal intensity: $I \propto N (g_P)_{\text{av}} B_1 \text{th}(h\nu/2k_B T)$

$$(g_P)_{\text{av}} \approx \left\{ \frac{2}{3} [(g_x^2 + g_y^2 + g_z^2) / 3]^{1/2} + \frac{1}{3} [(g_x + g_y + g_z) / 3] \right\}$$

Influence of the transition probability

Higher sensitivity for signals with high g-values (low magnetic field)

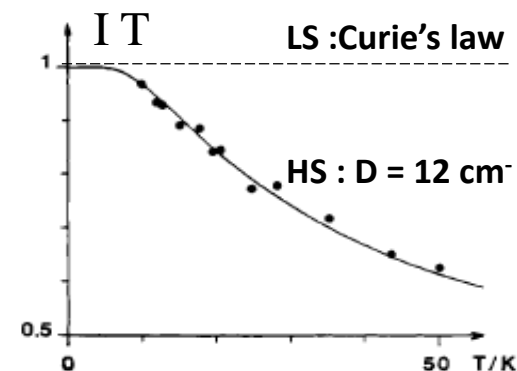
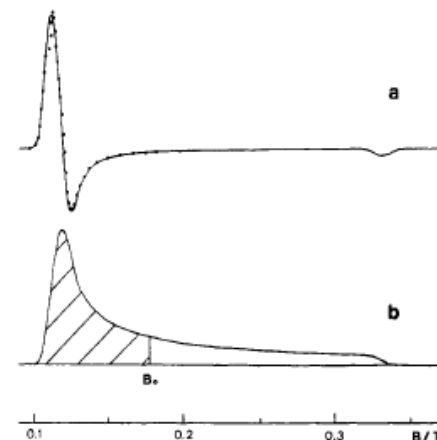
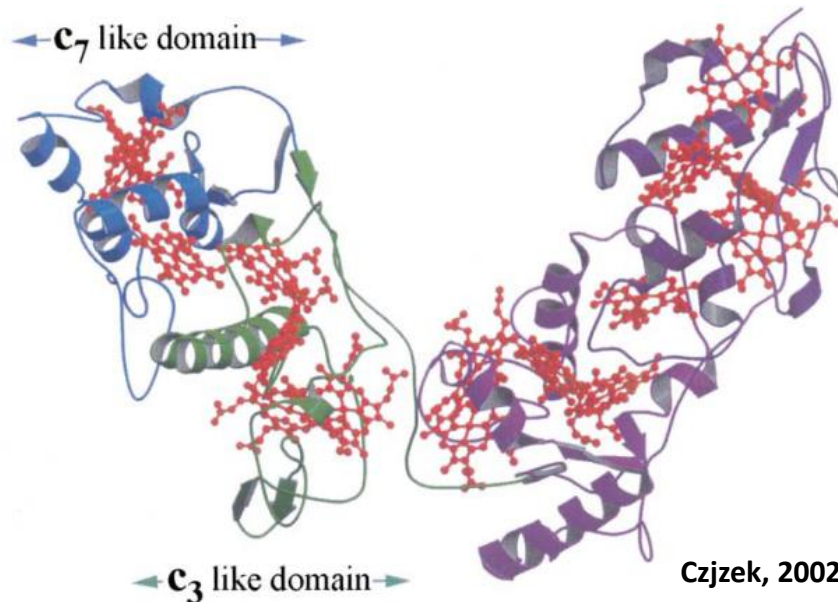
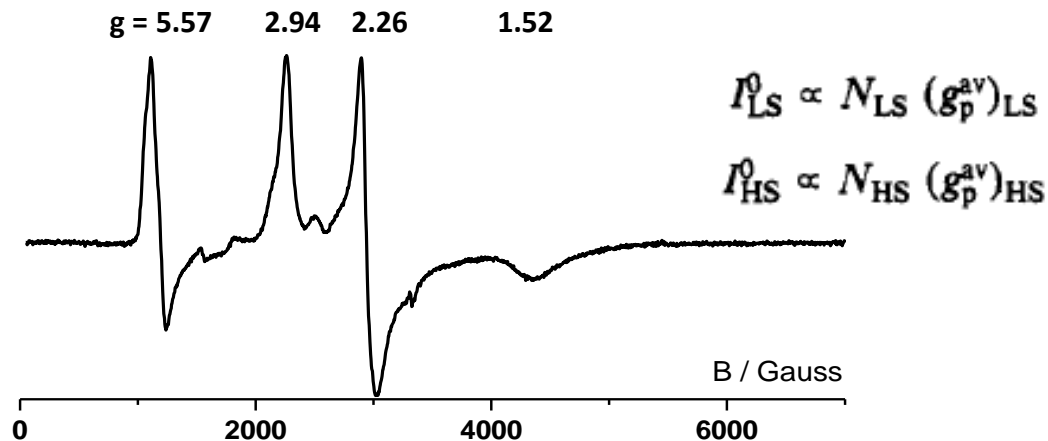
Equimolar solution of myoglobin (HS) and cytochrome c (LS)



High spin / Low spin Fe³⁺ systems

High Molecular weight Cytochrome (HMC) : 16 hemes

High Spin + Low Spin hemes ?

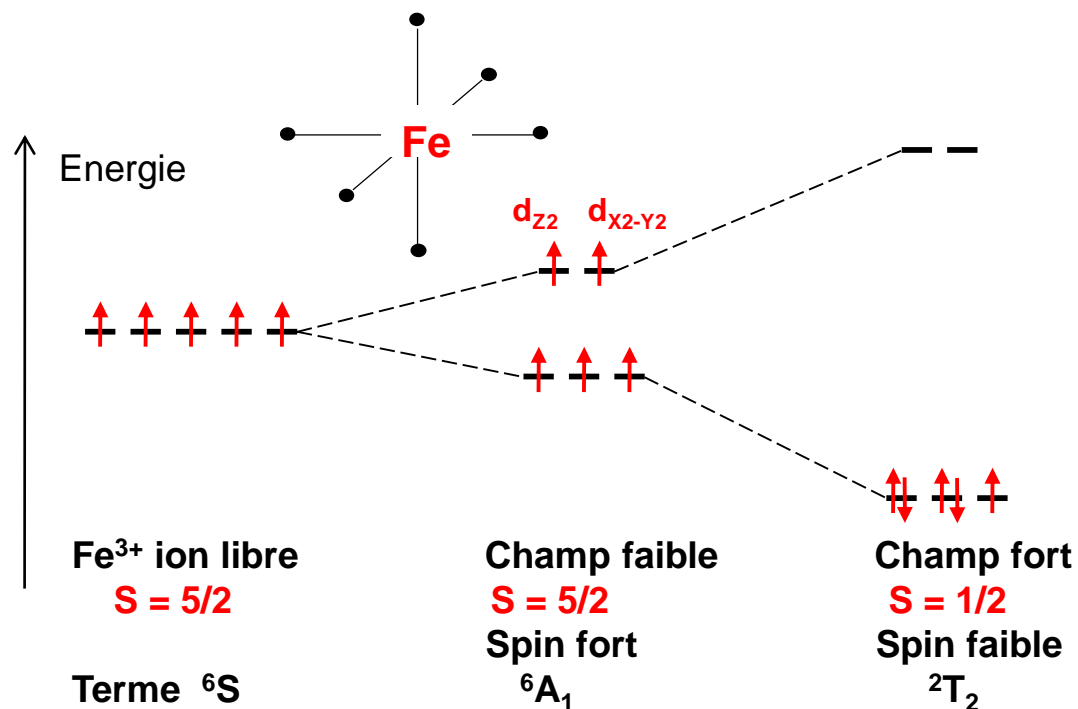


Determination of HS heme spin intensity by spectral simulation and comparison with a standard

$$(g_p^{av})_{LS} n_{LS} + (g_p^{av})_{HS} n_{HS} f(16 \text{ K}) = 38$$

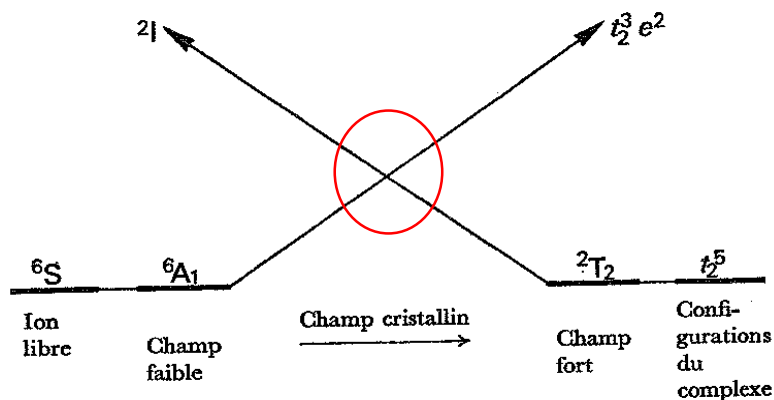
16 hemes : 1 HS + 15 LS

Spin transitions in Fe³⁺ systems



Valence ion Fe	1+	2+	3+	4+	5+
3d ⁿ	7	6	5	4	3
HS	3/2	2	5/2	2	3/2
LS	1/2	0	1/2	0	1/2

Spin Transitions



Spin transitions are induced by:

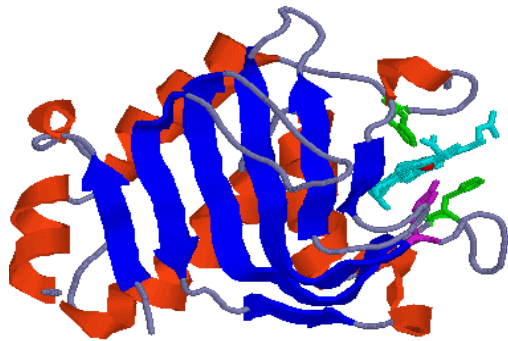
- Change of ligand field strength: change of ligand, compression
- T variations

Spin transitions in Fe^{3+} systems: HasA protein

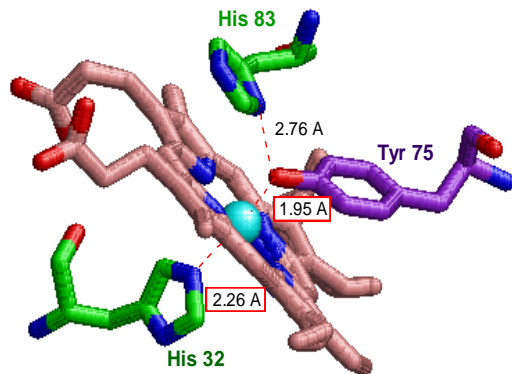
HasA protein : Heme acquisition system

Enable pathogenic bacteria (*Serratia marcescens* *Yersinia pestis*)
to take heme group from hemoglobin in human

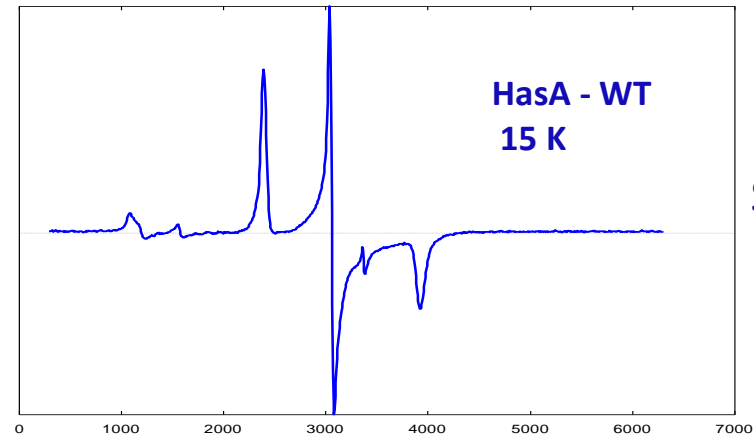
Very strong affinity for heme: $K_D = 10^{-11}$ M



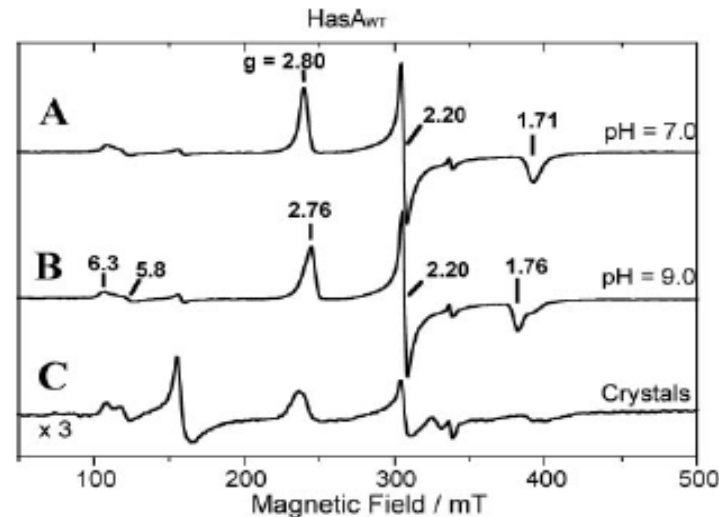
Axial coordination of Fe^{3+}
by His32-Tyr78



(Arnoux, NSB 1999)



Low spin Fe^{3+}
 $S = 1/2$



Same coordination
of Fe^{3+} in solution and
in the cristal state

Polycrystals

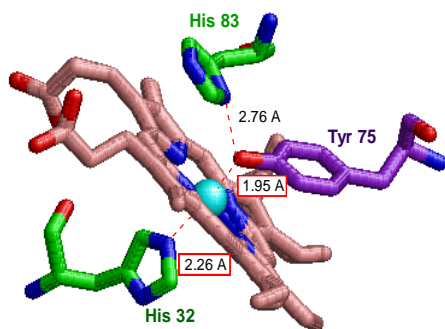
Spin transitions in Fe^{3+} systems: HasA protein

HasA protein : Heme acquisition system

Enable pathogenic bacteria (*Serratia marcescens* *Yersinia pestis*)

to take heme group from hemoglobin in human

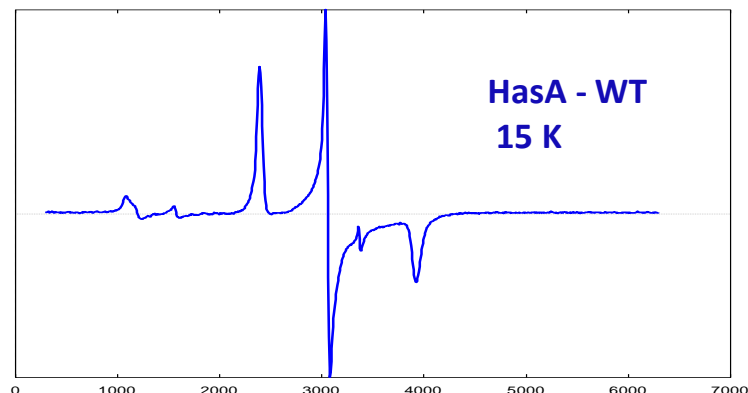
Very strong affinity for heme: $K_D = 10^{-11}$ M



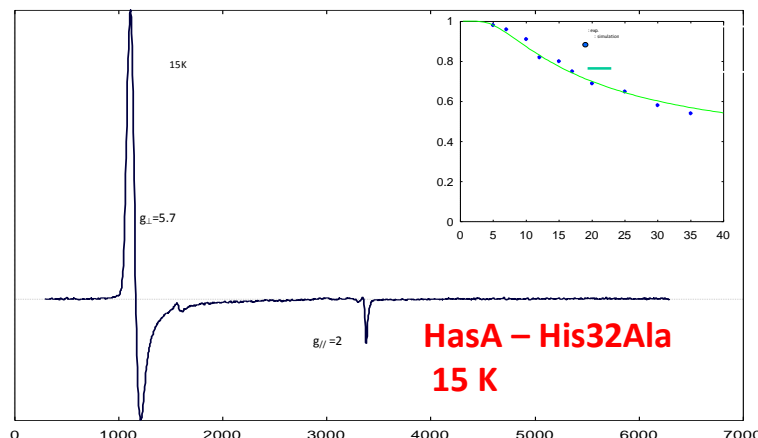
Mutant of the axial coordination:

His32Ala

Lack of sixth ligand or H_2O molecule



Low spin Fe^{3+}
 $S = 1/2$



High spin Fe^{3+}
 $S = 5/2$

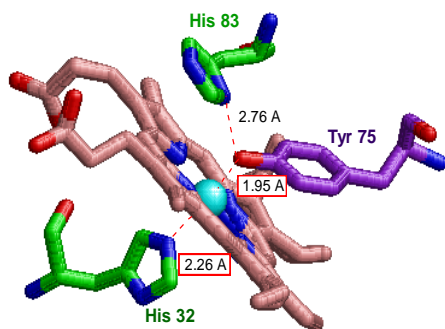
Spin transitions in Fe³⁺ systems: HasA protein

HasA protein : Heme acquisition system

Enable pathogenic bacteria (*Serratia marcescens* *Yersinia pestis*)

to take heme group from hemoglobin in human

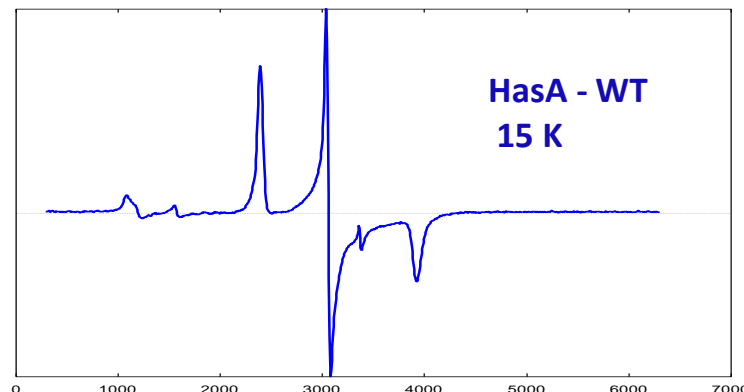
Very strong affinity for heme: $K_D = 10^{-11}$ M



Mutant of the axial coordination:

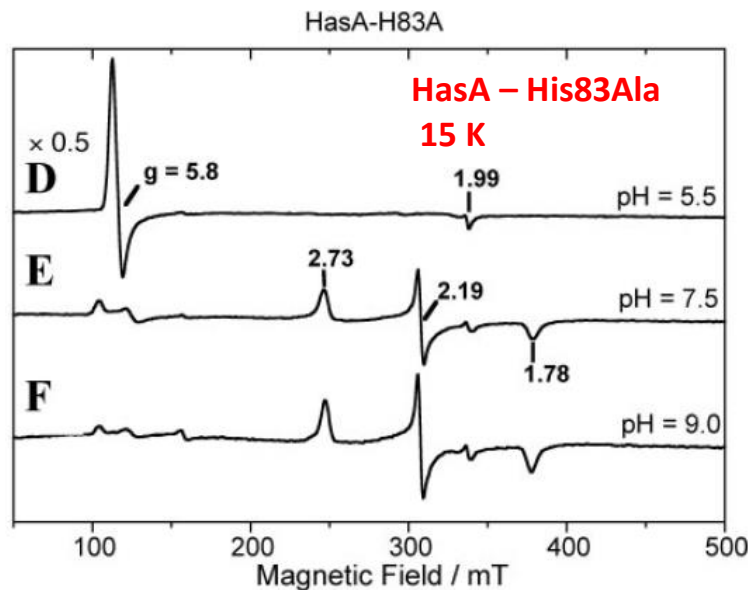
His83Ala

Decoordination of Tyr75 at acidic pH



HasA - WT
15 K

Low spin Fe³⁺
 $S = 1/2$



HasA - His83Ala
15 K

pH = 5.5
High spin
Fe³⁺ $S = 5/2$

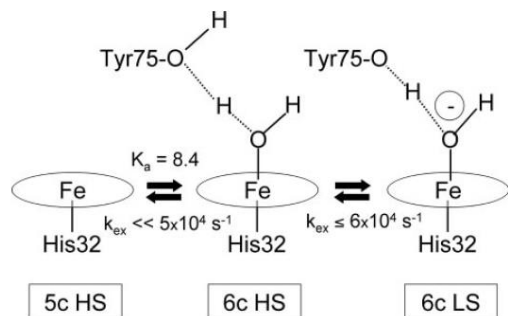
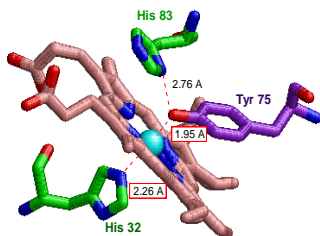
Spin transitions in Fe³⁺ systems: HasA protein

HasA protein : Heme acquisition system

Enable pathogenic bacteria (*Serratia marcescens* *Yersinia pestis*)

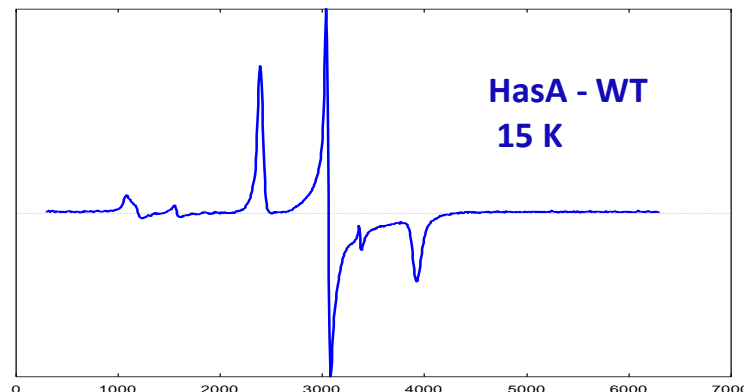
to take heme group from hemoglobin in human

Very strong affinity for heme: $K_D = 10^{-11}$ M

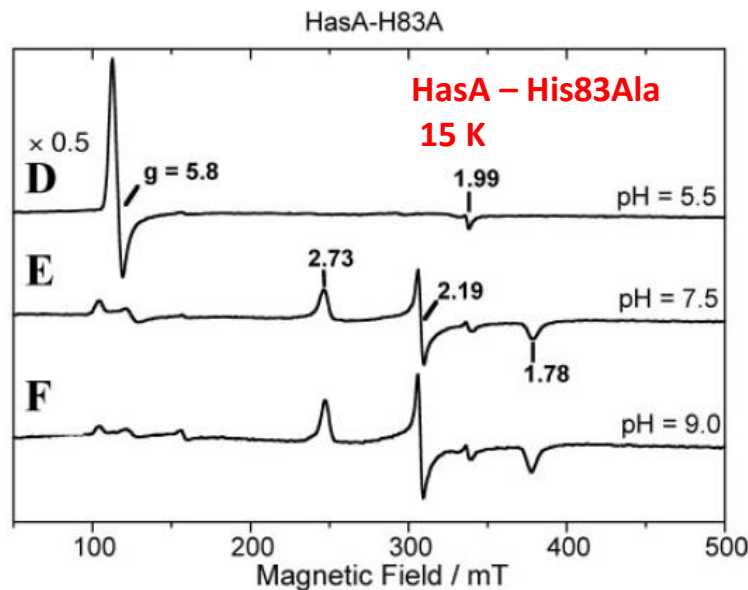


Model : Breaking the His83-Tyr75 H-bond decrease heme affinity and enable the transfer to the membrane bound receptor HasR

(Caillet, *J.Biol.Chem.*, 2008)

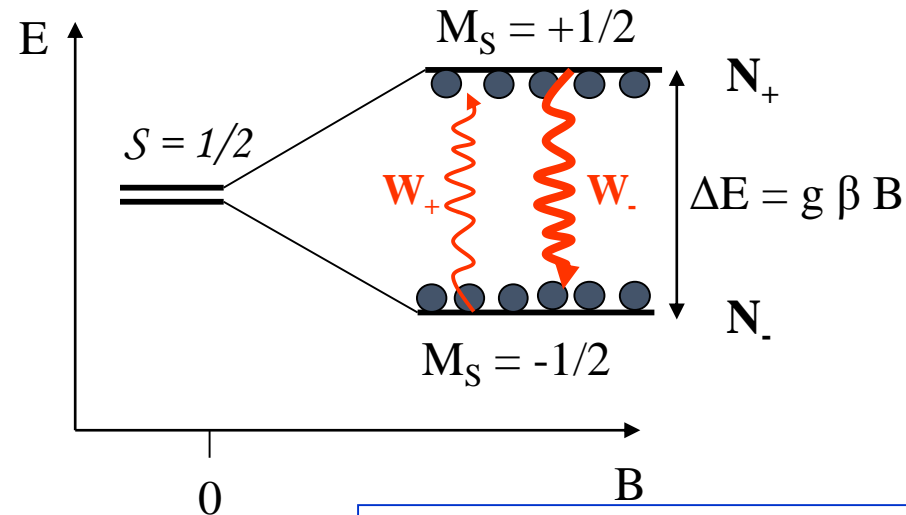


Low spin Fe³⁺
 $S = 1/2$



pH = 5.5
High spin
Fe³⁺ $S = 5/2$

Electron spin relaxation



Thermal equilibrium (Boltzmann)

$$N_+ / N_- = \exp (- g \beta B / k T) = W_+ / W_-$$

$$N_+ W_- = N_- W_+$$

Spontaneous transitions (W_+ , W_-) maintain thermal equilibrium

\Rightarrow Induced by fluctuations of magnetic field: $B = B_0 + B(r, t)$

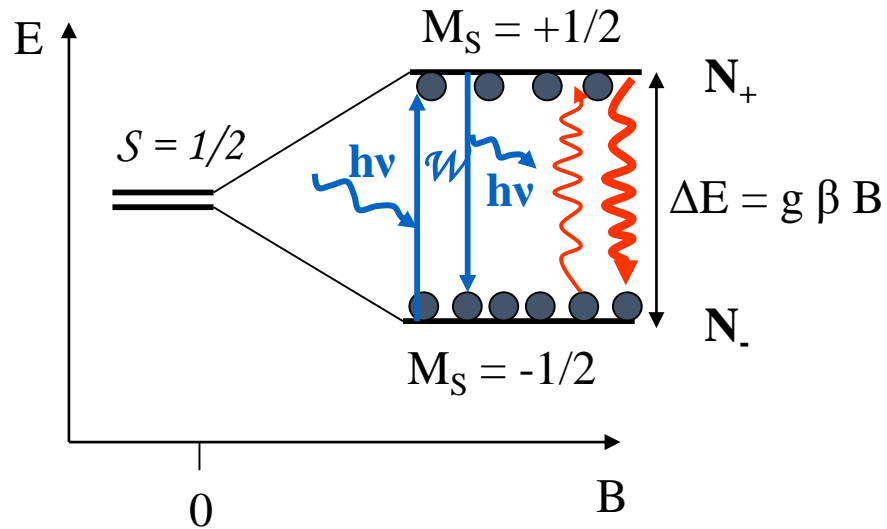
Fluctuations of the environment:

- Thermal motions: translations, rotations, vibrations, collisions
- Magnetic neighbours: nuclei, other paramagnetic centers
- Thermal radiation



- Energy exchange between spins : spin-spin relaxation (T_2)
- Energy exchange between spins and surrounding : spin-lattice relaxation (T_1)

Electron spin relaxation



Upon microwave irradiation, competition between **Absorption/Relaxation**

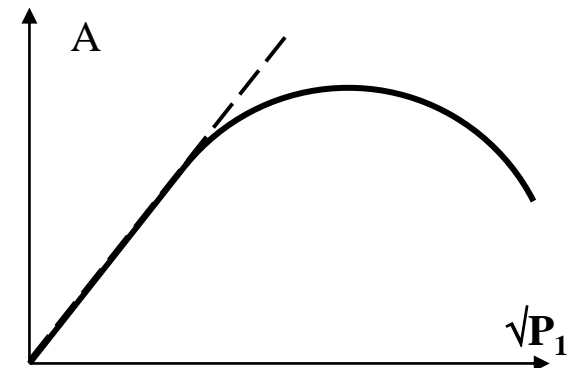
$$\frac{dn}{dt} = -2 \mathcal{W} n + (n_0 - n) / T_1 \quad (\mathcal{W} \propto B_1^2)$$

=> Steady state in continuous wave EPR

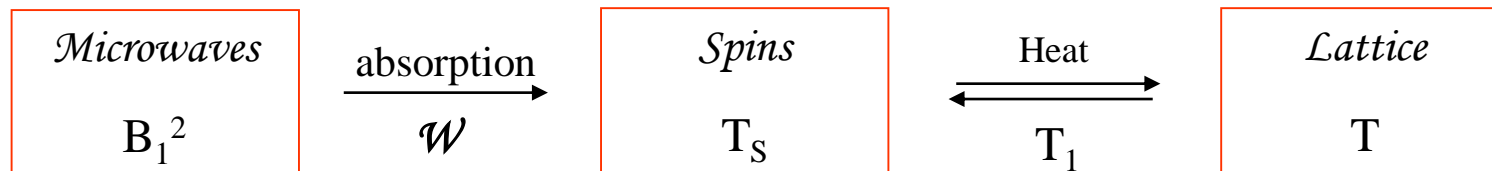
Net absorbed microwave power at steady state

$$P_{\text{abs}} = h\nu (\mathcal{W} N_- - \mathcal{W} N_+) = h\nu \mathcal{W} n_{\text{Stat}}$$

High power: $n_{\text{stat}} \rightarrow 0$: **Power saturation**



=> **T_1 and T_2 measurements**



Electron spin relaxation: Temperature dependence

Spin-lattice relaxation :

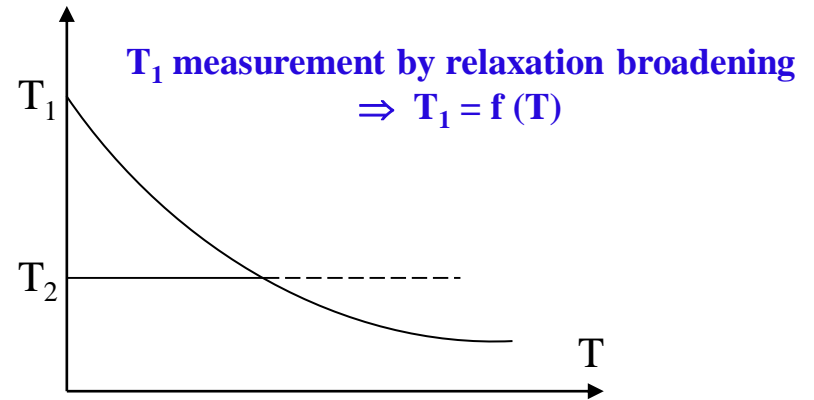
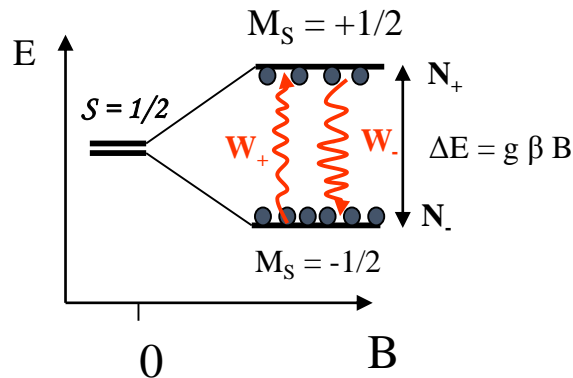
- Coupling between spins and vibrations (phonons)
- Strong dependence on spin-orbit coupling

$$\mathbf{H}_{\text{SO}} = \lambda \mathbf{L} \cdot \mathbf{S}$$

- If T increases, T_1 decreases.

When $T_1 \approx T_2$ broadening of the resonance line:

$$\delta B = \hbar / g\beta \cdot 1/T_1$$



Relaxation broadening

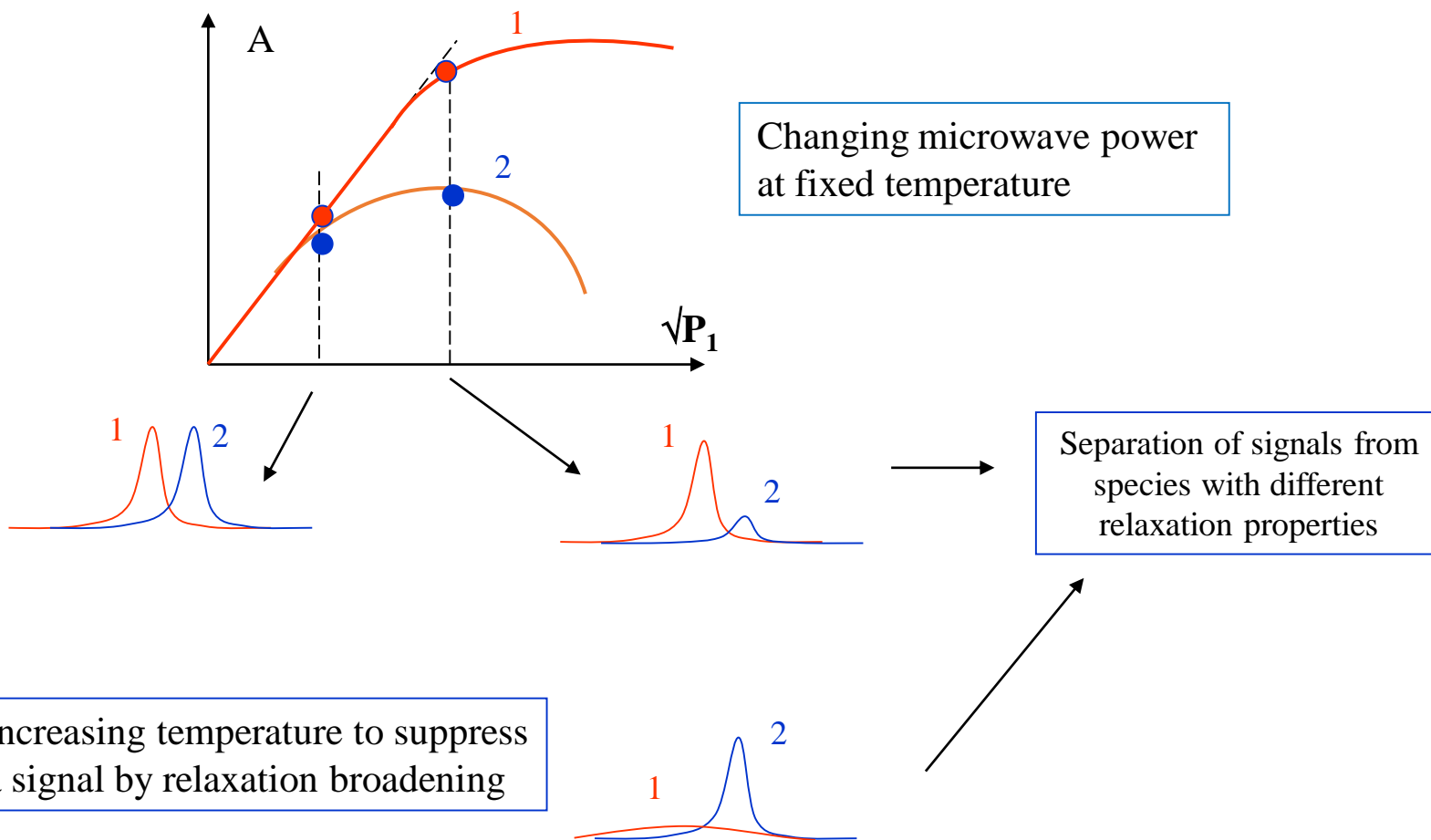
Disappearance of the signal by broadening

**For transition metal ions
Strong spin-orbit coupling**

- ***g*-tensor anisotropy**
- **Fast relaxation**
- **EPR study at low T**

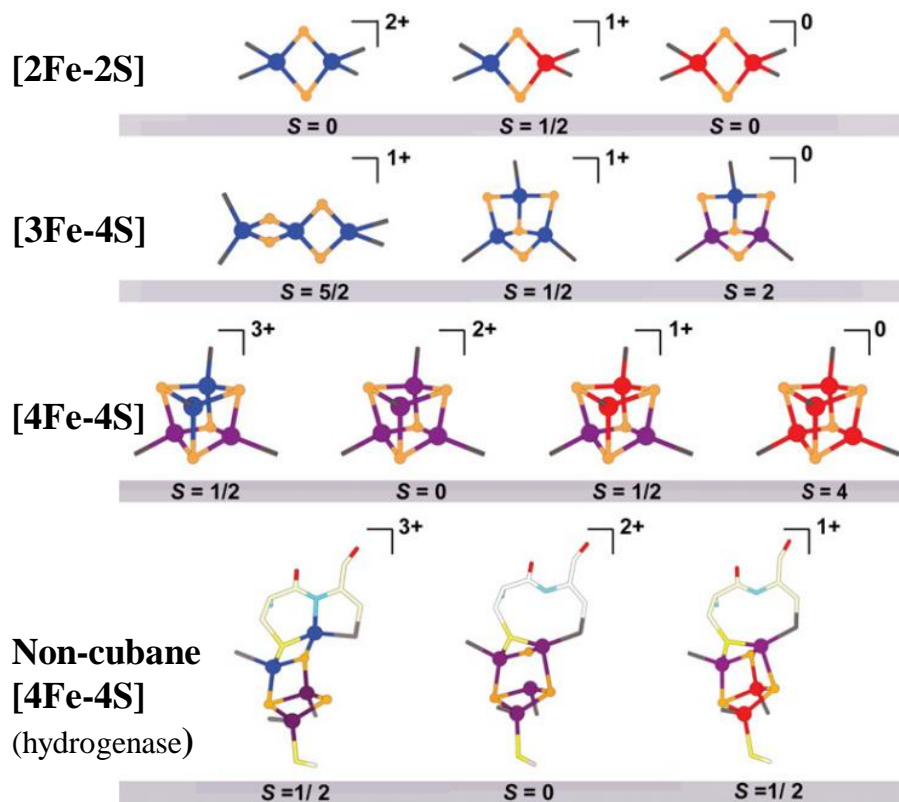
Electron spin relaxation: Temperature dependence

Strategies for separating signals from different species



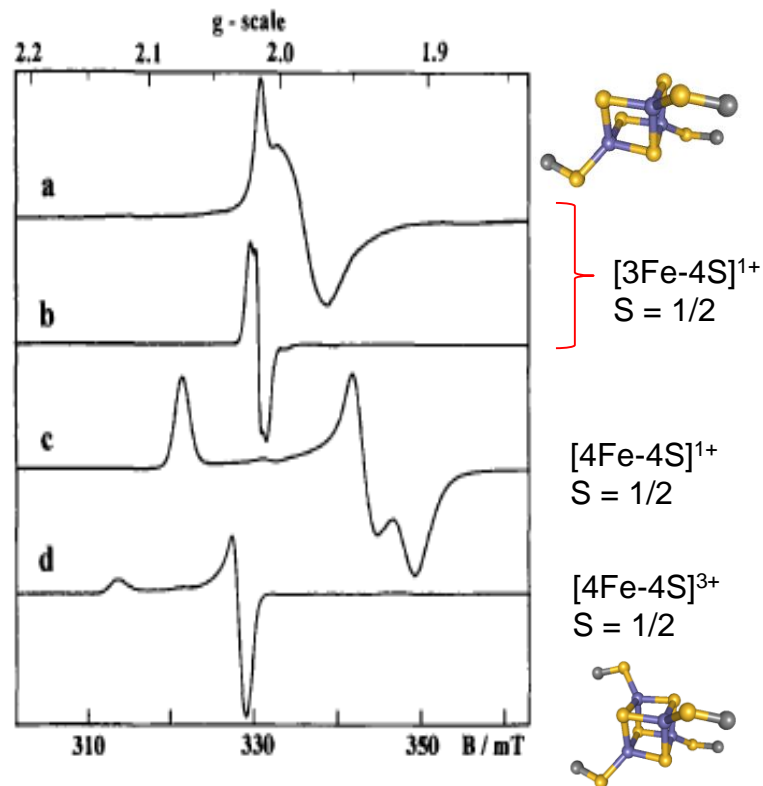
Fe-S clusters

Magnetic properties arise from exchange coupling between Fe^{3+} ($S=5/2$) and Fe^{2+} ($S=2$) ions



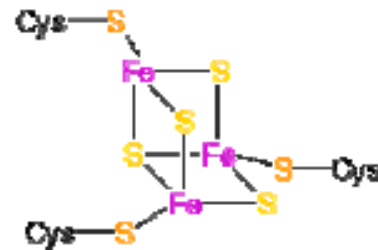
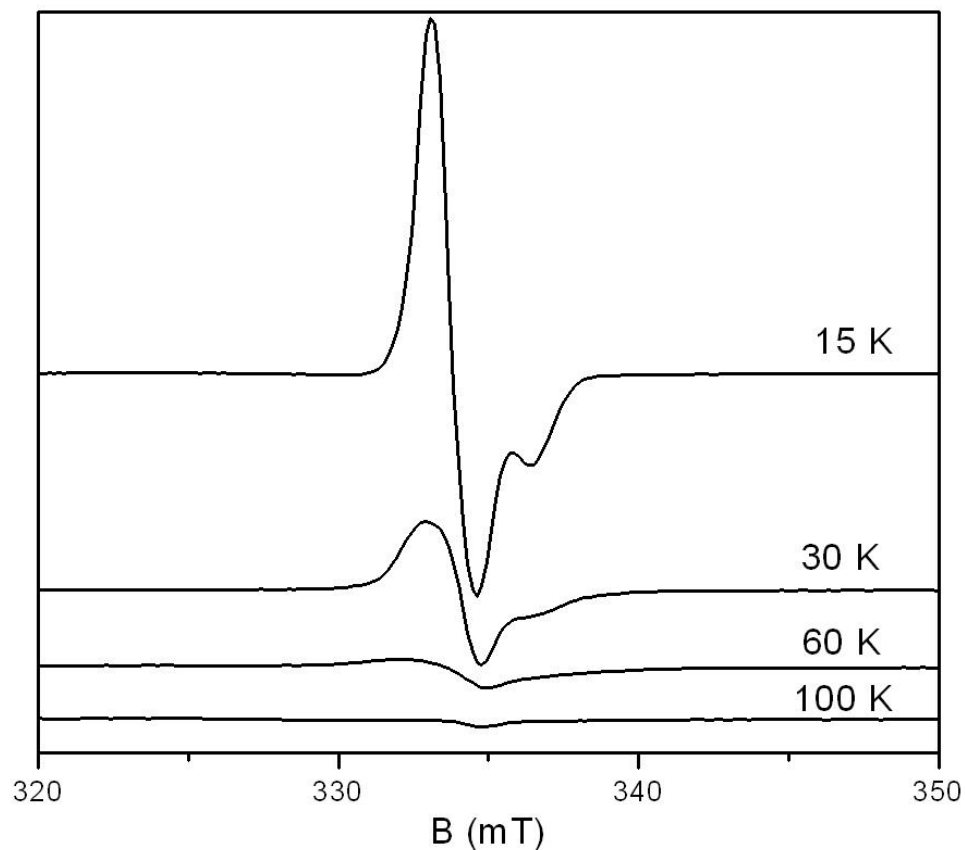
[Pandelia, BBA 2015]

Typical Fe-S EPR signals



Fe-S clusters: fast electron spin relaxation

Relaxation broadening of a $[3\text{Fe-4S}]^{1+}$ signal ($S = 1/2$) upon T increase



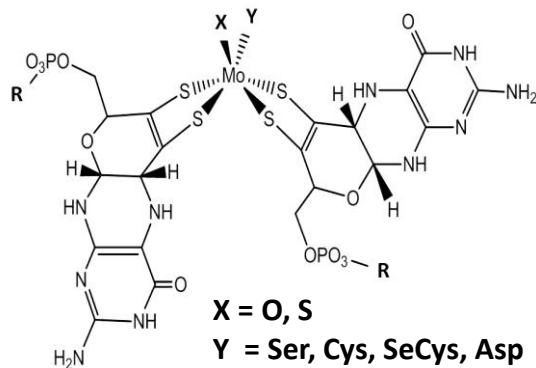
Fe-S clusters: fast electron spin relaxation

Selective EPR view of metal cofactors in *E. coli* respiratory nitrate reductase

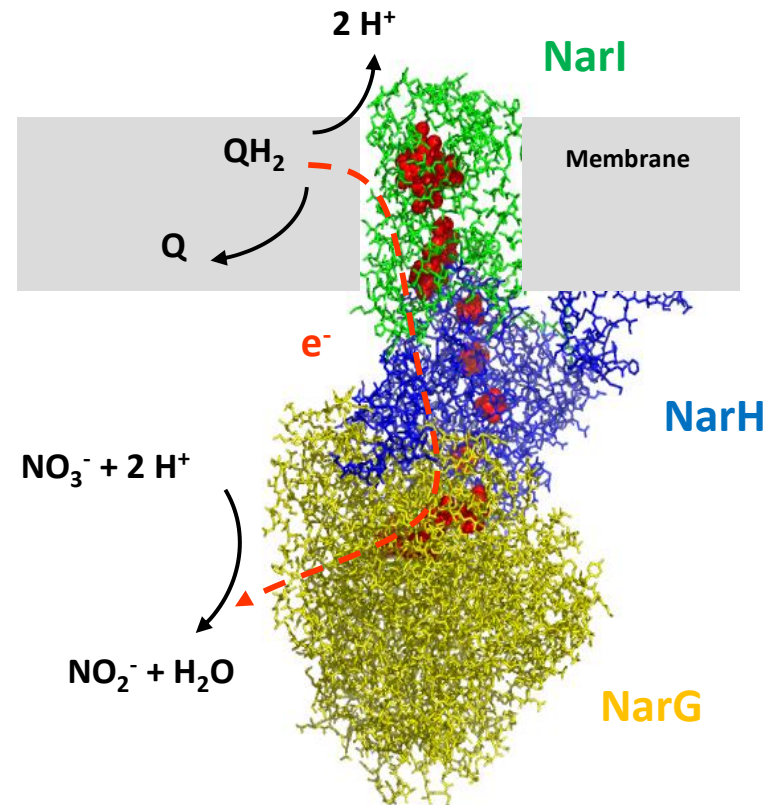
NarGHI

- Structure
- Mechanism
- Interaction with quinones
- Reactivity of Molybdenum cofactor
- Substrate specificity
- Biogenesis

(Coll. A. Magalon, CNRS Marseille)



Mo-bisPGD cofactor

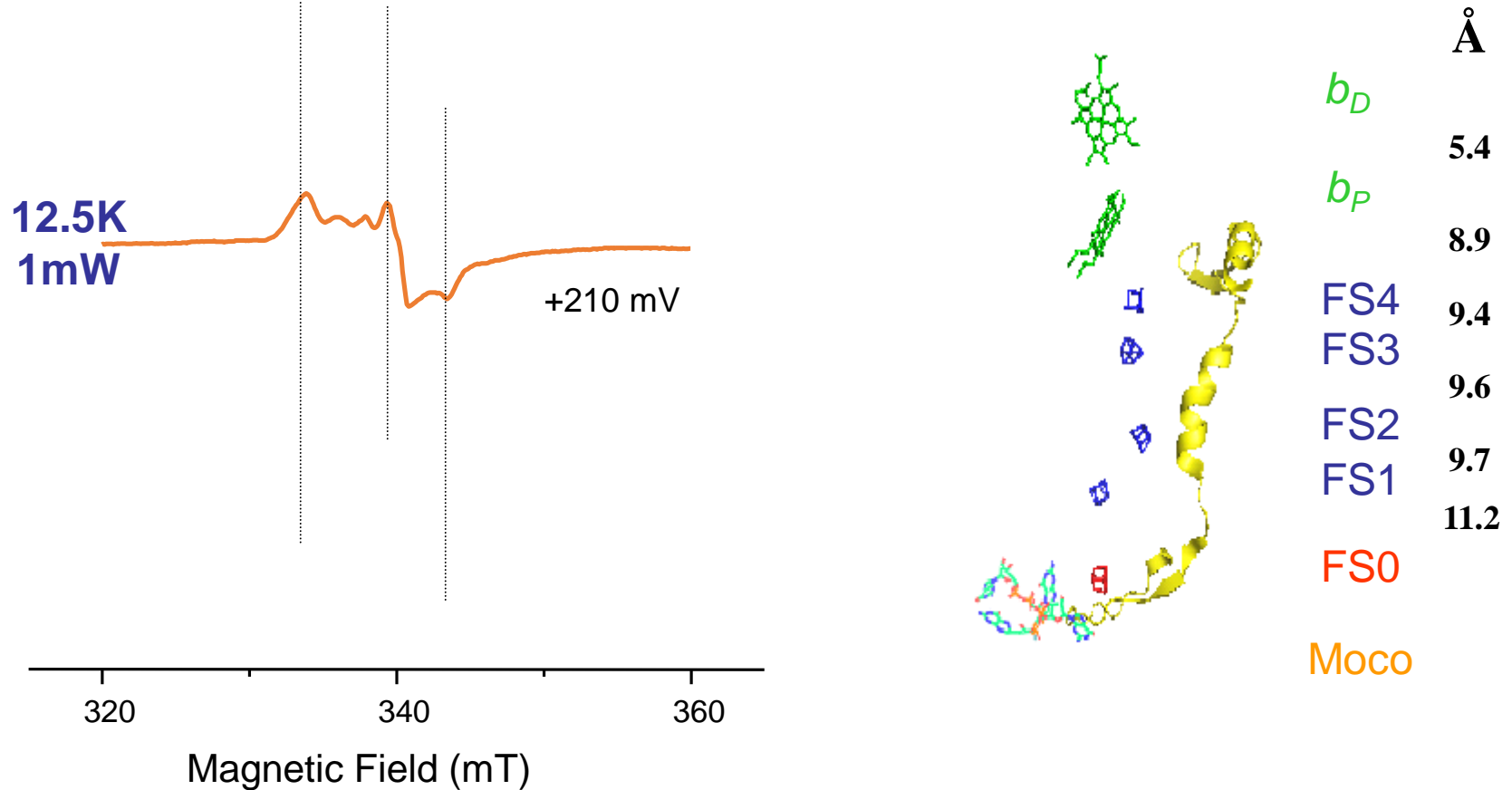


Membrane-bound Nitrate reductase
from *E. coli* (NarGHI)

Fe-S clusters: fast electron spin relaxation

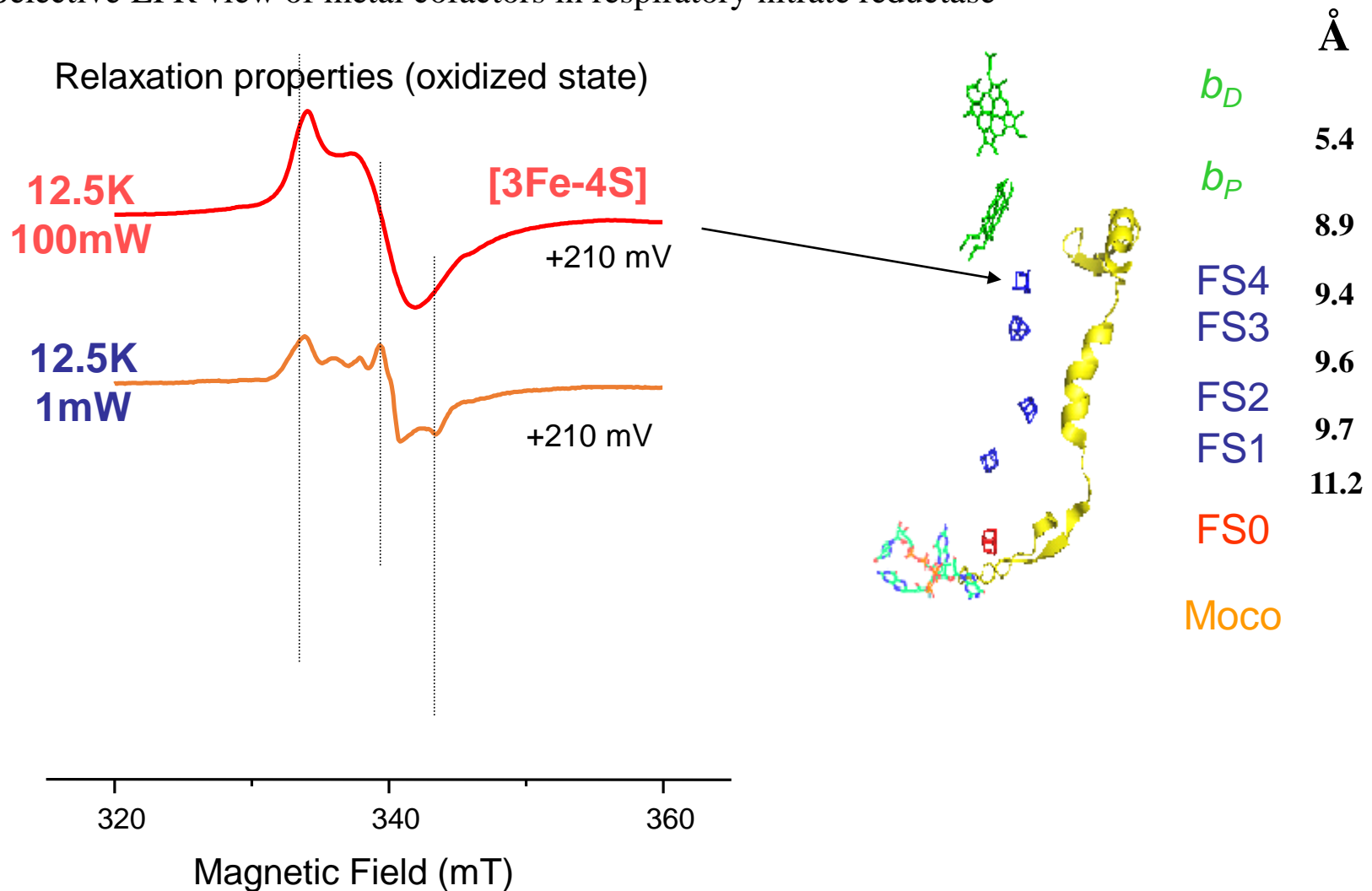
Selective EPR view of metal cofactors in respiratory nitrate reductase

Relaxation properties (oxidized state)



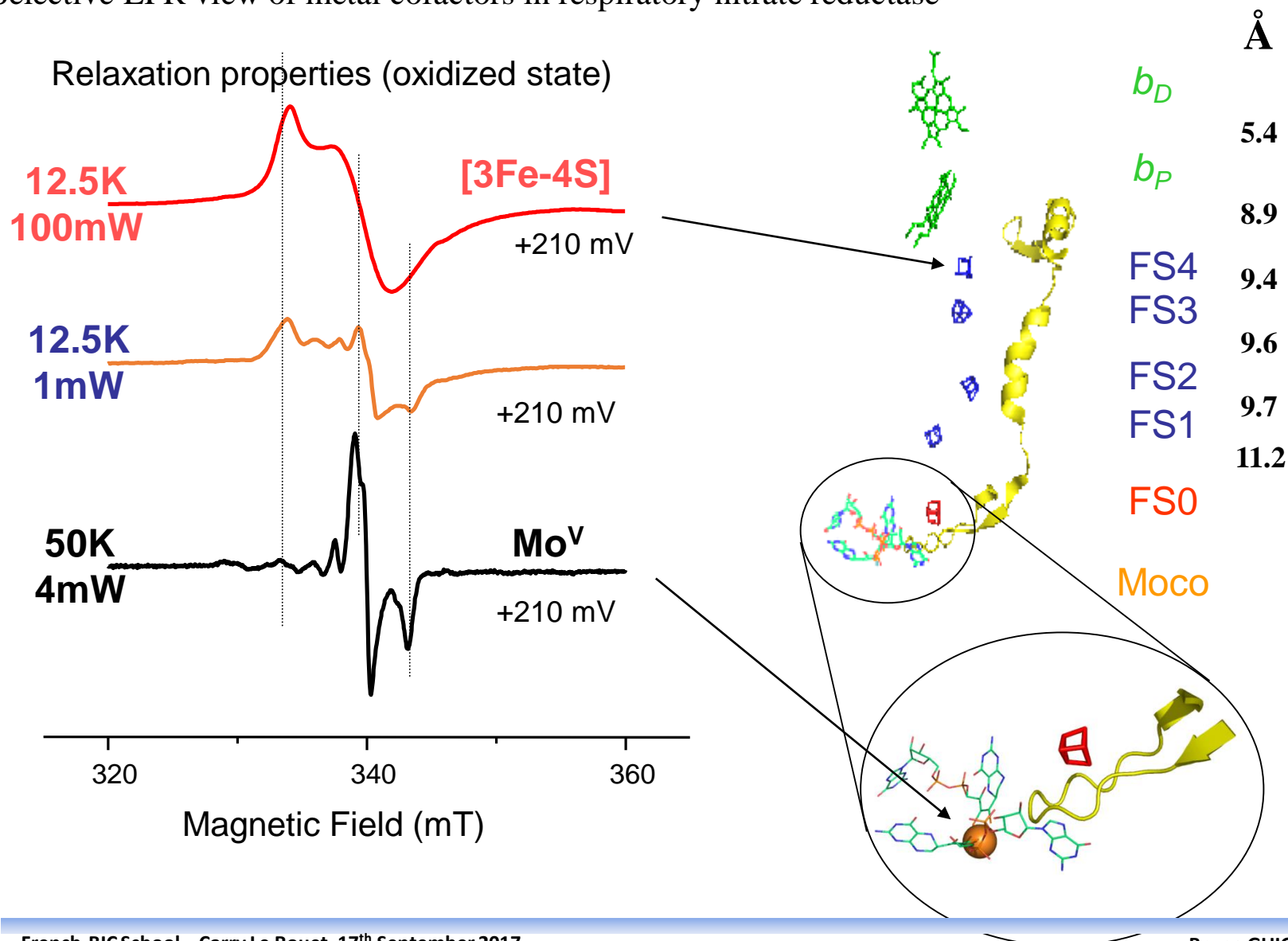
Fe-S clusters: fast electron spin relaxation

Selective EPR view of metal cofactors in respiratory nitrate reductase

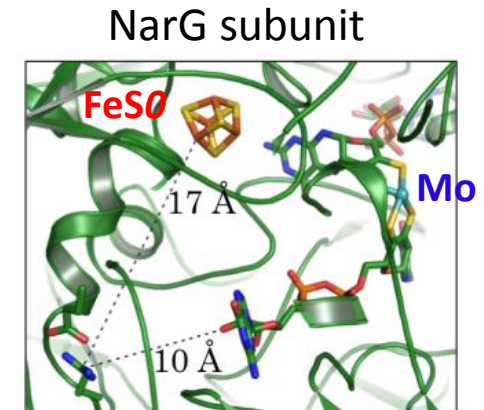
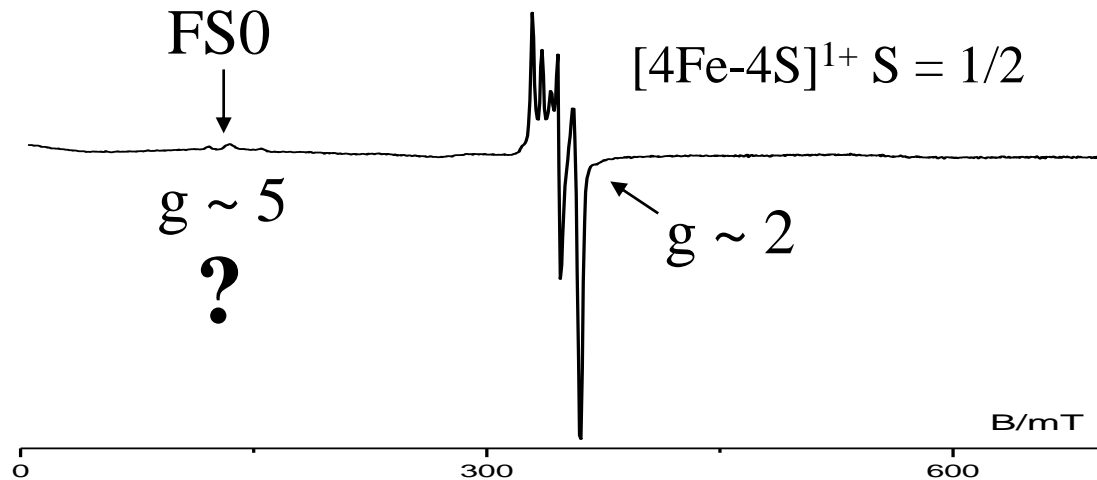


Fe-S clusters: fast electron spin relaxation

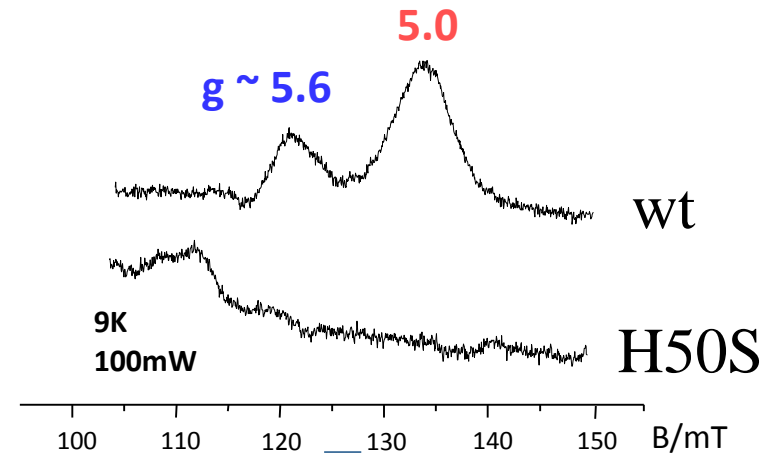
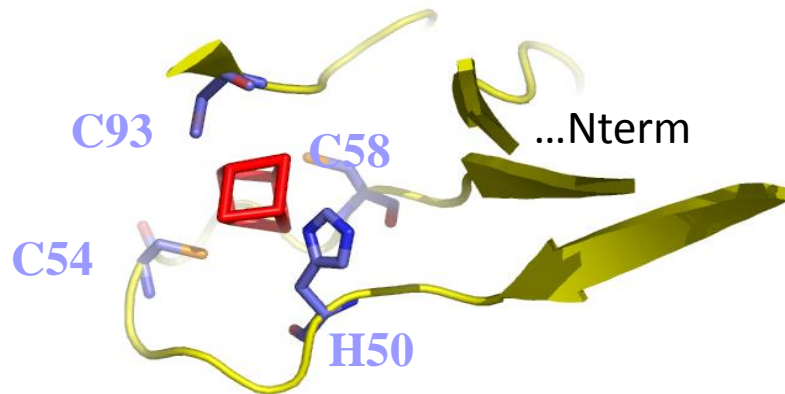
Selective EPR view of metal cofactors in respiratory nitrate reductase



Unusual FeS cluster in NarGHI nitrate reductase

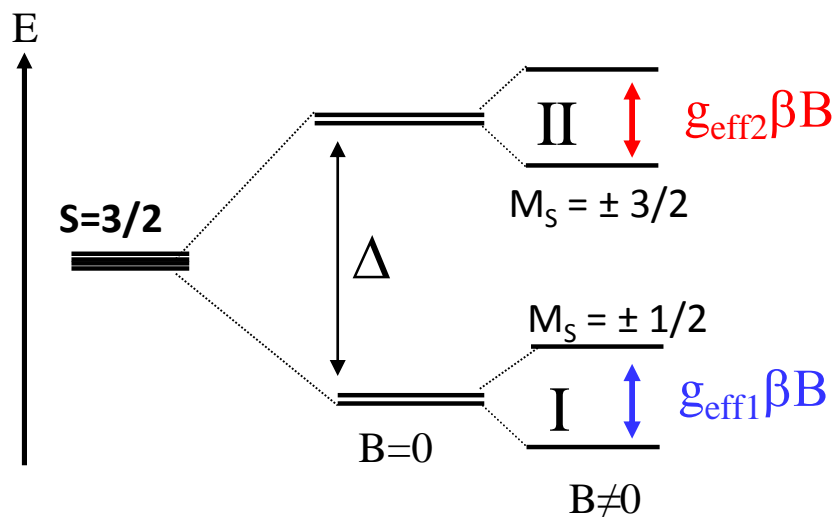
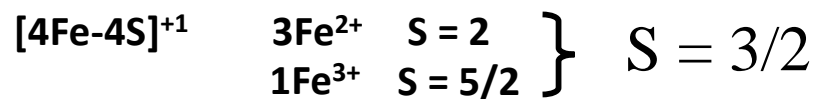


Unusual coordination of FeS0 cluster:
Cys motive HxxxCxxxC...C



FeS0 : a $S=3/2$ $[4\text{Fe-4S}]^{+1}$ cluster
coordinated by His
(Lanciano, *J.Phys.Chem.* 2007)

Unusual FeS cluster in NarGHI nitrate reductase



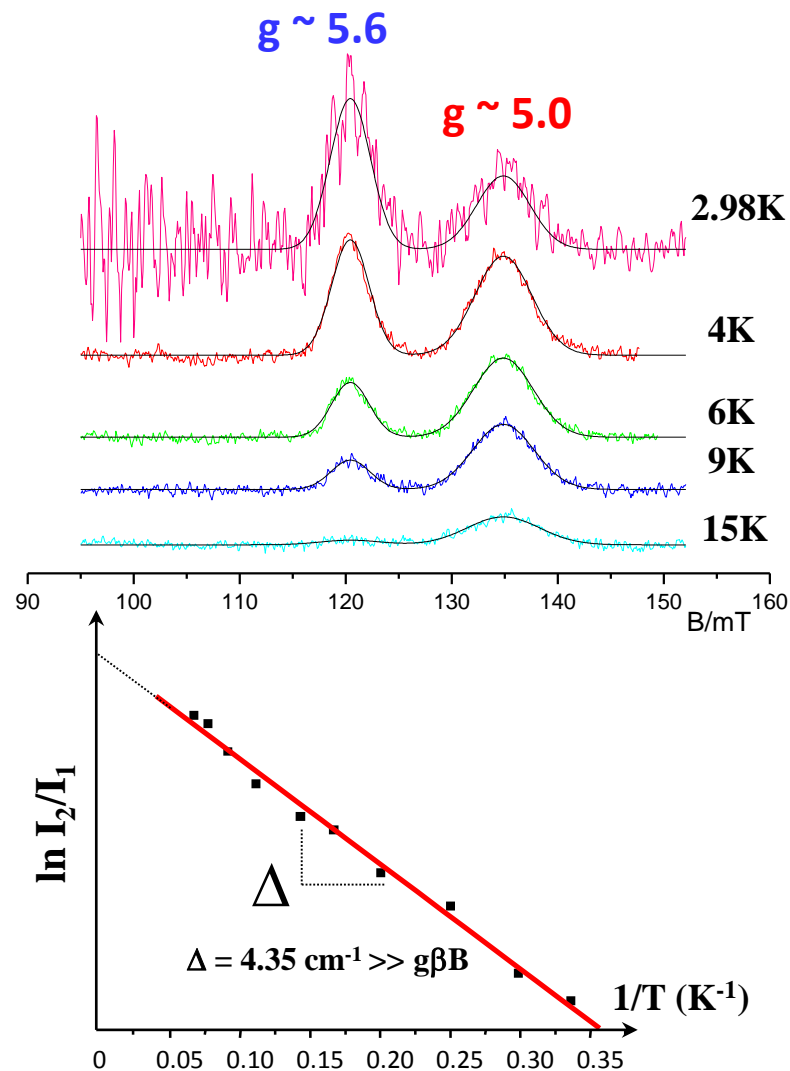
$$\tilde{H}_S = \tilde{H}_{\text{ZFS}} + \tilde{H}_{\text{Zeeman}}$$

$$\tilde{H}_S = D \left[S_z^2 - \frac{1}{3} S(S+1) + \frac{E}{D} (S_x^2 - S_y^2) \right] + \beta \vec{B} \tilde{g} \vec{S}$$

$$\Delta = [D^2 (1 + 3(E/D)^2)]^{1/2}$$

(Lanciano, J.Phys.Chem. 2007)

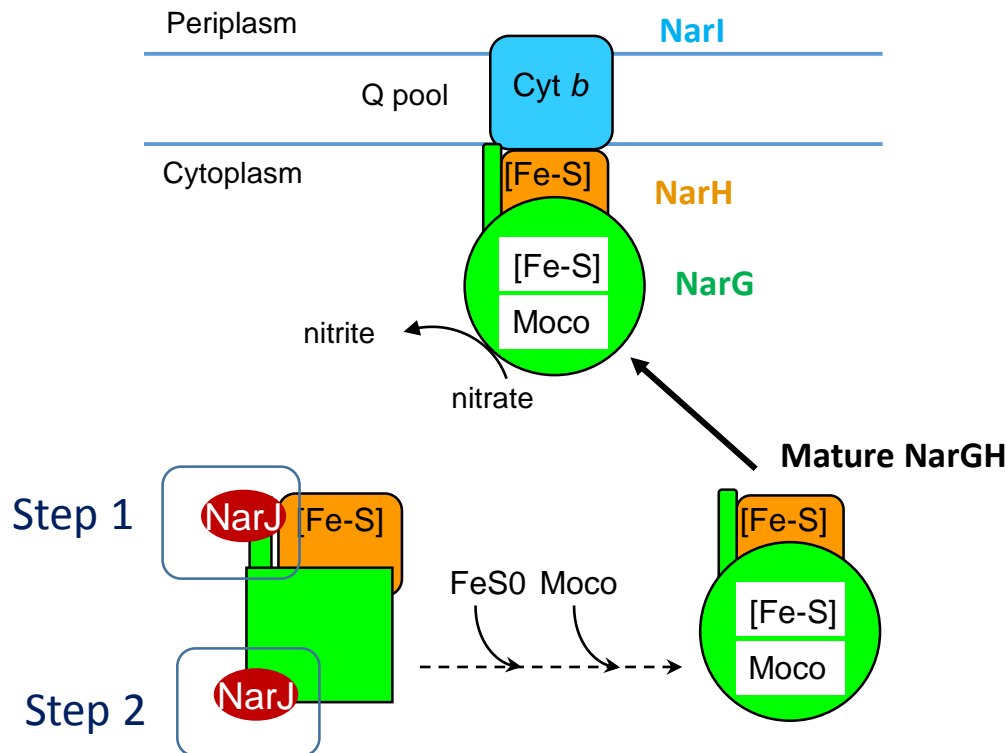
T dependence EPR study



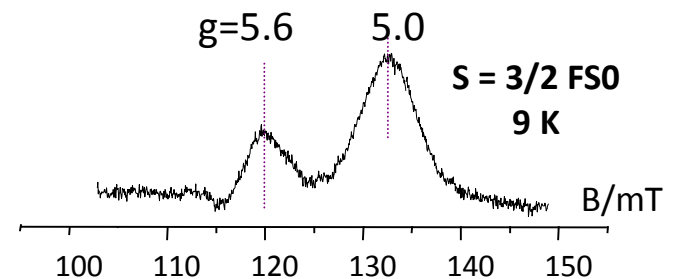
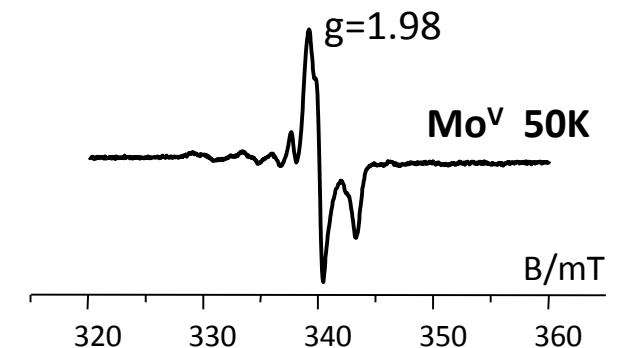
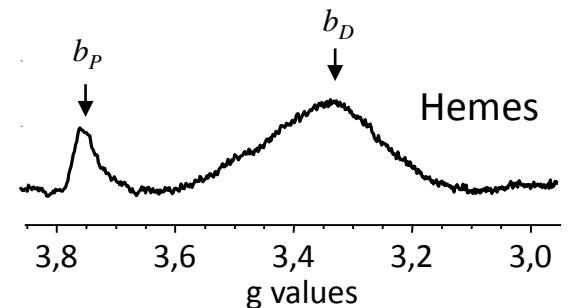
Insertion of the Mo cofactor in NarGHI nitrate reductase – EPR view

NarJ : a specific chaperone of NarGH complex
a multifunctional protein

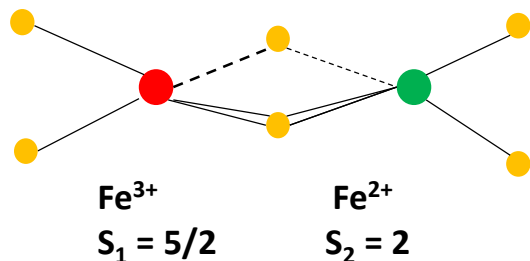
- ✓ Association to the N-ter of NarG
- prevent premature membrane anchoring
- ✓ Sequential Insertion of metal centers (FeS et Moco)



Vergnes A. *et al*, **2006**, *J. Biol. Chem.*
 Lanciano P. *et al*, **2007**, *J. Biol. Chem.*



Fe-S clusters: Exchange interaction determination from relaxation broadening



Exchange interaction between Fe ions in [2Fe-2S]⁺

$$H_{ex} = J \vec{S}_1 \cdot \vec{S}_2$$

$$S_T = \vec{S}_1 + \vec{S}_2$$

$$|S_1 - S_2| \leq S_T \leq S_1 + S_2$$

$$S_T = 1/2, 3/2, 5/2, 7/2, 9/2$$

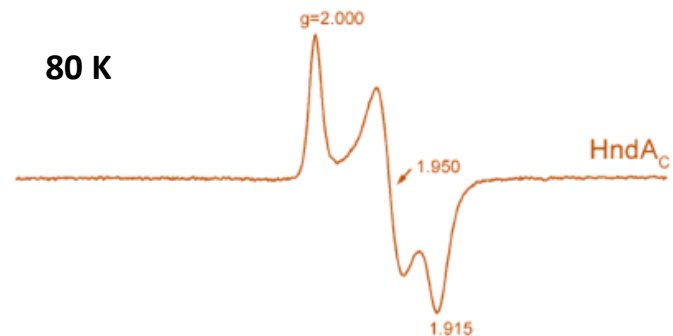
$$H_{ex} = \frac{J}{2} (S^2 - S_1^2 - S_2^2)$$

$$E = J S(S+1) + Cte$$

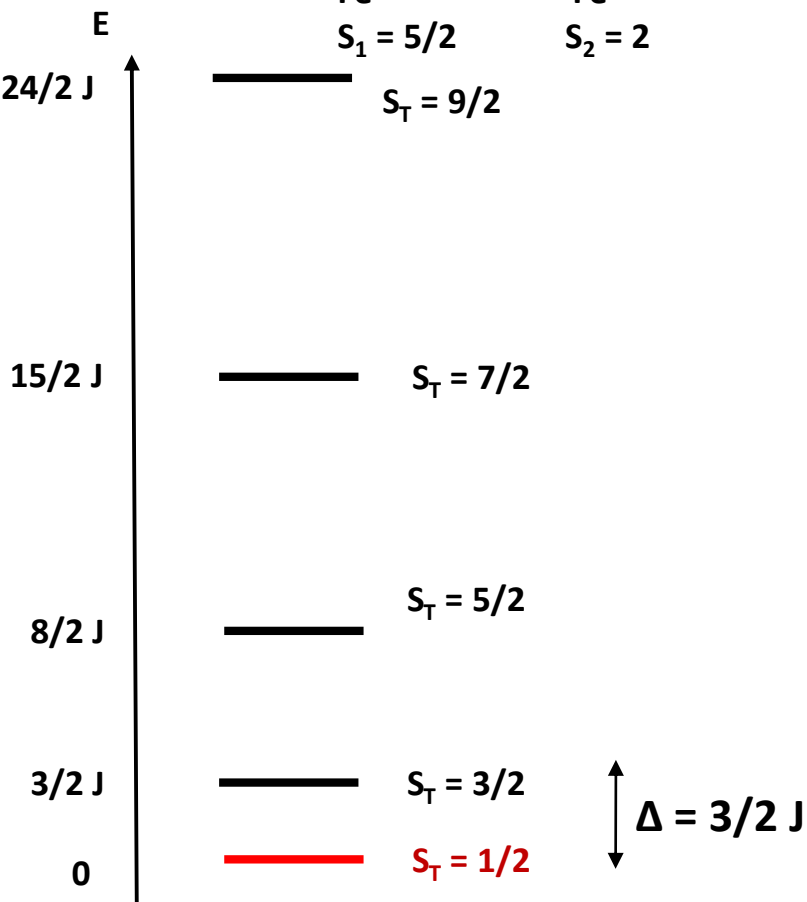
Antiferromagnetic coupling: $J > 0$



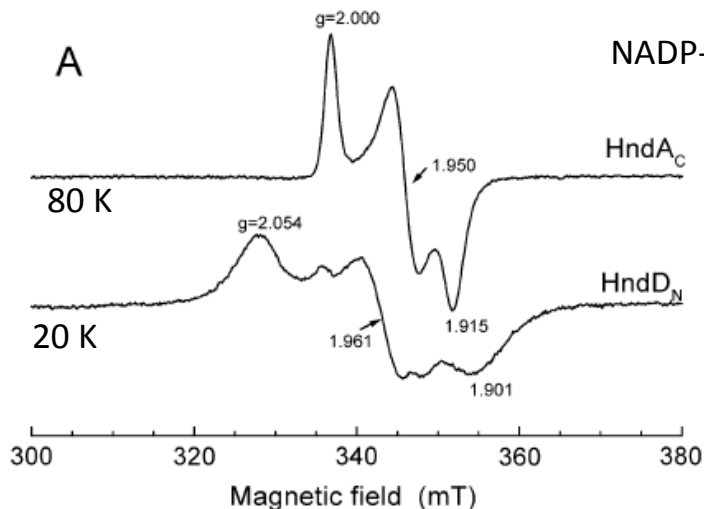
Ground state: $S_T = 1/2$



Fast relaxation of the EPR signal: Orbach process



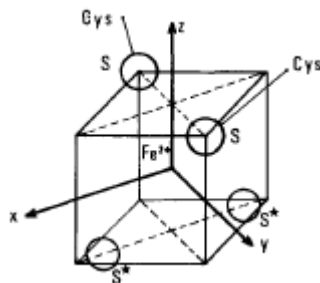
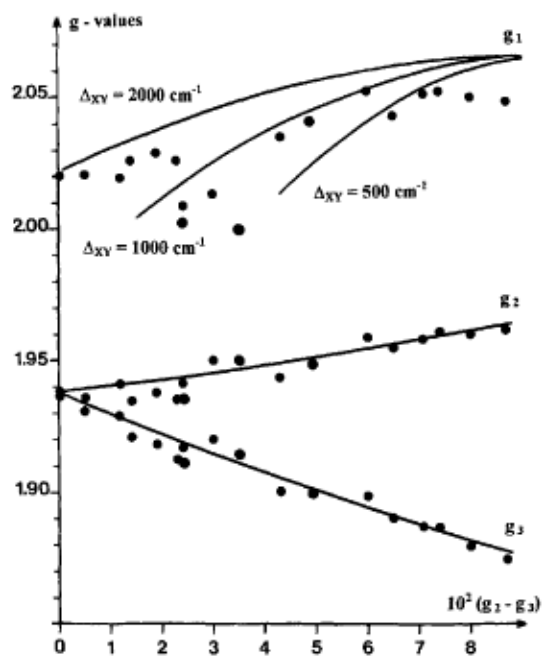
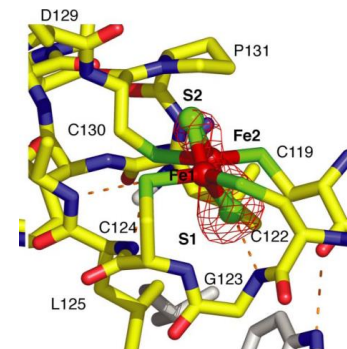
Fe-S clusters: Exchange interaction determination from relaxation broadening



NADP-dependent Fe-Fe hydrogenase from *D. fructosovorans*

Cys motive $\text{C-X}_4\text{-C-X}_{35}\text{-C-X}_3\text{-C}$
Signal broadening for $T > 160$ K

Cys motive $\text{C-X}_{15}\text{-C-X}_2\text{-C-X}_{13}\text{-C}$
Signal broadening for $T > 50$ K
Disappearance at $T = 100$ K



For each S manifold: $\tilde{g} = K_1 \tilde{g}_1 + K_2 \tilde{g}_2$

$$K_1 = \frac{S(S+1) + S_1(S_1+1) - S_2(S_2+1)}{2S(S+1)}$$

$$K_2 = \frac{S(S+1) + S_2(S_2+1) - S_1(S_1+1)}{2S(S+1)}$$

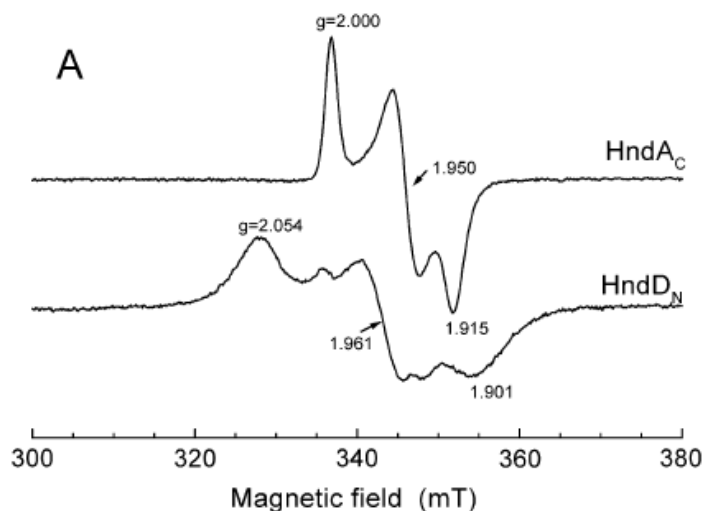
$$K_1 + K_2 = 1$$

For the ground state $S = 1/2$: $g = 7/3 g_1 - 4/3 g_2$
 Fe^{3+} , $S_1 = 5/2$, state 6A_1 , only weak variations of g_1
 Fe^{2+} , $S_2 = 5/2$, state 2T_2 , g_2 very sensitive to structure variations
 \Rightarrow Correlations between g-values variations reflect structural changes of the Fe^{2+} site

(Bertrand & Guigliarelli, Adv.Inorg.Chem1999)

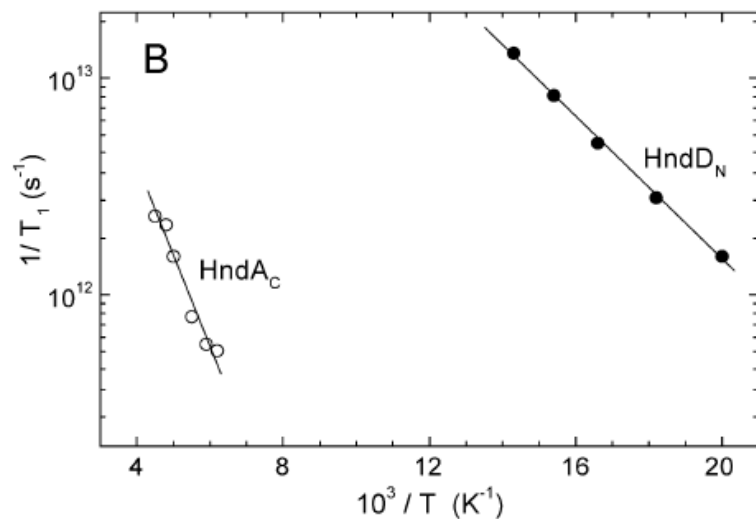
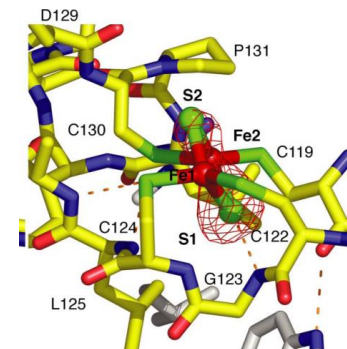
Fe-S clusters: Exchange interaction determination from relaxation broadening

NADP-dependent Fe-Fe hydrogenase from *D. fructosovorans*



Cys motive **C-X₄-C-X₃₅-C-X₃-C**
Signal broadening for T > 160 K

Cys motive **C-X₁₅-C-X₂-C-X₁₃-C**
Signal broadening for T > 50 K
Disappearance at T = 100 K



Broadening by Orbach relaxation process

$$1 / T_1 \propto \exp (- \Delta / kT)$$

$$\Delta = 3/2 J$$

$$\text{HndD}_N : J = 180 \text{ cm}^{-1}$$

$$\text{HndA}_C : J = 560 \text{ cm}^{-1}$$

Hyperfine coupling

$$H_S = \vec{S} \tilde{D} \vec{S} + \beta \vec{S} \tilde{g} \vec{B} + \vec{S} \tilde{A} \vec{I}$$

Magnetic coupling between electron and nuclear spins

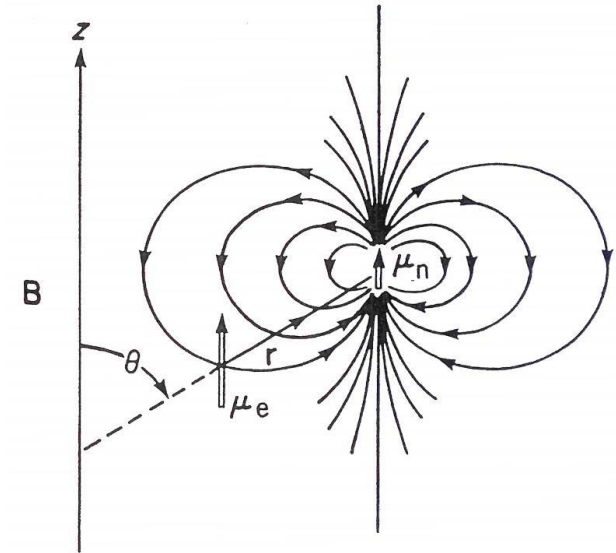
Two physical contributions:

- Dipolar magnetic coupling

$$E_{\text{dip}} = -\vec{\mu}_e \cdot \vec{B}_{\text{induit}} = \frac{\mu_0}{4\pi} \left(\frac{\vec{\mu}_e \cdot \vec{\mu}_n}{r^3} - \frac{3(\vec{\mu}_n \cdot \vec{r})(\vec{\mu}_e \cdot \vec{r})}{r^5} \right)$$

$$\hat{H}(\mathbf{r}) = -\frac{\mu_0}{4\pi} g_e \beta_e g_n \beta_n \left(\frac{\hat{\mathbf{S}} \cdot \hat{\mathbf{I}}}{r^3} - \frac{3(\hat{\mathbf{S}} \cdot \vec{r})(\hat{\mathbf{I}} \cdot \vec{r})}{r^5} \right)$$

$$\hat{H} = \hat{\mathbf{S}} \tilde{\mathbf{T}} \hat{\mathbf{I}} \quad \text{Anisotropic term, } \text{Tr}(\mathbf{T}) = 0$$



- Fermi contact term (non-zero probability of electron on nucleus)

$$\hat{H}_{\text{Fermi}} = \frac{2\mu_0}{3} g \beta_e g_n \beta_n |\psi(0)|^2 \vec{S} \cdot \vec{I} = a_{\text{iso}} \vec{S} \cdot \vec{I} \quad \text{isotropic, reflects spin density on the nucleus}$$

$$\boxed{\mathbf{H}_{\text{Hyp}} = \vec{S} \tilde{\mathbf{A}} \vec{I}} \quad \text{Anisotropic term, with } \text{Tr}(\mathbf{A}) = a_{\text{iso}}$$

Hyperfine coupling: spectral effects

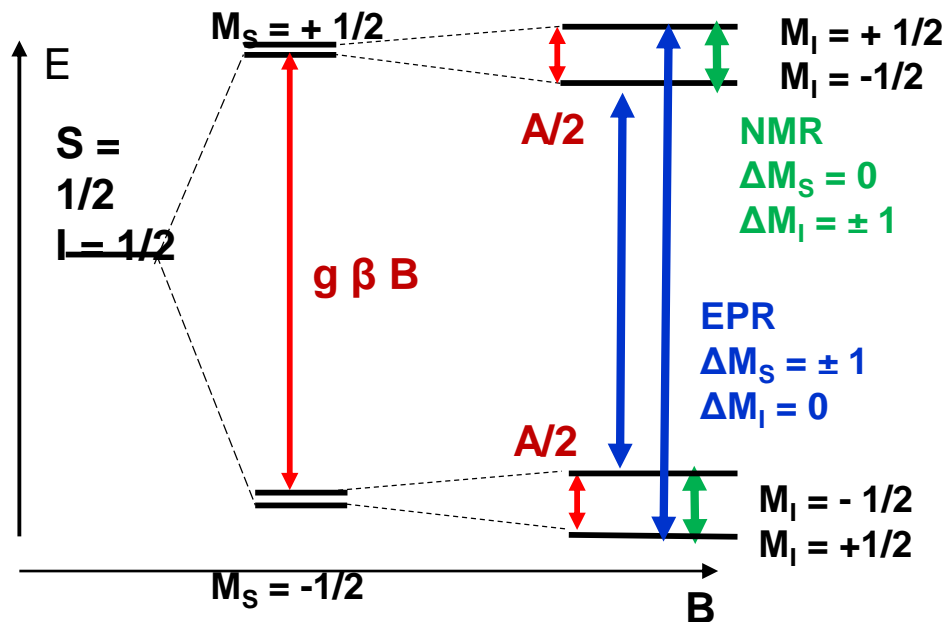
$$H_S = \vec{S} \tilde{D} \vec{S} + \beta \vec{S} \tilde{g} \vec{B} + \vec{S} \tilde{A} \vec{I}$$

Spin states: $|S, M_S\rangle, |I, M_I\rangle$: $(2S+1)(2I+1)$ states

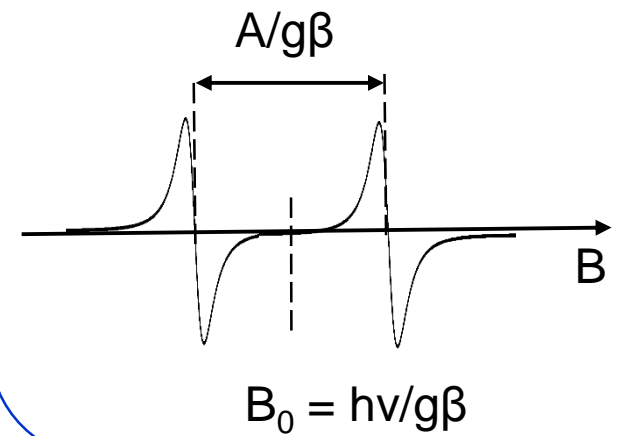
- For isotropic g and isotropic A tensor:

$$H_S = g\beta \vec{S} \cdot \vec{B} + A \vec{S} \cdot \vec{I} = g\beta S_z B + A(S_z I_z)$$

$$E_{(M_S, M_I)} = g\beta B M_S + A M_S M_I \quad (1^{\text{st}} \text{ order})$$



Splitting of the EPR line into
 $(2I + 1) = 2$
Hyperfine components

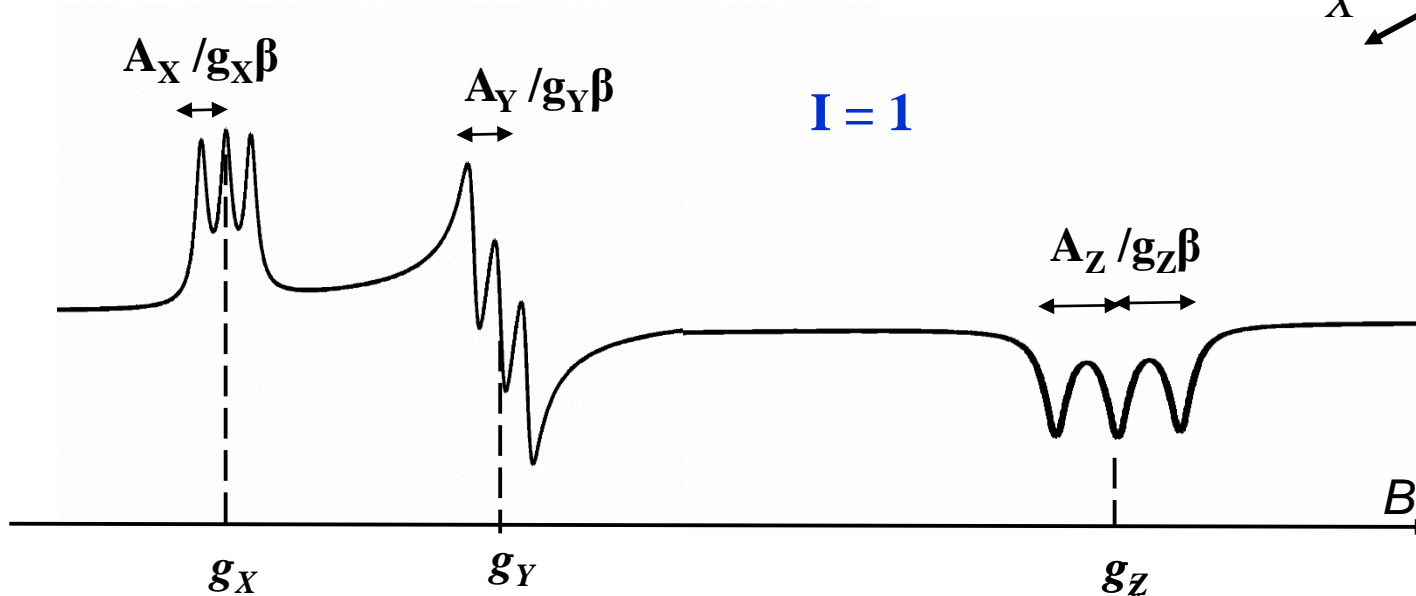
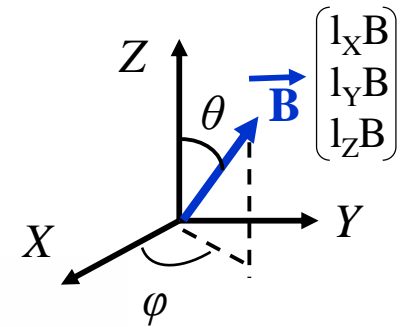


Hyperfine coupling: spectral effects

$$H_S = \vec{S} \tilde{D} \vec{S} + \beta \vec{S} \tilde{g} \vec{B} + \vec{S} \tilde{A} \vec{I}$$

General case: anisotropic g and A tensor

=> $(2I+1)$ hyperfine components for each principal direction of g



A and g with parallel axes

$$g^2 = l_X^2 g_X^2 + l_Y^2 g_Y^2 + l_Z^2 g_Z^2$$

$$A^2 g^2 = l_X^2 A_X^2 g_X^2 + l_Y^2 A_Y^2 g_Y^2 + l_Z^2 A_Z^2 g_Z^2$$

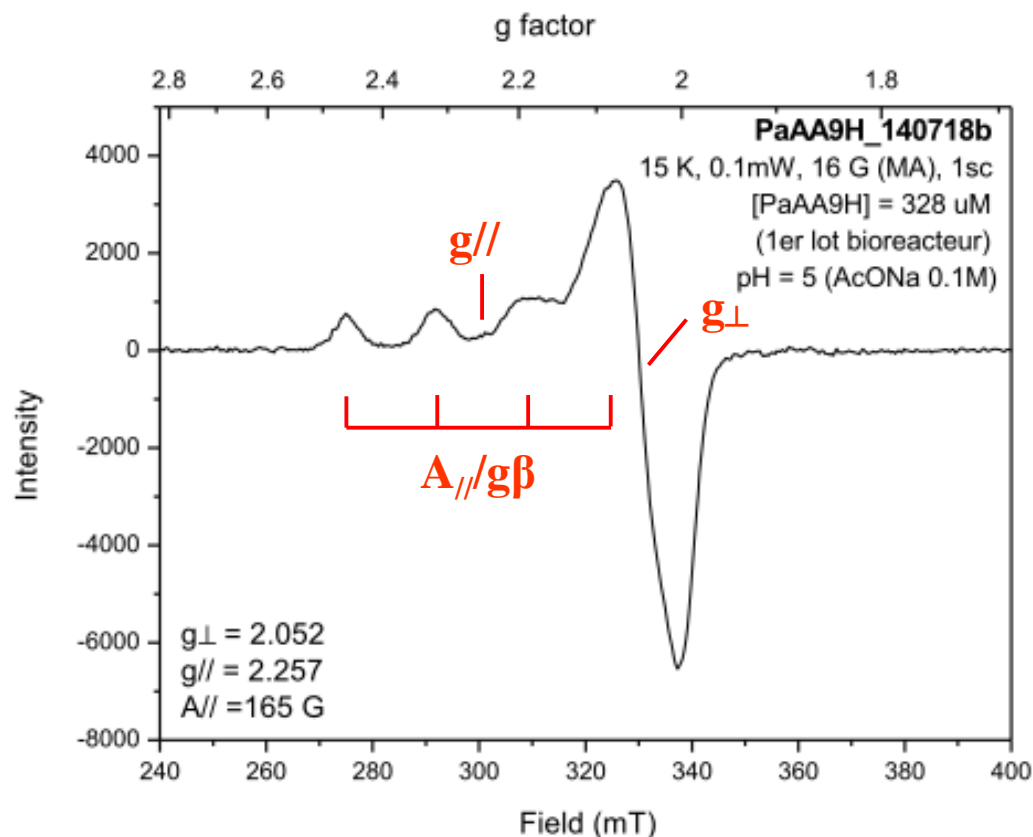
Hyperfine coupling: spectral effects

General case: anisotropic g and A tensor

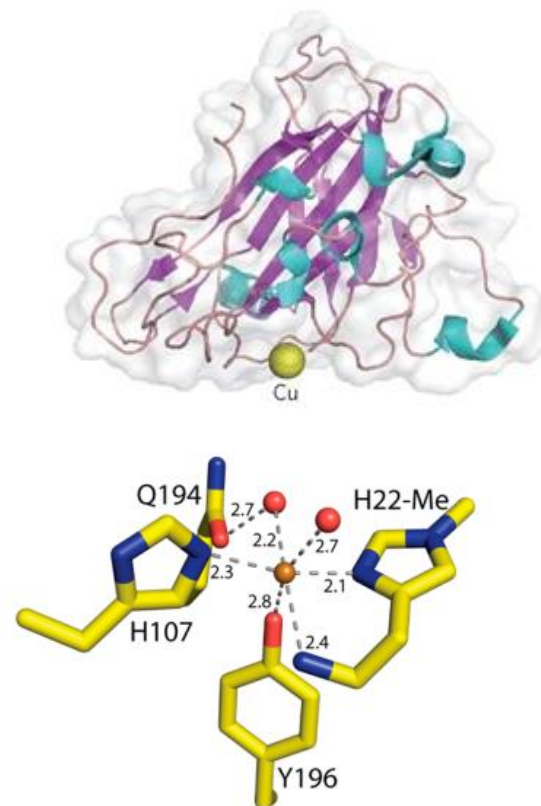
Exemple of copper enzymes

$\text{Cu}^{2+} : 3d^9 S=1/2$

$^{63}\text{Cu}, ^{65}\text{Cu} : I = 3/2 \quad 2I+1 = 4$



Lytic Polysaccharides Monooxygenases (LPMO), *Pseudospira ancerina*

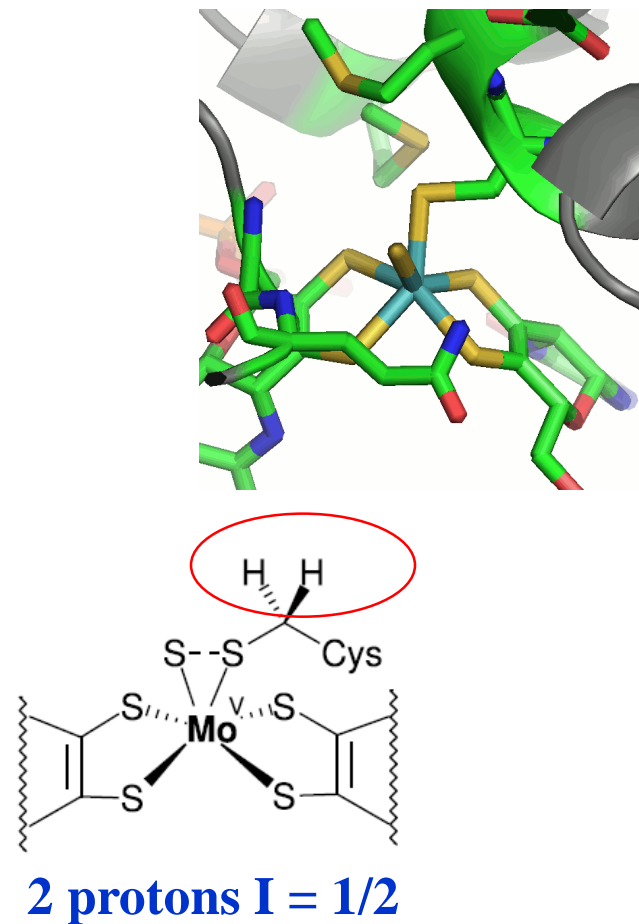
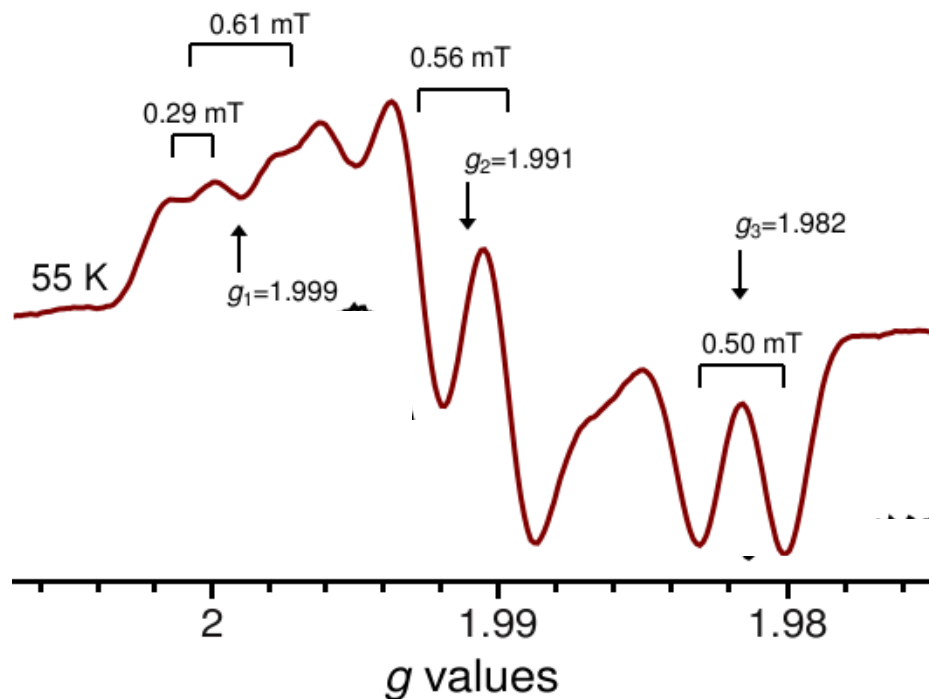


Partial resolution of
hyperfine lines / linewidths

Hyperfine coupling: spectral effects

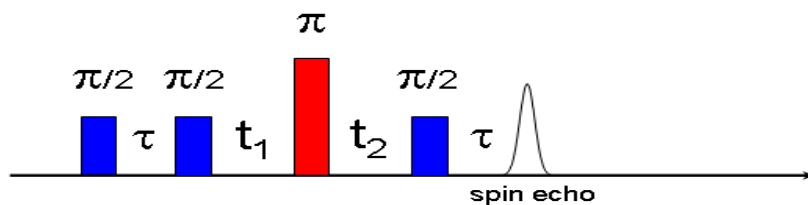
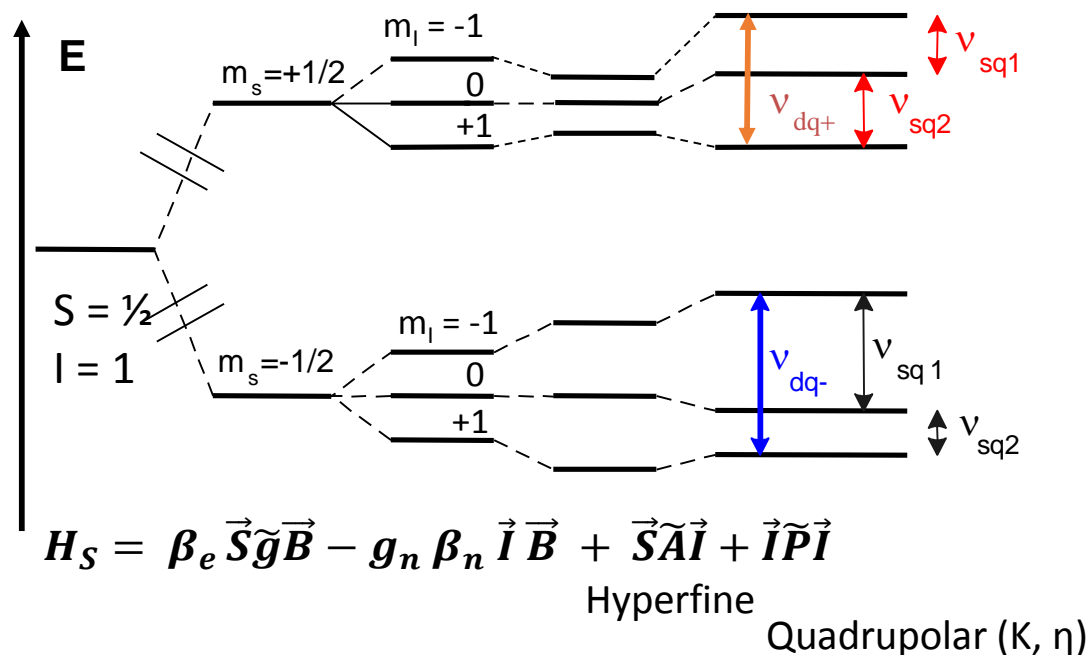
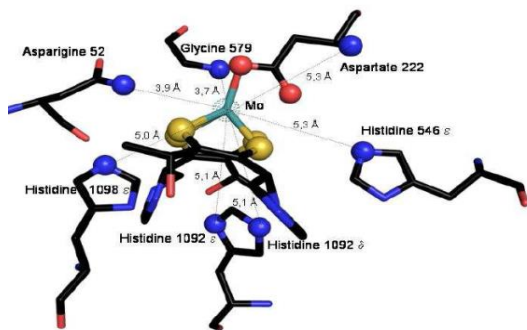
General case: anisotropic g and A tensor

Mo(V) cofactor ($4d^1$) of periplasmic nitrate reductase (*Rhodobacter sphaeroides*)

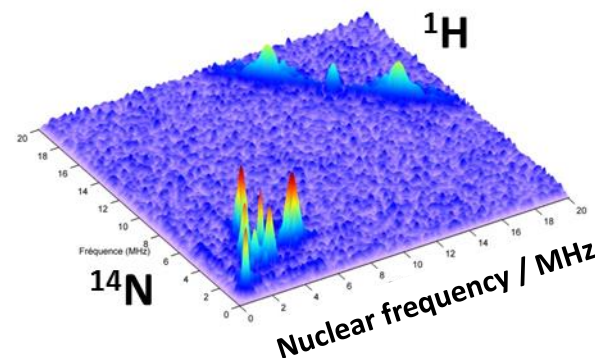


Detection of unresolved hyperfine coupling: HYSCORE spectroscopy

Hyperfine sublevels correlation for ^{14}N ($I = 1$)

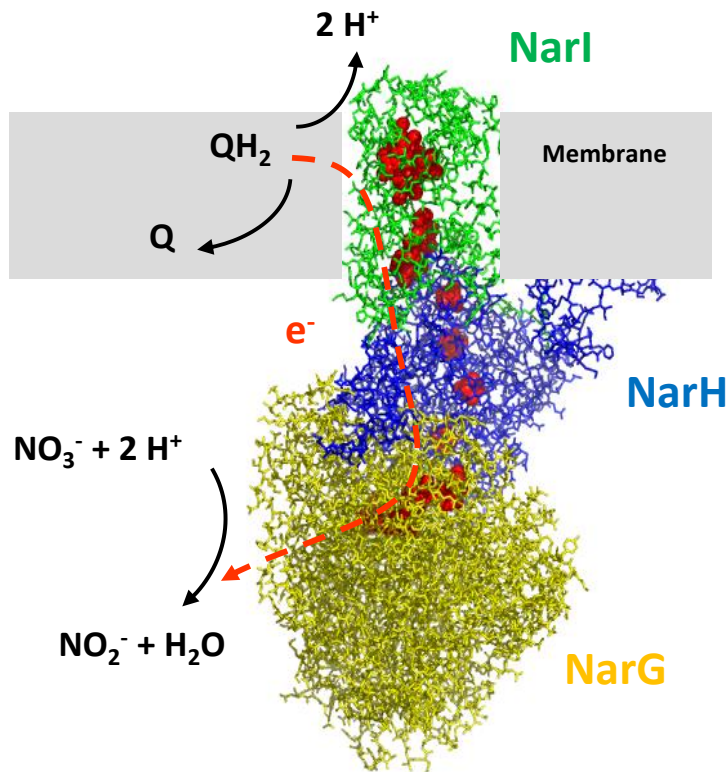


HYSCORE pulse sequence

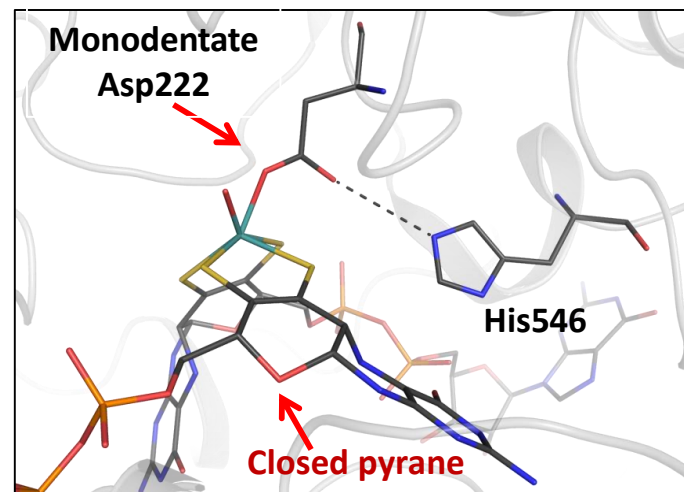


Detection of unresolved hyperfine coupling: HYSCORE spectroscopy

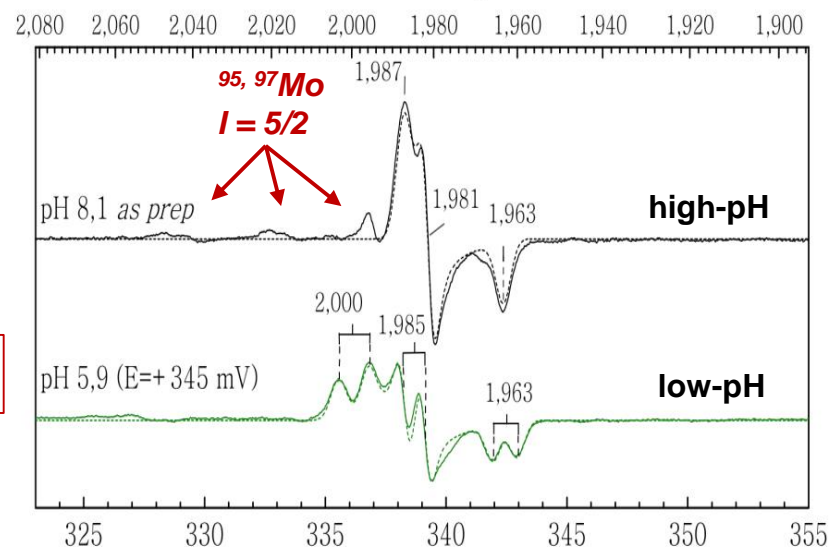
Membrane-bound Nitrate reductase from *E. coli* (NarGHI)



NarGH

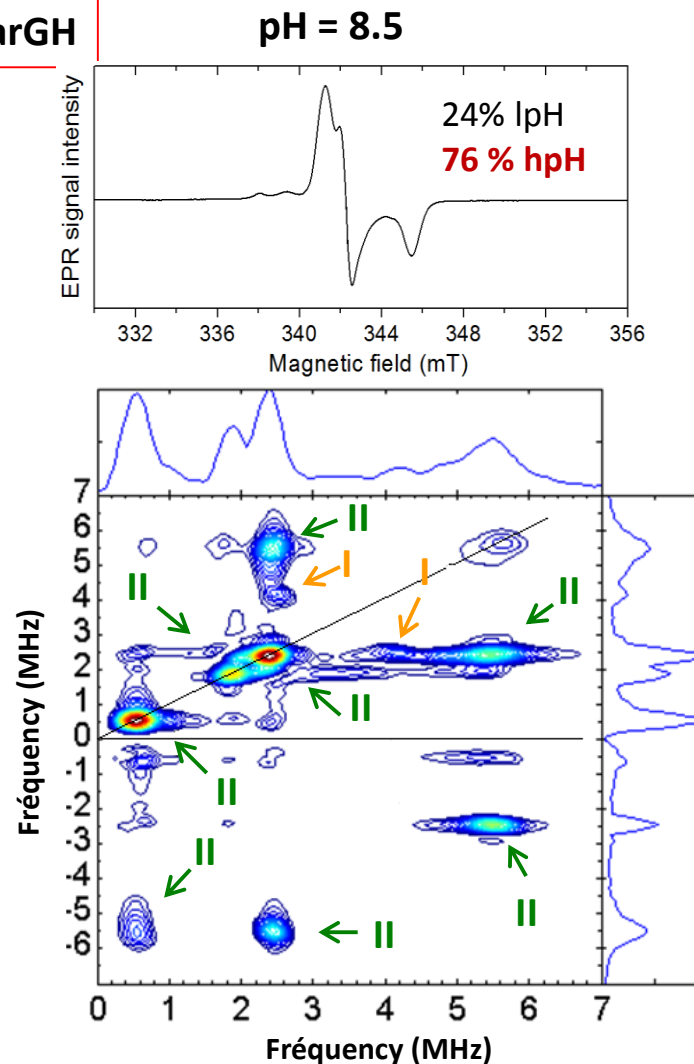
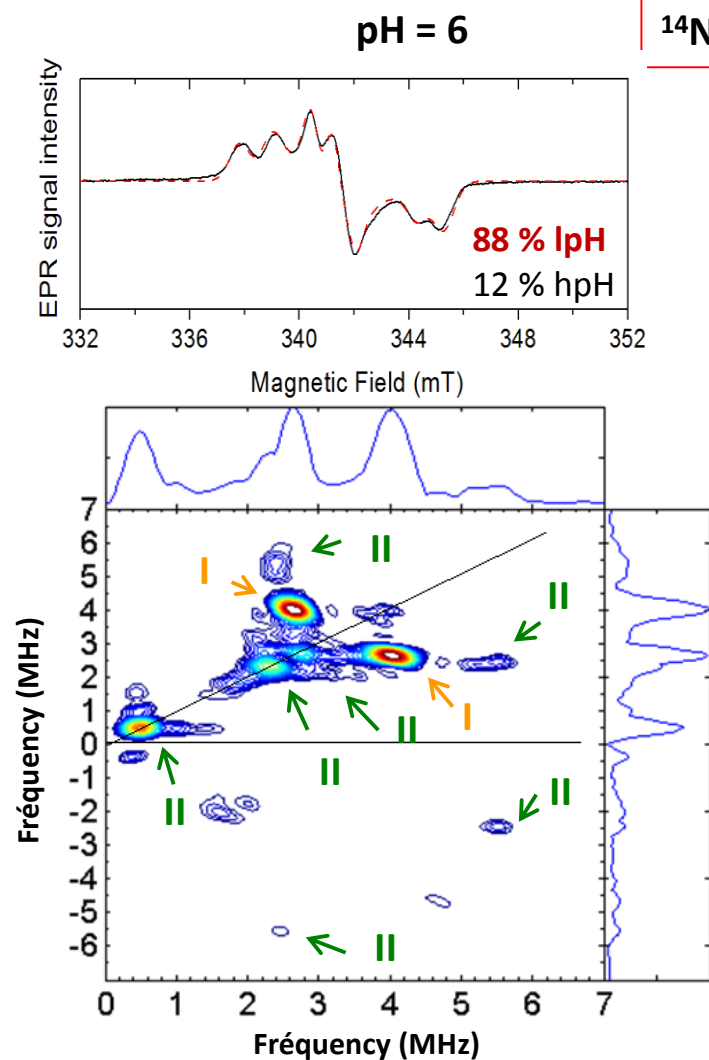


(Jormakka, 2004)



Structure of the different Mo(V) species ?

Detection of unresolved hyperfine coupling: HYSCORE spectroscopy

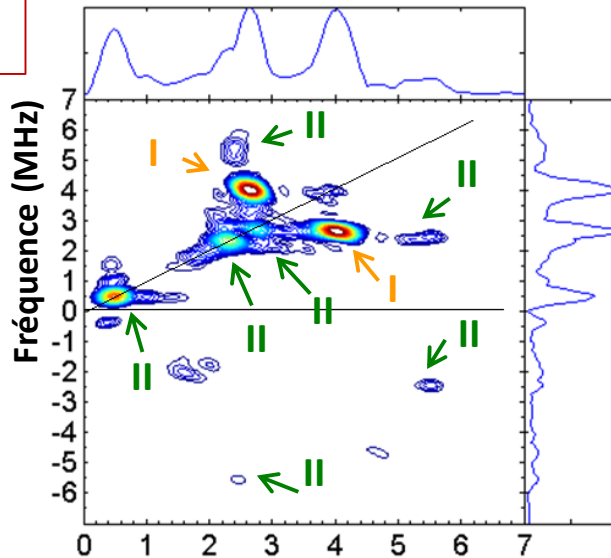


Evidence for two ^{14}N nuclei,
 N_{I} and N_{II} associated to low pH and high pH Mo(V), respectively

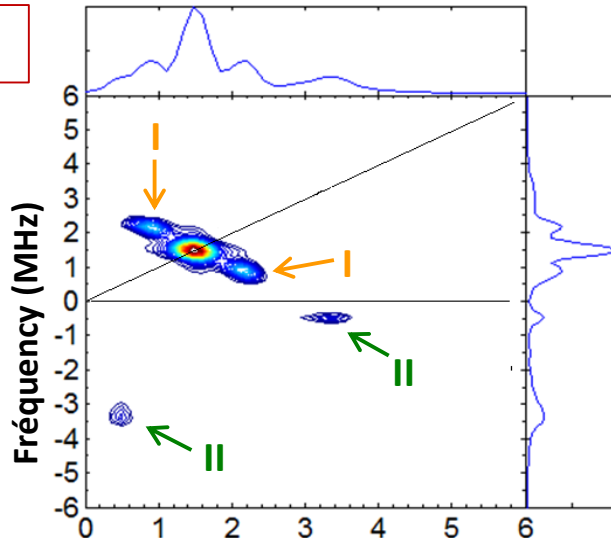
Detection of unresolved hyperfine coupling: HYSCORE spectroscopy

Simplify HYSCORE spectrum with double isotope labeling ^{15}N ($I=1/2$) - ^{98}Mo of NarGH

pH = 6



pH = 6



- N_I parameter determination

pH = 6 preparation of ^{14}N / ^{98}Mo -NarGH

- Hyperfine and quadrupolar parameters:

$$A_{\text{iso}} = 1.0 \text{ MHz}$$

$$T = 0.25 \text{ MHz}$$

$$\kappa = 0.6\text{-}0.7 \text{ MHz}$$

$$\eta = [0\text{-}1]$$

$$A < 2\nu_I(\text{N})$$



$$^{15}\text{N} : I = 1/2 ;$$

$$\frac{A(^{14}\text{N})}{A(^{15}\text{N})} = \frac{g_n(^{14}\text{N})}{g_n(^{15}\text{N})} = 0.712$$

Double isotope labelling:

pH = 6 preparation of ^{15}N / ^{98}Mo -NarGH

- Hyperfine parameters :

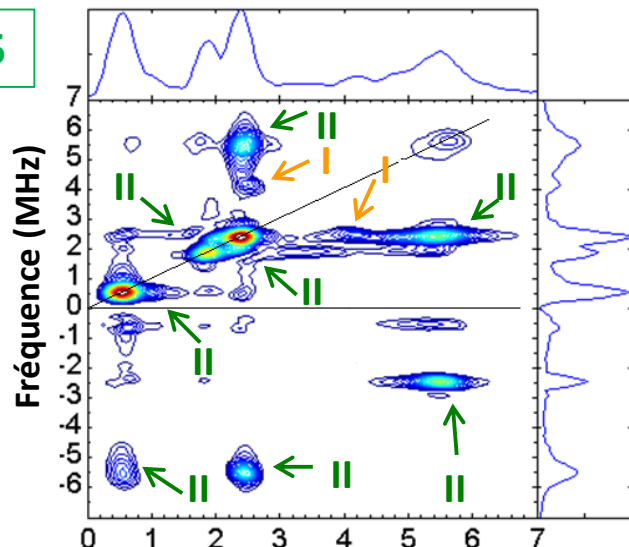
$$A_{\text{iso}} = 1.5 \text{ MHz}$$

$$T = 0.4 \text{ MHz}$$

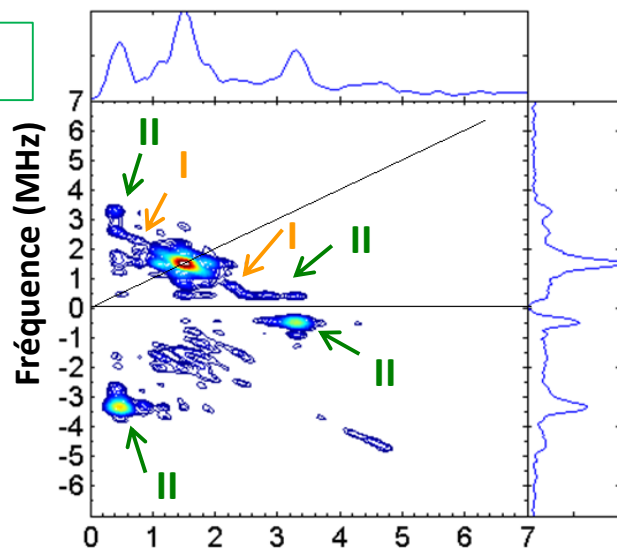
Detection of unresolved hyperfine coupling: HYSCORE spectroscopy

Simplify HYSCORE spectrum with double isotope labeling ^{15}N ($I=1/2$) - ^{98}Mo of NarGH

pH = 8.5



pH = 10



- $N_{||}$ parameter determination

pH 8.5 preparation of $^{14}\text{N}/^{98}\text{Mo}$ NarGH

- Hyperfine and quadrupolar parameters :

$$A_{\text{iso}} = 2.7 \text{ MHz} \quad \kappa = 0.7 \text{ MHz} \quad \text{Cancellation Condition}$$

$$T = 0.56 \text{ MHz} \quad \eta = 0.4 \text{ MHz} \quad A \sim 2\nu_l(N)$$

$$^{15}\text{N} : I = 1/2 ; \quad \frac{A(^{14}\text{N})}{A(^{15}\text{N})} = \frac{g_n(^{14}\text{N})}{g_n(^{15}\text{N})} = 0.712$$

pH10 preparation of $^{15}\text{N}/^{98}\text{Mo}$ NarGH

- Hyperfine coupling :

$$A_{\text{iso}} = 3.4 \text{ MHz}$$

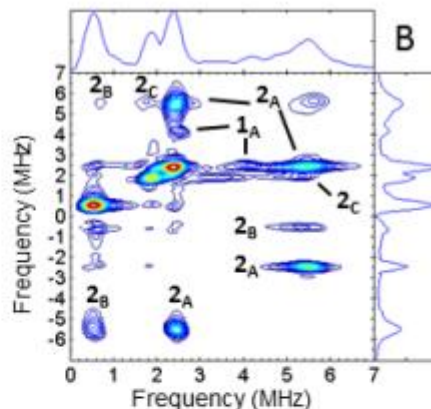
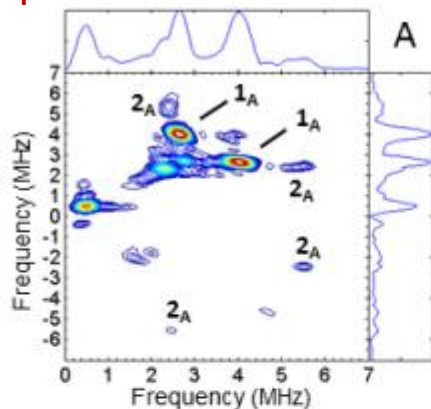
$$T = 0.7 \text{ MHz}$$

Detection of unresolved hyperfine coupling: HYSCORE spectroscopy

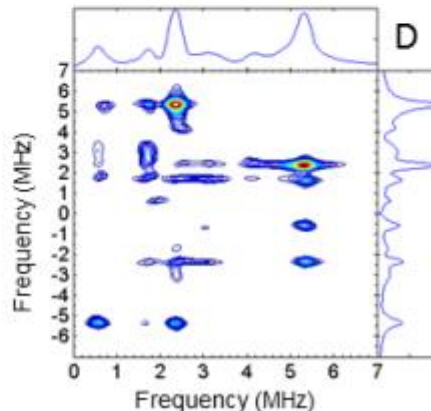
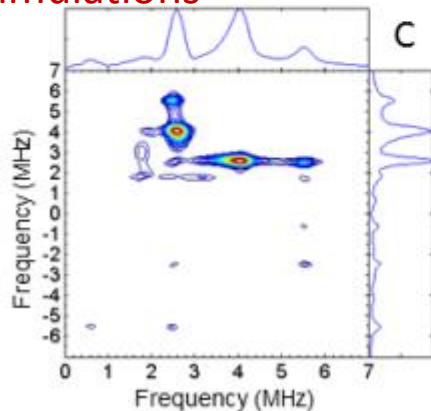
pH = 6.0

pH = 8.5

Experimental



Simulations

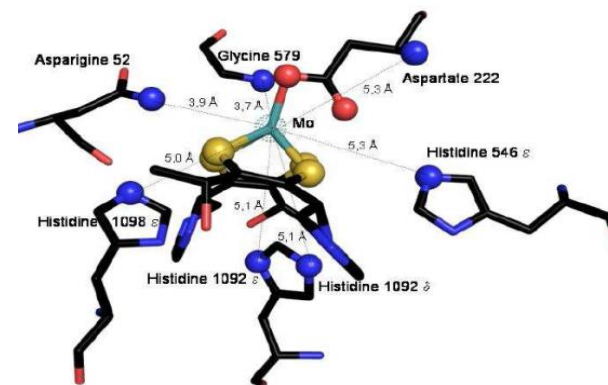


80% $^{14}\text{N}_I$ + 20% $^{14}\text{N}_{II}$

15% $^{14}\text{N}_I$ + 85% $^{14}\text{N}_{II}$

	^{14}N parameters	Assignment
$^{14}\text{N}_{II}$	$A = 2.7 \text{ MHz}$ $\kappa = 0.66 \text{ MHz}$ $\eta = 0.4$	High pH form
$^{14}\text{N}_I$	$A = 1.1 \text{ MHz}$ $\kappa = 0.69 \text{ MHz}$ $\eta = 0.44$	Low pH form

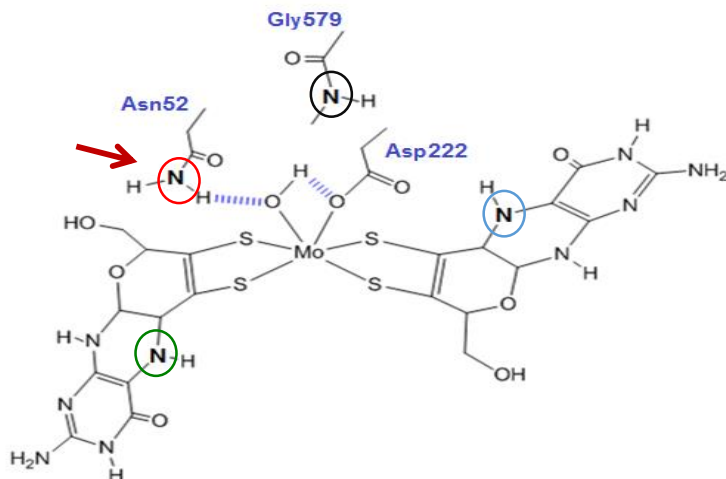
Similar quadrupole parameters for N_I et N_{II} :
Do they arise from the same chemical group ?



Detection of unresolved hyperfine coupling: HYSCORE spectroscopy

Structure model for Mo(V) low pH species

- Entire tetrahydropyranopterin
- Amino-acids with closest N atoms : Asn52, Gly579



DFT

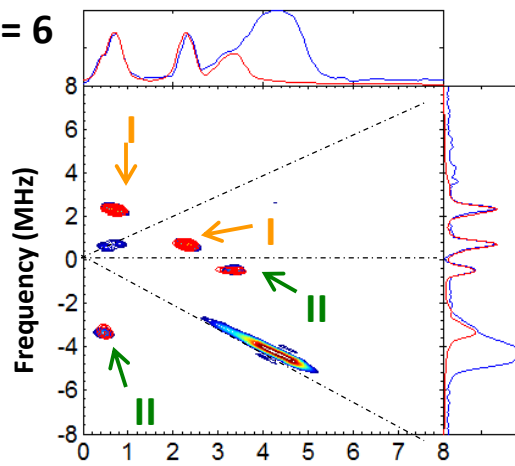
Nucleus	$ \kappa $ [MHz]	η
$^{14}\text{N}_Q$	1.433	0.162
$^{14}\text{N}_P$	1.422	0.168
$^{14}\text{N}_{\text{N52}}$	0.786	0.418
$^{14}\text{N}_{\text{G579}}$	0.916	0.205

HYSCORE

$^{14}\text{N}_I$	0.69	0.44	Low pH
$^{14}\text{N}_{II}$	0.66	0.4	High pH

Selective ^{15}N -Asn labeling of ^{98}Mo -NarGH

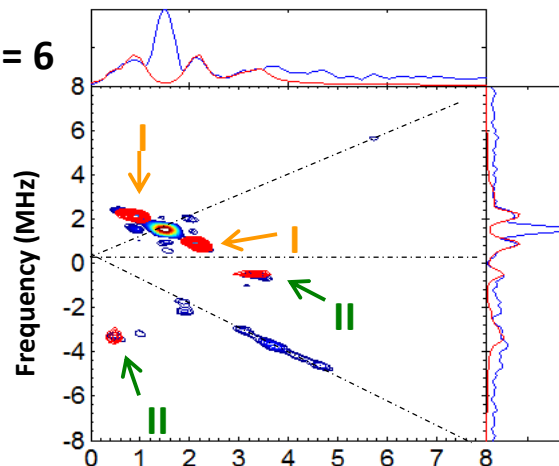
pH = 6



— Simulations

^{15}N / ^{98}Mo -NarGH

pH = 6

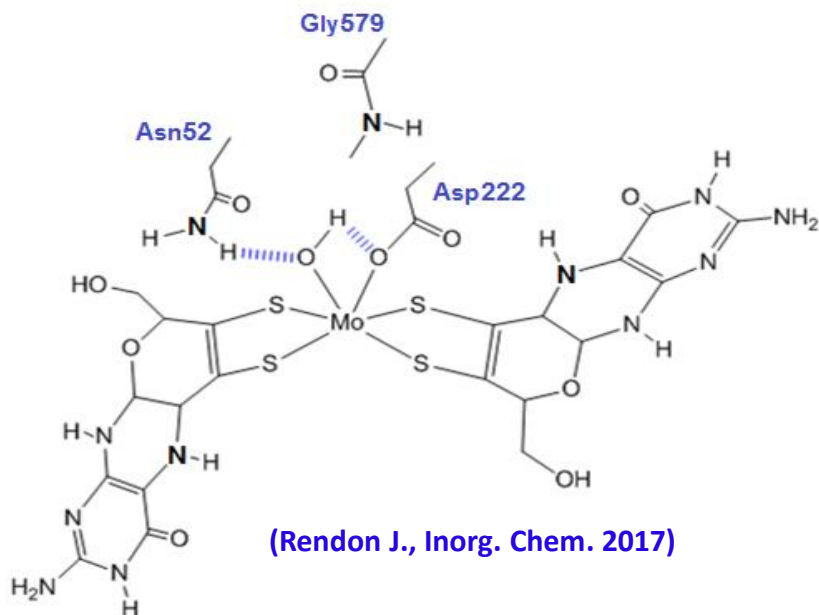


Assignment to Asn52- N_6
 - N_I to low pH Mo(V)
 - N_{II} to high pH Mo(V)

(Rendon, Inorg. Chem. 2017)

Detection of unresolved hyperfine coupling: HYSCORE spectroscopy

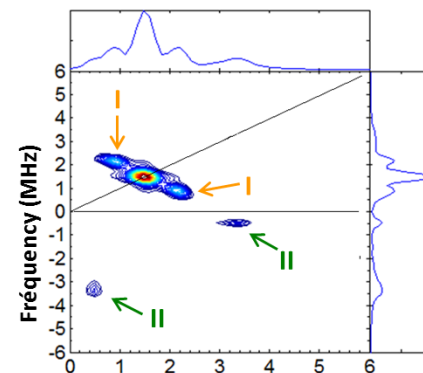
First structural model of the low pH Mo(V) species in NarGH



In progress:

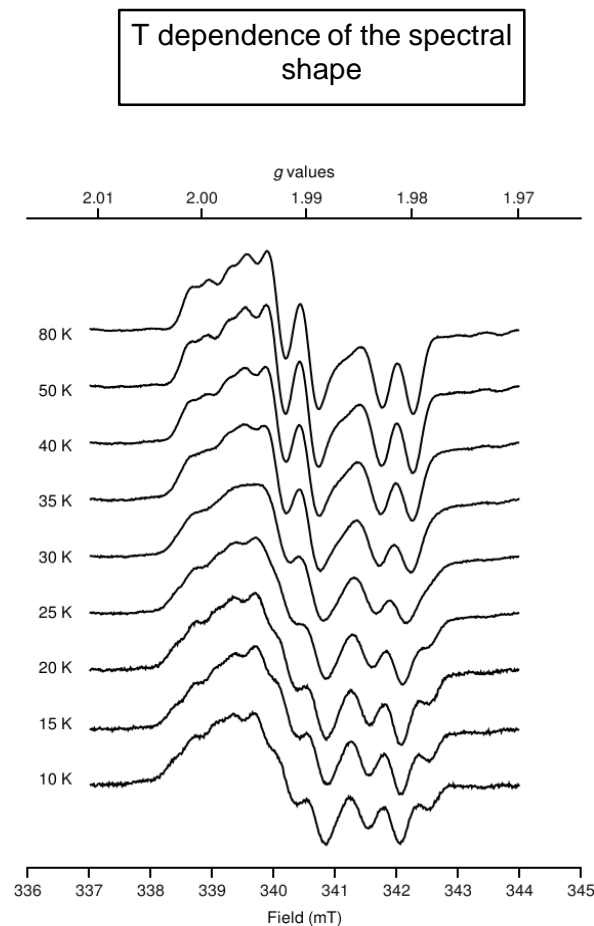
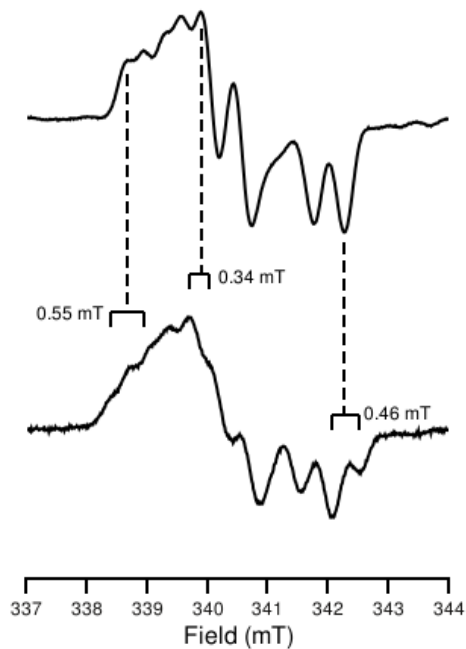
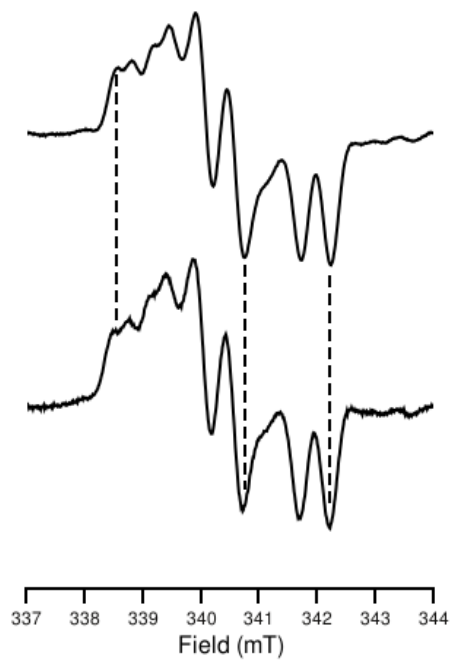
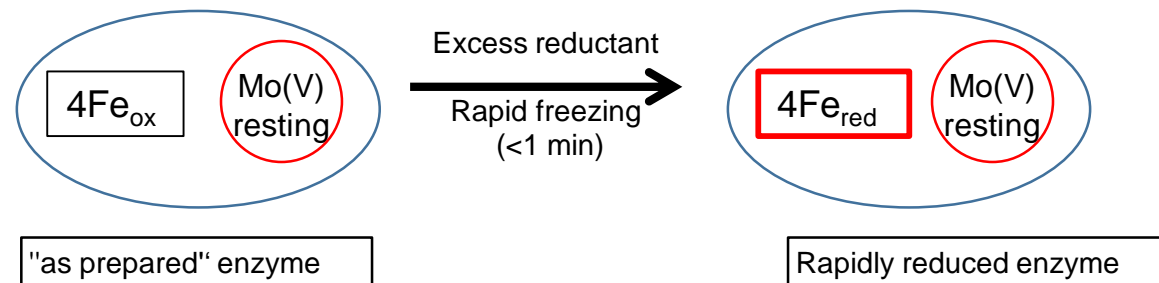
- ^1H , ^2H HYSCORE analysis in progress
- Structure of high pH Mo(V)
- Influence of distant amino-acids

HYSCORE Study of Nar



Detection of intercenter magnetic coupling

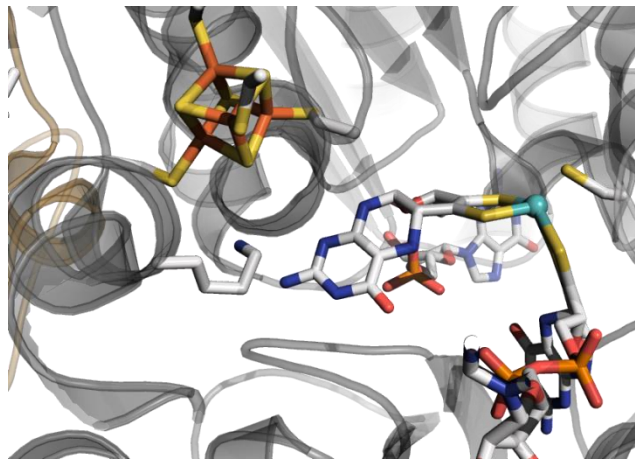
Analysis of spin-spin coupling between high g Mo(V) and reduced 4Fe-4S center in NapAB



Detection of intercenter magnetic coupling

Analysis of spin-spin coupling between high g Mo(V) and reduced 4Fe-4S center in NapAB

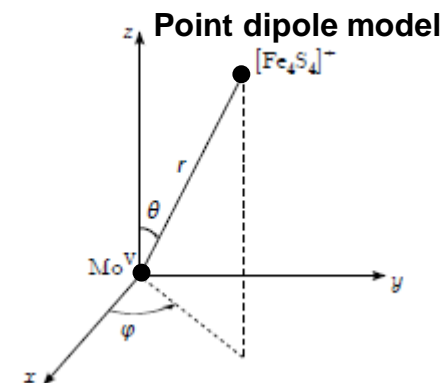
Mo(V) \leftrightarrow [4Fe-4S]⁺¹



$$\hat{H}_{\text{int}} = \hat{H}_{\text{exch}} + \hat{H}_{\text{dip}}$$

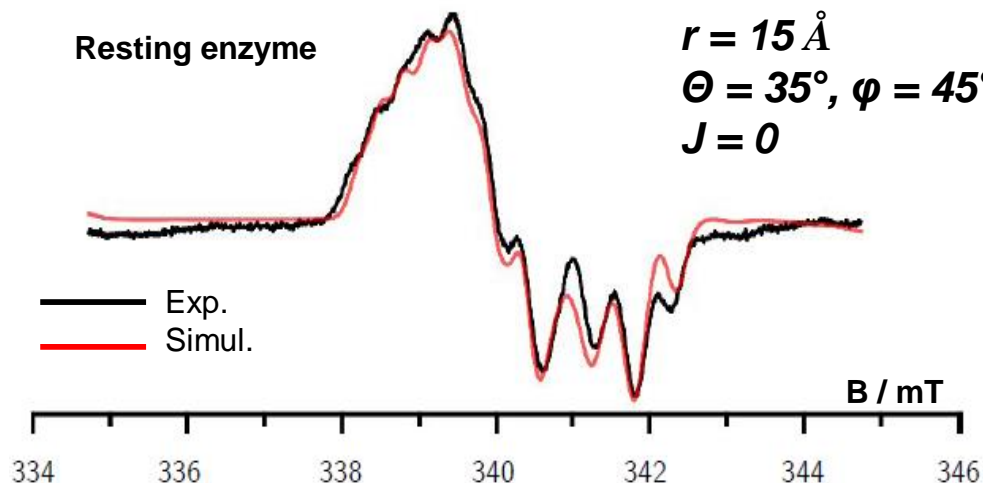
$$\downarrow \qquad \qquad \downarrow$$

$$J \vec{S}_1 \cdot \vec{S}_2 + \vec{S}_1 D_{\text{dip}} \vec{S}_2$$



Resting enzyme

$r = 15 \text{ \AA}$
 $\Theta = 35^\circ, \varphi = 45^\circ$
 $J = 0$

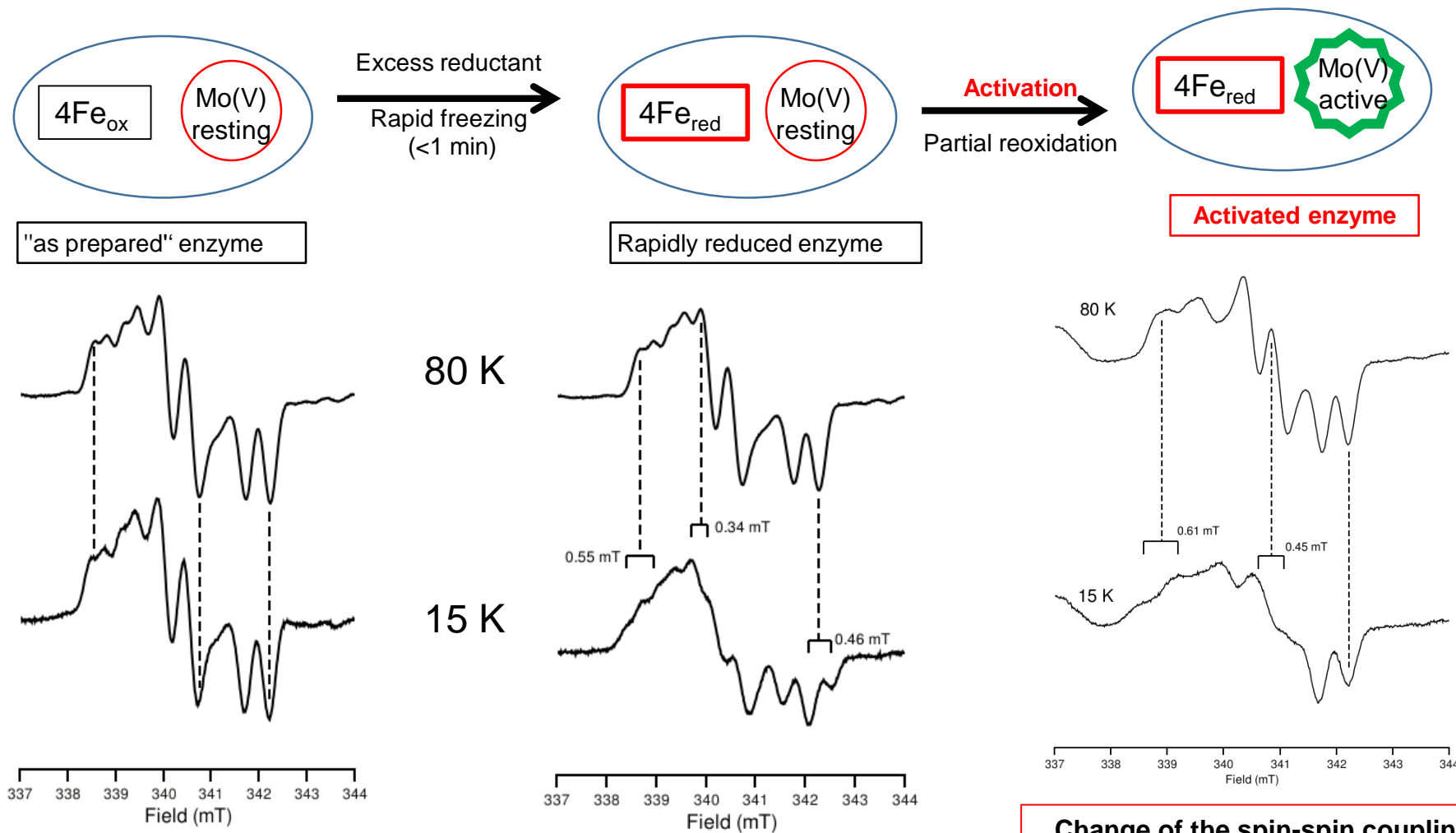


$J = 0$

No exchange coupling in inactive Nap between high g resting Mo(V) and FeS center

Detection of intercenter magnetic coupling

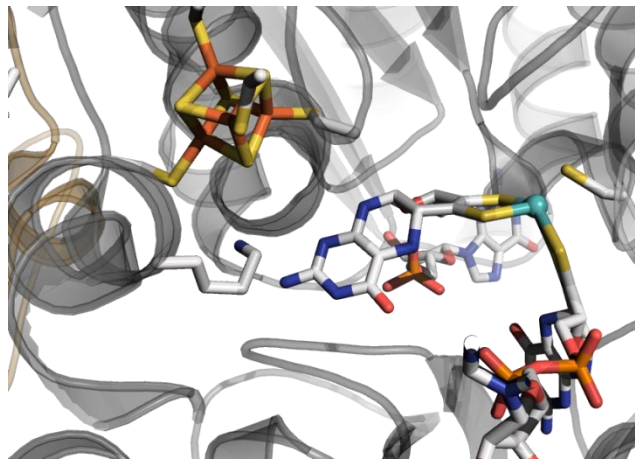
Influence of activation on the spin-spin coupling between high g Mo(V) and reduced Fe-S center



Detection of intercenter magnetic coupling

Analysis of spin-spin coupling between high g Mo(V) and reduced 4Fe-4S center in NapAB

Mo(V) \leftrightarrow [4Fe-4S]⁺¹

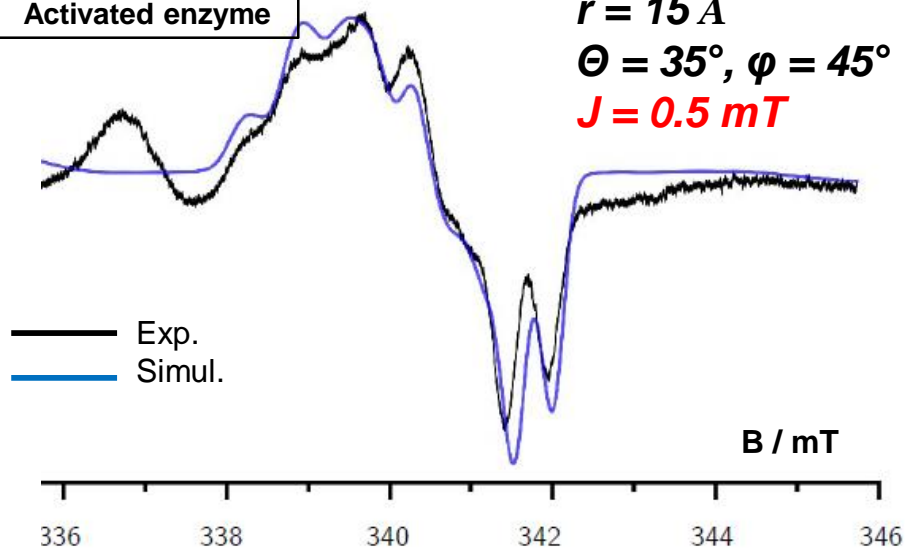


$$\hat{H}_{\text{int}} = \hat{H}_{\text{exch}} + \hat{H}_{\text{dip}}$$

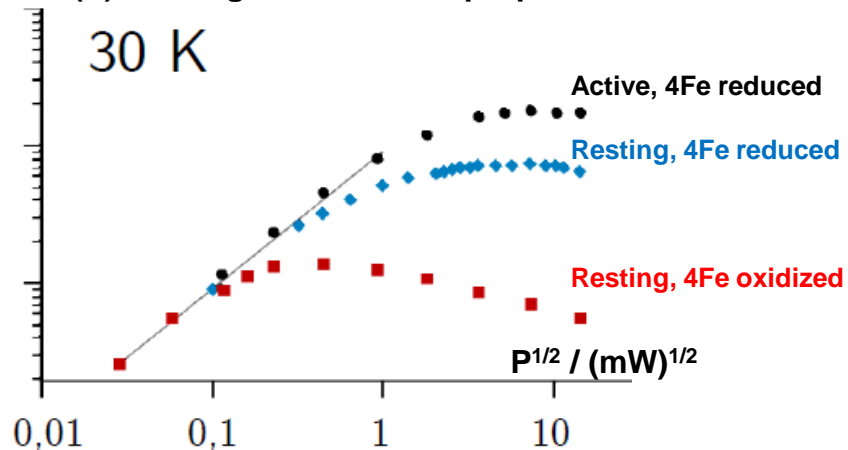
$$J \vec{S}_1 \cdot \vec{S}_2 + \vec{S}_1 D_{\text{dip}} \vec{S}_2$$

Activated enzyme

$r = 15 \text{ \AA}$
 $\Theta = 35^\circ, \varphi = 45^\circ$
 $J = 0.5 \text{ mT}$



Mo(V) EPR signal saturation properties



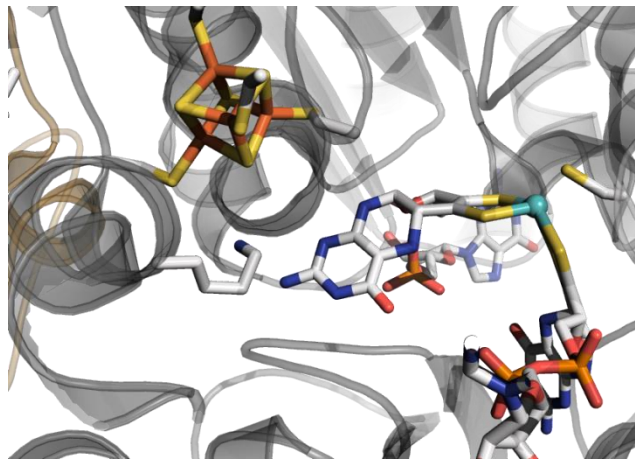
$$1/T_1 = 1/T_1^\circ + k_{1\text{dip}} + k_{1\text{ex}}$$

$$1/T_2 = 1/T_2^\circ + k_{2\text{dip}} + k_{2\text{ex}}$$

Detection of intercenter magnetic coupling

Analysis of spin-spin coupling between high g Mo(V) and reduced 4Fe-4S center in NapAB

Mo(V) \leftrightarrow [4Fe-4S]⁺¹



$$\hat{H}_{\text{int}} = \hat{H}_{\text{exch}} + \hat{H}_{\text{dip}}$$

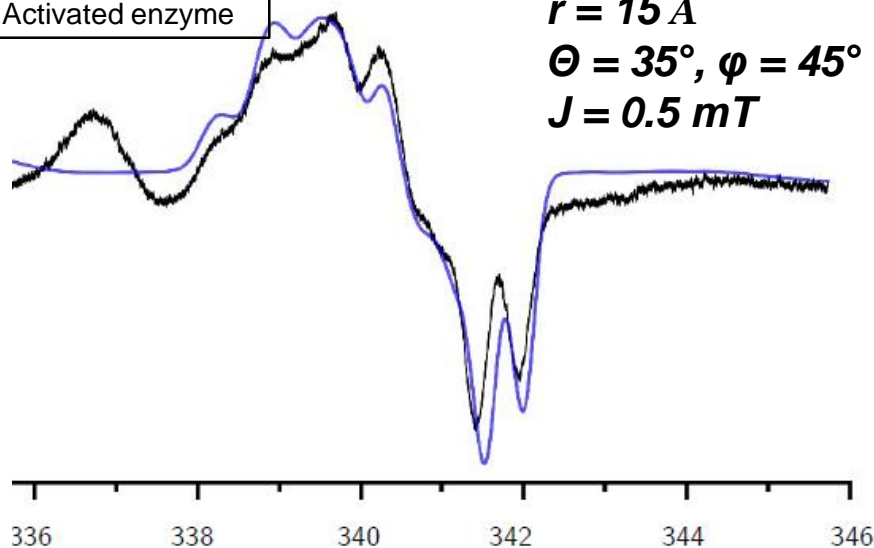
$\downarrow \qquad \qquad \downarrow$

$$J \vec{S}_1 \cdot \vec{S}_2 + \vec{S}_1 D_{\text{dip}} \vec{S}_2$$

- In resting and activated enzymes, the high-g Mo(V) signals are very similar
- No change of the first coordination sphere of the Mo ion in the activation process
- Change of the exchange coupling between Mo and Fe-S centers in the activation process.

Activated enzyme

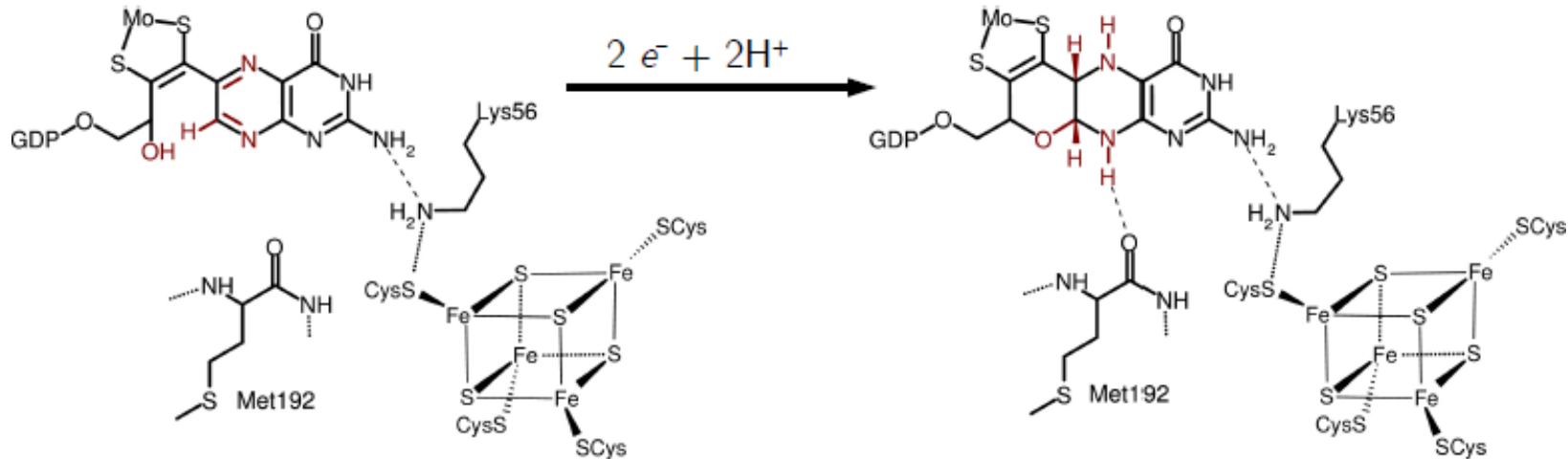
$r = 15 \text{ \AA}$
 $\Theta = 35^\circ, \varphi = 45^\circ$
 $J = 0.5 \text{ mT}$



Detection of intercenter magnetic coupling

Analysis of spin-spin coupling between high g Mo(V) and reduced 4Fe-4S center in NapAB

Model for NapAB activation : Pterin as a non-innocent ligand



Inactive enzyme

High g resting Mo(V), oxidized pterine

$J = 0$, no electron transfer

Activated enzyme

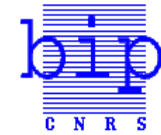
High g « activated » Mo(V), reduced pterine

$J = 0.5$ mT, restored electron transfer

Change of hydrogen bond network around Mo ion

(J. Jacques, BBA 2014)

Acknowledgements



BIP, CNRS & AMU
Stéphane GRIMALDI
Julia RENDON
Frédéric BIASO
Sinan AL ATTAR
Elisabetta MILEO
Alessio BONUCCI
Valérie BELLE
Bénédicte BURLAT
Kamal ZEAMARI



LBC, CEA, CNRS, AMU
David PIGNOL
Pascal ARNOUX
Monique SABATY

LCB, CNRS & AMU
Axel MAGALON
Sinan AL ATTAR
Anne WALBURGER



Thank you for your attention



**International EPR school
Carry-Le-Rouet / Marseille
3-7 June 2018**